

The *XMM* Cluster Survey: evolution of the velocity dispersion – temperature relation over half a Hubble time

Susan Wilson,^{1*} Matt Hilton,^{1†} Philip J. Rooney,² Caroline Caldwell,³ Scott T. Kay,⁴ Chris A. Collins,³ Ian G. McCarthy,³ A. Kathy Romer,² Alberto Bermeo,² Rebecca Bernstein,⁵ Luiz da Costa,^{6,7} Daniel Gifford,⁸ Devon Hollowood,⁹ Ben Hoyle,¹⁰ Tesla Jeltema,⁹ Andrew R. Liddle,¹¹ Marcio A. G Maia,^{6,7} Robert G. Mann,¹¹ Julian A. Mayers,³ Nicola Mehrrens,^{12,13} Christopher J. Miller,⁸ Robert C. Nichol,¹⁴ Ricardo Ogando,^{6,7} Martin Sahlén,¹⁵ Benjamin Stahl,⁹ John P. Stott,¹⁶ Peter A. Thomas,² Pedro T. P. Viana,^{17,18} and Harry Wilcox¹⁴

¹ Astrophysics & Cosmology Research Unit, School of Mathematics, Statistics & Computer Science, University of KwaZulu-Natal, Durban 4041, SA

² Astronomy Centre, University of Sussex, Falmer, Brighton, BN1 9QH, UK

³ Astrophysics Research Institute, Liverpool John Moores University, IC2, Liverpool Science Park, 146 Brownlow Hill, Liverpool, L3 5RF, UK

⁴ Jodrell Bank Centre for Astrophysics, School of Physics and Astronomy, The University of Manchester, Manchester, M13 9PL, UK

⁵ Observatories of the Carnegie Institution for Science, 813 Santa Barbara Street, Pasadena, CA 91101, USA

⁶ Observatório Nacional, Rua Gal. José Cristino 77, Rio de Janeiro, RJ - 22460-040, Brazil

⁷ Laboratório Interinstitucional de e-Astronomia - LIneA, Rua Gal. José Cristino 77, Rio de Janeiro, RJ - 20921-400, Brazil

⁸ Astronomy Department, University of Michigan, Ann Arbor, MI 48109, USA

⁹ Department of Physics and Santa Cruz Institute for Particle Physics, University of California, Santa Cruz, CA 95064, USA

¹⁰ Universitaets-Sternwarte, Fakultae fuer Physik, Ludwig-Maximilians Universitaet Muenchen, Scheinerstr. 1, D-81679 Muenchen, Germany

¹¹ Institute for Astronomy, University of Edinburgh, Royal Observatory, Blackford Hill, Edinburgh, EH9 3HJ, UK

¹² George P. and Cynthia Woods Mitchell Institute for Fundamental Physics and Astronomy, Texas A & M University, College Station, TX, 77843-4242 USA

¹³ Department of Physics and Astronomy, Texas A & M University, College Station, TX, 77843-4242 USA

¹⁴ Institute of Cosmology and Gravitation, University of Portsmouth, Dennis Sciama Building, Portsmouth, PO1 3FX, UK

¹⁵ BIPAC, Department of Physics, University of Oxford, Denys Wilkinson Building, 1 Keble Road, Oxford OX1 3RH, UK

¹⁶ Sub-department of Astrophysics, Department of Physics, University of Oxford, Denys Wilkinson Building, Keble Road, Oxford OX1 3RH, UK

¹⁷ Instituto de Astrofísica e Ciências do Espaço, Universidade do Porto, CAUP, Rua das Estrelas, 4150-762 Porto, Portugal

¹⁸ Departamento de Física e Astronomia, Faculdade de Ciências, Universidade do Porto, Rua do Campo Alegre, 687, 4169-007 Porto, Portugal

Accepted for publication in MNRAS

ABSTRACT

We measure the evolution of the velocity dispersion–temperature (σ_v – T_X) relation up to $z = 1$ using a sample of 38 galaxy clusters drawn from the *XMM* Cluster Survey. This work improves upon previous studies by the use of a homogeneous cluster sample and in terms of the number of high redshift clusters included. We present here new redshift and velocity dispersion measurements for 12 $z > 0.5$ clusters observed with the GMOS instruments on the Gemini telescopes. Using an orthogonal regression method, we find that the slope of the relation is steeper than that expected if clusters were self-similar, and that the evolution of the normalisation is slightly negative, but not significantly different from zero ($\sigma_v \propto T^{0.86 \pm 0.14} E(z)^{-0.37 \pm 0.33}$). We verify our results by applying our methods to cosmological hydrodynamical simulations. The lack of evolution seen in our data is consistent with simulations that include both feedback and radiative cooling.

Key words: galaxies: clusters: general, galaxies: clusters: intracluster medium, galaxies: distances and redshifts, X-rays: galaxies: clusters, cosmology: miscellaneous

1 INTRODUCTION

Clusters of galaxies are the largest coherent gravitationally bound objects in our Universe. By studying galaxy clusters, information

* E-mail: swilson072@gmail.com

† E-mail: hiltonm@ukzn.ac.za

can be gained about the formation of galaxies, and the effect of on-going processes such as merging and AGN feedback. They can also be used as a probe of cosmology by studying the evolution of their number density with mass and redshift (e.g., Vikhlinin et al. 2009; Hasselfield et al. 2013; Reichardt et al. 2013; Planck Collaboration et al. 2015). However, the mass of galaxy clusters is not a quantity that can be directly measured, and therefore it needs to be determined using observable mass tracers such as X-ray properties (e.g., luminosity and temperature), the Sunyaev-Zel'dovich (SZ) effect signal, and optical properties, such as richness, line-of-sight velocity dispersion of member galaxies, and shear due to gravitational lensing (e.g., Ortiz-Gil et al. 2004; Vikhlinin et al. 2006; Rozo et al. 2009; Sifón et al. 2013; Nastasi et al. 2014; von der Linden et al. 2014; Hoekstra et al. 2015).

Scaling relations are power laws between galaxy cluster properties that have the potential to allow us to measure the mass of clusters using easily observable properties such as the X-ray Luminosity, X-ray Temperature and the velocity dispersion. These power laws can be predicted if we assume clusters are formed in the manner described by Kaiser (1986). In this model, known as the self-similar model, all galaxy clusters and groups are essentially identical objects which have been scaled up or down (Maughan et al. 2012). Strong self-similarity refers to when galaxy clusters have been scaled by mass and weak self-similarity refers to a scaling due to the changing density of the Universe with redshift (Bower 1997). This model makes some key assumptions, as described by Kravtsov & Borgani (2012) and Maughan et al. (2012). The first assumption is that we are in an Einstein-de-Sitter Universe, $\Omega_m = 1$, so the clusters form via a single gravitational collapse at the observed redshift. Secondly, gravitational energy as a result of the collapse is the only source of energy to the intracluster medium (ICM). By introducing these assumptions we greatly simplify the problem so that properties of the density field depend on only two control parameters, the slope of the power spectrum of the initial perturbations and its normalisation. The strong self-similarity determines the slope and is not expected to evolve with redshift while the weak self-similarity is responsible for the evolution of the normalisation since in this simplified model it is due only to a change in density with redshift (Bryan & Norman 1998).

The most commonly studied scaling relation is the luminosity – temperature relation ($L_X - T$), however there is still no consensus on how it evolves with redshift and if self-similarity holds. Some studies have found that the evolution of the normalisation of this relation is consistent with self-similarity (e.g., Vikhlinin et al. 2002; Lumb et al. 2004; Maughan et al. 2006), while other studies have found zero or negative evolution (e.g., Ettori et al. 2004; Branchesi et al. 2007; Hilton et al. 2012; Clerc et al. 2012, 2014). Maughan et al. (2012) also found that the evolution of the $L_X - T$ relation was not self-similar, but concluded that this could plausibly be explained by selection effects.

In this paper we focus on the lesser studied relationship between the velocity dispersion of member galaxies (σ_v) and the X-ray temperature (T_X) of the ICM. Since the velocity dispersion is a measure of the kinetic energy of the galaxies in the cluster, and temperature is related to the kinetic energy of the gas, both the gas and galaxies are tracers of the gravitational potential. One would expect a self-similar relationship of the form $\sigma_v \propto T^{0.5}$, if clusters were formed purely due to the action of gravity (Quintana & Melnick 1982; Kaiser 1986; Voit 2005). However, almost all previous studies of the relation have found a steeper power-law slope than this (see Table 1). The relation is also not expected to evolve with redshift. To date this has been tested only by Wu et al. (1998) and

Nastasi et al. (2014). Even then, all but four clusters in the Wu et al. (1998) sample are at $z < 0.5$. Nastasi et al. (2014) made a measurement of the relation at $0.6 < z < 1.5$ using a sample of 12 clusters, obtaining results consistent with previous studies at low redshift.

One may expect evolution in cluster scaling relations due to the increase of star formation and AGN activity at high redshift (e.g., Silverman et al. 2005; Magnelli et al. 2009), or due to the increase in frequency of galaxy cluster mergers with increasing redshift (e.g., Cohn & White 2005; Kay et al. 2007; Mann & Ebeling 2012). Galaxy cluster mergers are among the most energetic events in the Universe, and simulations have shown that these could result in the boosting of cluster X-ray temperatures (e.g., Ritchie & Thomas 2002; Randall et al. 2002; Poole et al. 2007). Figure 9 in Ritchie & Thomas (2002) shows how the temperature is boosted when two equal mass systems have a head on collision with varying initial distances between their centres. All of these processes add energy into the ICM, and so we might expect to see an overall increase in the average temperatures of galaxy clusters above that expected from the self-similar case at a given redshift.

In this paper, we study a sample of 38 $z < 1.0$ galaxy clusters drawn from the XMM Cluster Survey (XCS; Mehrrens et al. 2012). We divide the sample into two groups: a low redshift sample ($0.0 < z < 0.5$), and a high redshift sample ($0.5 < z < 1.0$), such that each group has an equal number of clusters in each, and then proceed to test for evolution in the $\sigma_v - T$ relation. We describe the sample and processing of the optical and X-ray data in Section 2. Section 3 discusses the method used to determine cluster membership and for measuring the velocity dispersion and describes the methods used for fitting the $\sigma_v - T$ relation, and we present our results in Section 4. We discuss our findings in Section 5 and present our conclusions in Section 6.

We assume a cosmology with $\Omega_m = 0.27$, $\Omega_\Lambda = 0.73$, and $H_0 = 70 \text{ km s}^{-1} \text{ Mpc}^{-1}$ throughout.

2 SAMPLE AND DATA REDUCTION

The cluster sample for this work is drawn from XCS, a serendipitous X-ray cluster survey being conducted using archival XMM-Newton data. Data Release 1 (DR1) of the XCS is described in Mehrrens et al. (2012). The overall aims of the XCS project are to measure cosmological parameters through the evolution of the cluster mass function with redshift (Sahlén et al. 2009), study the evolution of galaxies in clusters (Collins et al. 2009; Hilton et al. 2009, 2010; Stott et al. 2010) and investigate the X-ray scaling relations as a way to study the evolution of the cluster gas with redshift (Hilton et al. 2012).

The XCS Automated Pipeline Algorithm (XAPA) described in Lloyd-Davies et al. (2011) was used to search the XMM archive for cluster candidates. Mehrrens et al. (2012) describes confirmation of a subset of these candidates as clusters using the combination of data from the literature and optical follow-up observations. This left a final sample of 503 X-ray confirmed galaxy clusters, 255 which were previously unknown and 356 of which were new X-ray detections. Of these, 464 have redshift estimates, and 402 have temperature measurements.

For XCS-DR1 the cluster-averaged X-ray temperatures (T_X) were measured using an automated pipeline described in detail in Lloyd-Davies et al. (2011). In summary this pipeline operates as follows: spectra were generated in the 0.3-7.9 keV band using photons in the XAPA source ellipse, (where the XAPA ellipse corresponds 0.08 – 0.56 of R500, with a median value of 0.36 R500,

Table 1. Previous measurements of the velocity dispersion–temperature relation. Here the relation is in the form $\sigma_v = 10^A T^B$, where σ_v is measured in km s^{-1} and T is measured in keV.

Paper	Number of clusters	A	B	Redshift range	Fitting method
Edge & Stewart (1991)	23	2.60 ± 0.08	0.46 ± 0.12	$z < 0.1$	Least squares
Lubin & Bahcall (1993)	41	2.52 ± 0.07	0.60 ± 0.11	$z < 0.2$	χ^2
Bird et al. (1995)	22	2.50 ± 0.09	0.61 ± 0.13	$z < 0.1$	Bisector
Girardi et al. (1996)	37	2.53 ± 0.04	0.61 ± 0.05	$z < 0.2$	Bisector
Ponman et al. (1996)	27	2.54 ± 0.04	0.55 ± 0.05	$z < 0.15$	Bisector
White et al. (1997)	35	2.53 ± 0.08	0.60 ± 0.10	$z < 0.2$	Orthogonal
Wu et al. (1998)	94	2.47 ± 0.06	0.67 ± 0.09	$z < 0.9$	Orthogonal
Wu et al. (1998)	110	2.57 ± 0.03	0.49 ± 0.05	$z < 0.1$	Orthogonal
Wu et al. (1998)	39	2.57 ± 0.08	0.56 ± 0.09	$0.1 < z < 0.9$	Orthogonal
Wu et al. (1999)	92	2.49 ± 0.03	0.64 ± 0.02	$z < 0.45$	Orthogonal
Xue & Wu (2000)	109	2.53 ± 0.03	0.58 ± 0.05	$z < 0.2$	Orthogonal
Nastasi et al. (2014)	12	2.47 ± 0.19	0.64 ± 0.34	$0.64 < z < 1.46$	Bisector

where R_{500} is calculated using Equation 2 and Table 2 from Arnaud et al. (2005); an in-field background subtraction method was used; and model fitting was done inside XSPEC (Schafer 1991) using an absorbed MEKAL (Mewe & Schrijver 1986) model and Cash statistics (Cash 1979). In the fit, the hydrogen column density was fixed to the Dickey (1990) value and the metal abundance to 0.3 times the Solar value. For this paper we have updated the T_X values compared to Mehrtens et al. (2012). The pipeline is very similar to that described in Lloyd-Davies et al. (2011), but using updated versions of the XMM calibration and XSPEC. The median X-ray count for all the clusters in our final sample was 1919 with a minimum count of 220. We note that for only 1 of the clusters in our sample are the X-ray counts used for the spectral analysis less than 300. This is the minimum threshold defined by Lloyd-Davies et al. (2011) for reliable, i.e. with a fractional error of < 0.4 , T_x measurements at $T_x > 5\text{keV}$ (See Figure 16 from Lloyd-Davies et al. (2011)). The remaining cluster was fit using 220 counts, but has a temperature of 3.5keV (so still has an expected fractional error of 0.4)

For this paper both the samples were constructed from XCS DR1, except for one of the high redshift sample clusters (XMMXCS J113602.9-032943.2) which is a previously unreported XCS cluster detection. Fig. 1 shows the redshift and temperature distributions of the two samples. The high redshift sample contains more high temperature clusters than the low redshift sample, which may be due to selection effects which result in higher luminosity and hence higher temperature clusters being chosen at higher redshift.

2.1 Low redshift sample

The low redshift sample contains 19 clusters whose properties can be found in Table 3. In order to obtain this sample we excluded all clusters from the DR1 sample that did not have temperatures or which had a redshift $z > 0.5$, leaving us with a sample of 320 clusters. We performed a search in NED¹ for galaxies surrounding each cluster. We included only clusters which had spectroscopic redshifts resulting in our sample size being decreased from 320 to 296. Since NED collects data from many different sources the reliability of the redshifts can not be guaranteed. Hence, where possible

¹ This research has made use of the NASA/IPAC Extragalactic Database (NED) which is operated by the Jet Propulsion Laboratory, California Institute of Technology, under contract with the National Aeronautics and Space Administration.

we use only one source of redshifts per cluster to ensure homogeneity. These redshifts are specified to the 4th decimal place but unfortunately for most an uncertainty is not included in the original sample and therefore we assumed an accuracy of 1%.

We excluded galaxies located at a projected radial distance $> R_{200}$ (the radius within which the mean density is 200 times the critical density of the Universe at the cluster redshift) as such galaxies are unlikely to be cluster members. To ensure we did not exclude possible members, for this initial step R_{200} was calculated using a fiducial velocity dispersion of 2000 km s^{-1} following Finn et al. (2005),

$$R_{200} (\text{Mpc}) = 2.47 \frac{\sigma_v}{1000\text{ km s}^{-1}} \frac{1}{\sqrt{\Omega_\Lambda + \Omega_0(1+z)^3}}. \quad (1)$$

Here σ_v is the line of sight velocity dispersion (see Section 3.1.3) and z is the redshift of the cluster. Equation 1 assumes that the galaxy velocity distribution follows an isothermal sphere dark matter profile. The fiducial R_{200} values span the range 2–4 Mpc. Section 3.1.2 below describes how this initial cluster membership selection was refined to give the final cluster members. We then excluded all clusters which had less than 10 galaxies as this would provide us with too few members for accurate velocity dispersion calculation leaving us with a sample size of 19 clusters.

2.2 High redshift sample

The high redshift sample is made up of 19 clusters whose properties can be found in Table 4. Member redshifts were determined from observations using the Gemini telescopes for 12 of these clusters (see Section 2.2.1). The other seven clusters used data obtained from Nastasi et al. (2014). They drew both on new observations and on existing data. For example, the observations of three of the Nastasi et al. (2014) clusters we have used in this paper (XMMXCS J105659.5-033728.0, XMMXCS J113602.9-032943.2 and XMMXCS J182132.9+682755.0 in Table 4) were presented in Tran et al. (1999) respectively. The observations of the other 4 clusters we have used in this paper were presented for the first time in Nastasi et al. (2014). These four were discovered independently (to XCS) by the XMM Newton Distant Cluster Project (XDCP; Fassbender et al. 2011). Nastasi et al. (2014) also presented galaxy redshift data for another six XDCP clusters, however we have not used those in this paper because there are insufficient galaxies to derive

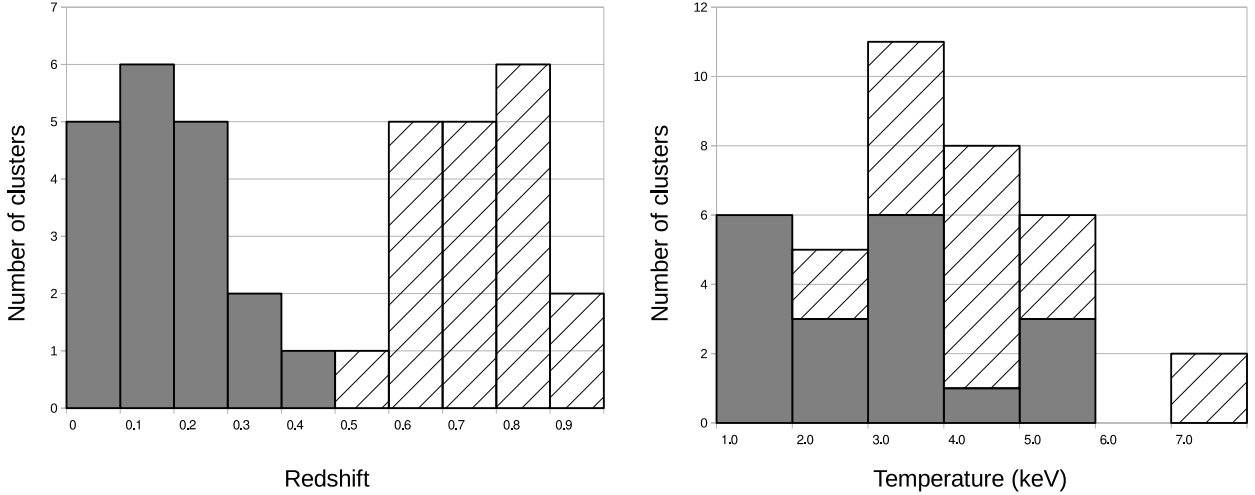


Figure 1. The redshift and temperature distributions of the low and high redshift cluster samples used in this work. The solid grey marks the low redshift sample ($z < 0.5$) and the shading with diagonal lines marks the high redshift sample ($z > 0.5$). Note that the high redshift sample ($T_{\text{median}} = 4.5$ keV) contains more high temperature clusters than the low redshift sample ($T_{\text{median}} = 3.0$ keV).

an accurate velocity dispersion². For the seven clusters that relied on [Nastasi et al. \(2014\)](#) data, new temperatures were obtained using XCS pipelines and the velocity dispersion was recalculated using the [Nastasi et al. \(2014\)](#) cluster redshift together with the method described in Section 3.

2.2.1 Observations

Observations of 12 $z > 0.5$ clusters were obtained using the Gemini Multi Object Spectrographs (GMOS) on both the Gemini telescopes from 2010 to 2012. The nod-and-shuffle mode ([Glazebrook & Bland-Hawthorn 2001](#)) was used to allow better sky subtraction and shorter slit lengths when compared to conventional techniques. For all observations the R400 grating and OG515 order blocking filter were used, giving wavelength coverage of 5400 – 9700 Å. The GMOS field of view samples out to R200 at the redshifts of our sample [Sifón et al. \(2013\)](#). A total of 30 masks were observed with a varying number of target slitlets. Each slitlet had length 3'' and width 1''. Target galaxies were selected to be fainter than the brightest cluster galaxy (which was also targeted in the slit masks), on the basis of *i*-band pre-imaging obtained from Gemini. We also used colour or photo-*z* information, where available, to maximise our efficiency in targeting cluster members. For five clusters which had *r*, *z*-band photometry from the National Optical Astronomy Observatory–XMM Cluster Survey (NXS; described in [Mehrtens et al. 2012](#)), we preferentially selected galaxies with *r* – *z* colours expected for passively evolving galaxies at the cluster redshift (see [Mehrtens et al. 2012](#), for details). For four clusters, we used photometric redshifts for galaxies from SDSS DR7 ([Abazajian et al. 2009](#)). For XMMXCS J113602.9-032943.2, we used galaxy photo-*z*s that were measured from our own *riz* photometry obtained at the William Herschel Telescope (WHT) on 2011 May 5. Observations at three different central wavelengths (7500, 7550 and 7600 Å) were used to obtain coverage over the gaps between the GMOS CCDs. For all observations an 85 percentile image quality and 50

percentile sky transparency were requested. The details of the individual observations are given in Table A1.

2.2.2 Spectroscopic data reduction

The data were reduced in a similar manner to [Hilton et al. \(2010\)](#), using PYRAF and the Gemini IRAF² package. We used the tools from this package to subtract bias frames; make flat fields; apply flat field corrections and create mosaic images. We then applied nod-and-shuffle sky subtraction using the `gnsksysub` task. Wavelength calibration was determined from arc frames taken between the science frames, using standard IRAF tasks. All data were then combined using a median, rejecting bad pixels using a mask constructed from the nod-and-shuffle dark frames. Finally, we combined the pairs of spectra corresponding to each nod position, and extracted one-dimensional spectra using a simple boxcar algorithm.

2.2.3 Galaxy redshift measurements

We measured galaxy redshifts from the spectra by cross-correlation with SDSS spectral templates³ using the RVSAO/XCSAO package for IRAF ([Kurtz & Mink 1998](#)). XCSAO implements the method described by [Tonry & Davis \(1979\)](#). The spectra were compared to six different templates over varying redshifts with the final redshift measurement being determined after visual inspection. Redshifts were assigned a quality flag according to the following scheme: $Q = 3$ corresponds to two or more strongly detected features; $Q = 2$ refers to one strongly detected or two weakly detected features; $Q = 1$ one weakly detected feature and $Q = 0$ when no features could be identified. The features used were spectral lines, with the most commonly identified being [OII] 3727 Å, H, K, H β , and the [OIII] 4959, 5007 Å lines. Only galaxies with a quality rating of

² The methodology described in Section 3 was applied to these six clusters before they were excluded from our study.

² IRAF is distributed by the National Optical Astronomy Observatories, which are operated by the Association of Universities for Research in Astronomy, Inc., under cooperative agreement with the National Science Foundation.

³ <http://www.sdss.org/dr7/algorithms/spectemplates/index.html>

$Q \geq 2$ were used in this study because these have reasonably secure redshifts. Fig. 2 shows spectra of some member galaxies of the cluster XMMXCS J025006.4-310400.8 as an example. Tables of redshifts for galaxies in each cluster field as well as histograms depicting the included/excluded members and the best-fit Gaussian¹⁶ can be found in Appendix B.

Table 2 is shown, as an example, below for cluster XMMXCS J025006.4-310400.8.

3 ANALYSIS

3.1 Membership determination and velocity dispersion measurements

In this section we describe the methodology used to determine cluster membership and calculate the velocity dispersion of each cluster.

3.1.1 Cluster redshifts

For all of the clusters an estimate of the redshift is known either from the literature or from previous observations and this is used as a starting point. The peculiar velocity of each of the galaxies is calculated relative to this redshift estimate using

$$v_i = c \times \frac{z_i - \bar{z}}{1 + \bar{z}}, \quad (2)$$

where v_i is the peculiar velocity of the i th galaxy, z_i is the redshift of the i th galaxy, \bar{z} is the redshift of the cluster and c is the speed of light. Extreme foreground and background sources were removed by applying a 3000 km s^{-1} cut with respect to the cluster redshift and then the redshift was recalculated using the biweight location method described by Beers et al. (1990). This process was iterated until the redshift converged.

3.1.2 Cluster membership

A fixed gapper method, similar to that of Fadda et al. (1996) and Crawford et al. (2014), was applied to determine which galaxies are cluster members. The reasoning behind this method is that by studying a histogram of the redshifts of possible members there should be a clear distinction between the cluster and the fore/background galaxies. Therefore we can exclude interlopers by finding the velocity difference between adjacent galaxies and setting a fixed gap that should not be exceeded. De Propriis et al. (2002) found this optimum gap to be 1000 km s^{-1} , which avoids the merging of subclusters but also prevents the breaking up of real systems into smaller groups. Therefore all our galaxies were sorted by peculiar velocity and the difference between all adjacent pairs was calculated. Any galaxies which had a difference between adjacent galaxies of greater than 1000 km s^{-1} were considered interlopers and were removed. This process was iterated until the number of galaxies converged.

3.1.3 Velocity dispersion

We used our confirmed galaxy cluster members to calculate an initial estimate of the velocity dispersion of each cluster using the biweight scale method described in Beers et al. (1990). We then calculated R_{200} using Equation 1, and excluded all galaxies located

at projected cluster-centric radial distances outside R_{200} . The velocity dispersion of each cluster was then recalculated. This final radial cut did not remove more than two galaxies from the final sample for each cluster. Tables 3 and 4 list the final redshifts, velocity dispersions, and R_{200} values for the low and high redshift samples respectively.

3.2 Fitting the velocity dispersion – temperature relation

To determine the scaling relation between the velocity dispersion and temperature, we fitted a power law of the form

$$\log \left(\frac{\sigma_v}{1000 \text{ km s}^{-1}} \right) = A + B \log \left(\frac{T}{5 \text{ keV}} \right) + C \log E(z). \quad (3)$$

Here, 5 keV and 1000 km s^{-1} are the pivot temperature and velocity dispersion respectively for our fit. These were chosen to reduce the covariance between the normalisation A and the slope B , and for ease of comparison to previous studies. In the above, evolution of the normalisation is parametrised as $E(z)^C$, where $E(z) = \sqrt{\Omega_m(1+z)^3 + \Omega_\Lambda}$ describes the redshift evolution of the Hubble parameter. For the self similar case, $B = 0.5$ and $C = 0$ are expected.

Similarly to Hilton et al. (2012), the best fit values for these parameters were found using Markov Chain Monte-Carlo (MCMC) with the Metropolis algorithm. Both orthogonal and bisector regression methods were used. For the orthogonal method, the probability for a given cluster to be drawn from the model scaling relation is

$$P_{\text{model}} = \frac{1}{\sqrt{2\pi}(\Delta r^2 + \Delta S^2)} \exp \left[\frac{-(r - r_{\text{model}})^2}{2(\Delta r^2 + S^2)} \right], \quad (4)$$

where $r - r_{\text{model}}$ is the orthogonal distance of the cluster from the model relation, Δr is the error on the orthogonal distance and S is the intrinsic scatter orthogonal to the model relation. Δr is calculated from the projection in the direction orthogonal to the model line of the ellipse defined by the errors on $\log \sigma_v$ and $\log T$, chosen according to the position of a given point relative to the model fit line. For the bisector method, the intrinsic scatter and measurement errors are treated independently for each axis. Therefore in the equation for P_{model} , r_{model} is replaced by

$$y_{\text{model}} = \log \left(\frac{\sigma_v}{1000 \text{ km s}^{-1}} \right) - \left[A + B \log \left(\frac{T}{5 \text{ keV}} \right) + C \log E(z) \right], \quad (5)$$

and

$$x_{\text{model}} = \log \left(\frac{T}{5 \text{ keV}} \right) - \left[\frac{\log \left(\frac{\sigma_v}{1000 \text{ km s}^{-1}} \right) - A - C \log E(z)}{B} \right], \quad (6)$$

where r and Δr are replaced by x , Δx or y , Δy as appropriate. The intrinsic scatter S is replaced by two parameters S_x and S_y .

For both methods, the likelihood \mathcal{L} of a given model is simply the product of P_{model} for each cluster in the sample, i.e., in the orthogonal case

$$\mathcal{L}(\sigma_v, T | A, B, C, S) \propto P_{\text{prior}}(A, B, C, S) \prod_i P_{\text{model}, i}, \quad (7)$$

where we assume generous, uniform priors on each parameter, as listed in Table 5.

ID	Mask	RA(J2000)	Dec(J2000)	z	Quality	Member
1	GS-2010B-Q-46-06	02 ^h 50 ^m 22.92 ^s	-31°03′53.0″	0.8337	3	
8	GS-2010B-Q-46-06	02 ^h 50 ^m 15.25 ^s	-31°03′33.5″	0.7263	3	
9	GS-2010B-Q-46-06	02 ^h 50 ^m 13.27 ^s	-31°03′35.7″	0.6168	3	
10	GS-2010B-Q-46-06	02 ^h 50 ^m 12.05 ^s	-31°03′08.0″	0.7146	3	
14	GS-2010B-Q-46-06	02 ^h 50 ^m 06.63 ^s	-31°03′13.7″	0.8496	3	
15	GS-2010B-Q-46-06	02 ^h 50 ^m 08.70 ^s	-31°03′49.7″	0.9052	3	✓
16	GS-2010B-Q-46-06	02 ^h 50 ^m 03.78 ^s	-31°03′51.5″	0.3533	3	
17	GS-2010B-Q-46-06	02 ^h 50 ^m 06.89 ^s	-31°03′51.5″	0.9217	3	✓
18	GS-2010B-Q-46-06	02 ^h 50 ^m 05.48 ^s	-31°03′53.0″	0.6972	3	
19	GS-2010B-Q-46-06	02 ^h 50 ^m 04.50 ^s	-31°03′51.5″	0.9149	3	✓
21	GS-2010B-Q-46-06	02 ^h 50 ^m 02.79 ^s	-31°04′04.9″	0.9831	3	
22	GS-2010B-Q-46-06	02 ^h 50 ^m 06.48 ^s	-31°03′56.9″	0.9069	3	✓
23	GS-2010B-Q-46-06	02 ^h 50 ^m 09.04 ^s	-31°04′06.3″	0.7567	3	
25	GS-2010B-Q-46-06	02 ^h 50 ^m 03.83 ^s	-31°04′34.0″	0.8988	3	✓
26	GS-2010B-Q-46-06	02 ^h 50 ^m 04.24 ^s	-31°04′50.6″	0.9095	3	✓
28	GS-2010B-Q-46-06	02 ^h 50 ^m 04.59 ^s	-31°05′41.7″	0.6197	3	
34	GS-2010B-Q-46-06	02 ^h 50 ^m 04.26 ^s	-31°07′05.2″	0.1261	3	
1	GS-2012B-Q-011-09	02 ^h 50 ^m 22.92 ^s	-31°03′53.0″	0.5924	2	
2	GS-2012B-Q-011-09	02 ^h 50 ^m 18.11 ^s	-31°03′10.5″	0.9326	2	
4	GS-2012B-Q-011-09	02 ^h 50 ^m 16.05 ^s	-31°03′23.1″	1.0077	2	
5	GS-2012B-Q-011-09	02 ^h 50 ^m 14.89 ^s	-31°03′32.1″	0.7245	3	
6	GS-2012B-Q-011-09	02 ^h 50 ^m 14.94 ^s	-31°02′56.8″	0.9927	2	
9	GS-2012B-Q-011-09	02 ^h 50 ^m 08.98 ^s	-31°03′01.1″	0.9086	3	✓
10	GS-2012B-Q-011-09	02 ^h 50 ^m 10.24 ^s	-31°03′27.8″	0.9056	3	✓
11	GS-2012B-Q-011-09	02 ^h 50 ^m 07.01 ^s	-31°01′00.9″	0.5204	3	
13	GS-2012B-Q-011-09	02 ^h 50 ^m 06.54 ^s	-31°03′44.7″	0.9126	3	✓
17	GS-2012B-Q-011-09	02 ^h 50 ^m 03.99 ^s	-31°03′53.0″	0.9176	3	✓
18	GS-2012B-Q-011-09	02 ^h 50 ^m 07.33 ^s	-31°04′10.6″	0.9106	3	✓
19	GS-2012B-Q-011-09	02 ^h 50 ^m 02.67 ^s	-31°03′26.0″	0.9797	3	
20	GS-2012B-Q-011-09	02 ^h 50 ^m 07.38 ^s	-31°05′28.7″	0.6494	2	
21	GS-2012B-Q-011-09	02 ^h 49 ^m 58.10 ^s	-31°03′39.6″	0.8696	3	✓
22	GS-2012B-Q-011-09	02 ^h 50 ^m 05.48 ^s	-31°04′40.5″	0.9026	2	
27	GS-2012B-Q-011-09	02 ^h 49 ^m 58.68 ^s	-31°05′25.8″	0.6274	3	
28	GS-2012B-Q-011-09	02 ^h 49 ^m 59.99 ^s	-31°05′07.8″	0.8816	2	
29	GS-2012B-Q-011-09	02 ^h 49 ^m 58.60 ^s	-31°04′59.2″	0.9216	3	✓
30	GS-2012B-Q-011-09	02 ^h 50 ^m 00.51 ^s	-31°04′44.5″	0.5654	3	
31	GS-2012B-Q-011-09	02 ^h 50 ^m 04.26 ^s	-31°07′05.2″	0.9827	3	

Table 2. We depict the galaxy redshifts for the cluster XMMXCS J025006.4-310400.8. Column 1 gives an arbitrary ID for each galaxy, column 2 and 3 give the right ascension and declination respectively, and column 4 gives the redshift of the galaxy. Column 5 gives the quality flag as explained in Section 2.2.3 and column 6 shows whether or not the galaxy was included as a member for the determination of the velocity dispersion.

4 RESULTS

4.1 Evolution of the slope and intrinsic scatter

For the model given in Equation 3, it is assumed that the slope (parameter B) is not evolving with redshift. To test this, the σ_v-T relation was fitted with $C = 0$ in two redshift bins, $0.0 < z < 0.5$ and $0.5 < z < 0.9$, with 19 clusters in each bin. The parameters A , B and S were obtained using the MCMC method described above for the high and low redshift samples individually. The results for this are shown in Fig. 3 and Fig. 4.

Using the orthogonal method we found $B = 1.12 \pm 0.41$ for the high redshift sample and $B = 0.89 \pm 0.16$ for the low redshift sample. However, we found that the slope of the relation for the high redshift sample is unconstrained if the prior on B is relaxed further. We assume for the remainder of this paper that the slope does not evolve with redshift, though clearly either a larger sample or more accurate measurements of individual clusters are needed to confirm that this is true.

The intrinsic scatter is $S = 0.05 \pm 0.02$ for the low redshift sample and $S = 0.08 \pm 0.04$ for the high redshift sample. Therefore there is no evidence that the intrinsic scatter varies with redshift.

4.2 Evolution of the normalisation

To test for the evolution of the normalisation (parameter A in Equation 3), the low and high redshift samples were combined and C was allowed to vary in the MCMC analysis. The results obtained are shown by the the scaling relation plot in Fig. 6. We found $C = -0.53 \pm 0.27$, meaning that for a given σ_v , a higher T is obtained at higher redshift. However, the no evolution relation falls within the 95 per cent confidence interval and therefore we conclude that there is no significant evidence in favour of evolution.

We also applied a statistical test known as the Akaike information criterion (AIC) to determine whether the model with or without evolution (Fig. 5) was preferred. The AIC estimates the quality of each model relative to each other and is therefore a means of model selection. It is defined by (Burnham & Anderson 2002) as

$$\text{AIC} = 2k - 2\ln(\mathcal{L}), \quad (8)$$

where \mathcal{L} is the maximised likelihood function (Equation 7) and k is the number of free parameters. The AIC includes a penalty for using extra parameters as a way to discourage overfitting and rewards goodness of fit based on the likelihood function. Therefore the lower the value of the AIC, the better the fit. For the combined

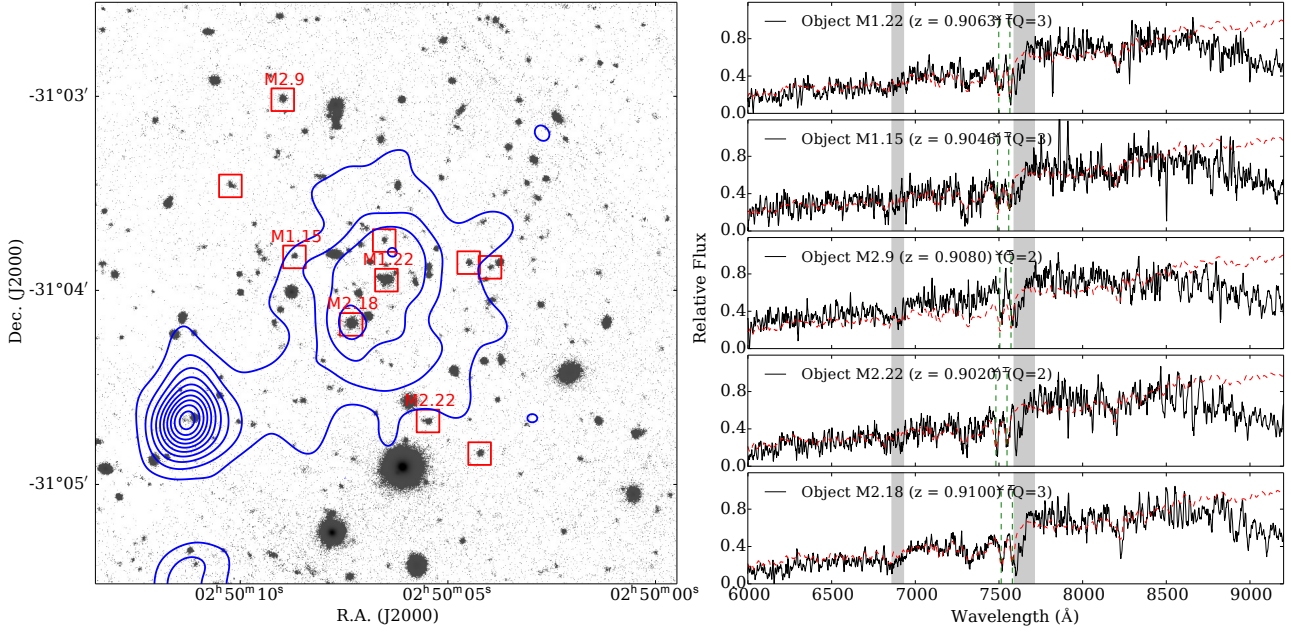


Figure 2. The $z=0.91$ cluster XMMXCS J025006.4 – 310400.8. The left hand panel shows the Gemini *i*-band image overlaid with the X–ray contours in blue. The red squares represent possible galaxy cluster members. Each possible member is labeled Mx.y, where x is the mask number and y is the object ID. The right hand panel shows the Gemini spectra (black lines) for a subset of these galaxies. The grey bands indicate regions affected by telluric absorption lines. The red line is the best fit SDSS template. The green dotted vertical lines show the positions of the H and K lines at the galaxy redshift.

Table 3. Low redshift sample ($0.0 < z < 0.5$): column 1 gives the name of the XCS Cluster, columns 2 and 3 give its J2000 right ascension and declination. Column 4 gives the redshift, with the uncertainty found using bootstrapping and column 5 gives the redshift from literature¹⁵. Column 6 gives the temperature with its positive and negative 1σ uncertainty. Column 7 gives the number of confirmed members and columns 8 and 9 give the calculated velocity dispersion and R_{200} respectively. The references for the redshifts are as follows: 1. [Mehrtens et al. \(2012\)](#) 2. [Cappi et al. \(1998\)](#) 3. [Yoon et al. \(2008\)](#) 4. [Mulchaey et al. \(2006\)](#) 5. [Vikhlinin et al. \(1998\)](#) 6. [Takey et al. \(2013\)](#) 7. [Finoguenov et al. \(2007\)](#) 8. [Takey et al. \(2011\)](#) 9. [Hao et al. \(2010\)](#) 10. [Hennawi et al. \(2008\)](#) 11. [Struble & Rood \(1999\)](#) 12. [Burenin et al. \(2007\)](#) 13. [Koester et al. \(2007\)](#) 14. [Mullis et al. \(2003\)](#) and 15. [Sakelliou & Merrifield \(1998\)](#)

Name	RA (J2000)	Dec (J2000)	z	z_{lit}	T (keV)	Members	σ_v (km s^{-1})	R_{200} (Mpc)
XMMXCS J000013.9-251052.1	00 ^h 00 ^m 13.9 ^s	-25° 10′ 52.1″	0.0845 ± 0.0004	0.08 ¹	$1.80^{+0.40}_{-0.20}$	19	410 ± 80	1.11
XMMXCS J003430.1-431905.6	00 ^h 34 ^m 30.1 ^s	-43° 19′ 05.6″	0.3958 ± 0.0010	0.40 ¹	$3.50^{+0.20}_{-0.20}$	22	920 ± 150	1.96
XMMXCS J005603.0-373248.0	00 ^h 56 ^m 03.0 ^s	-37° 32′ 48.0″	0.1659 ± 0.0009	0.16 ²	$5.20^{+0.30}_{-0.20}$	22	900 ± 140	2.06
XMMXCS J015315.0+010214.2	01 ^h 53 ^m 15.0 ^s	+01° 02′ 14.2″	0.0593 ± 0.0002	0.06 ³	$1.08^{+0.02}_{-0.02}$	12	240 ± 80	0.55
XMMXCS J072054.3+710900.5	07 ^h 20 ^m 54.3 ^s	+71° 09′ 00.5″	0.2309 ± 0.0005	0.23 ⁴	$2.90^{+0.50}_{-0.40}$	29	550 ± 60	1.20
XMMXCS J081918.6+705457.5	08 ^h 19 ^m 18.6 ^s	+70° 54′ 57.5″	0.2298 ± 0.0005	0.23 ⁵	$3.00^{+0.80}_{-0.60}$	19	410 ± 70	0.83
XMMXCS J094358.2+164120.7	09 ^h 43 ^m 58.2 ^s	+16° 41′ 20.7″	0.2539 ± 0.0005	0.25 ¹	$1.50^{+0.40}_{-0.20}$	27	590 ± 90	1.54
XMMXCS J095957.6+251629.0	09 ^h 59 ^m 57.6 ^s	+25° 16′ 29.0″	0.0523 ± 0.0005	0.08 ⁶	$1.40^{+0.20}_{-0.05}$	15	510 ± 220	1.79
XMMXCS J100047.4+013926.9	10 ^h 00 ^m 47.4 ^s	+01° 39′ 26.9″	0.2202 ± 0.0006	0.22 ⁷	$3.30^{+0.20}_{-0.20}$	16	560 ± 140	1.41
XMMXCS J100141.7+022539.8	10 ^h 01 ^m 41.7 ^s	+02° 25′ 39.8″	0.1233 ± 0.0005	0.12 ⁸	$1.43^{+0.06}_{-0.03}$	26	590 ± 130	1.05
XMMXCS J104044.4+395710.4	10 ^h 40 ^m 44.4 ^s	+39° 57′ 10.4″	0.1389 ± 0.0007	0.16 ⁹	$3.54^{+0.03}_{-0.03}$	17	860 ± 150	2.12
XMMXCS J111515.6+531949.5	11 ^h 15 ^m 15.6 ^s	+53° 19′ 49.5″	0.4663 ± 0.0010	0.47 ¹⁰	$5.40^{+1.50}_{-0.90}$	16	910 ± 310	1.75
XMMXCS J115112.0+550655.5	11 ^h 51 ^m 12.0 ^s	+55° 06′ 55.5″	0.0791 ± 0.0003	0.08 ¹¹	$1.66^{+0.04}_{-0.04}$	16	330 ± 100	1.50
XMMXCS J123144.4+413732.0	12 ^h 31 ^m 44.4 ^s	+41° 37′ 32.0″	0.1735 ± 0.0009	0.18 ¹²	$2.70^{+0.60}_{-0.40}$	10	480 ± 100	1.26
XMMXCS J151618.6+000531.3	15 ^h 16 ^m 18.6 ^s	+00° 05′ 31.3″	0.1200 ± 0.0005	0.13 ¹³	$5.40^{+0.10}_{-0.10}$	35	870 ± 220	2.01
XMMXCS J161132.7+541628.3	16 ^h 11 ^m 32.7 ^s	+54° 16′ 28.3″	0.3372 ± 0.0013	0.33 ⁸	$4.60^{+1.20}_{-0.80}$	12	790 ± 150	1.69
XMMXCS J163015.6+243423.2	16 ^h 30 ^m 15.6 ^s	+24° 34′ 23.2″	0.0625 ± 0.0003	0.07 ¹⁴	$3.50^{+0.60}_{-0.40}$	62	710 ± 130	2.20
XMMXCS J223939.3-054327.4	22 ^h 39 ^m 39.3 ^s	-05° 43′ 27.4″	0.2451 ± 0.0003	0.24 ¹⁴	$2.80^{+0.20}_{-0.20}$	68	560 ± 70	1.32
XMMXCS J233757.0+271121.0	23 ^h 37 ^m 57.0 ^s	+27° 11′ 21.0″	0.1237 ± 0.0007	0.12 ¹⁵	$3.40^{+0.60}_{-0.40}$	12	460 ± 110	1.49

Table 4. High redshift sample ($0.5 < z < 1.0$): all columns are as explained in Table 3. The superscripts in column one indicate the origin of redshift data when it did not come from our own observations. ¹ also known as MS1054-03 was observed with Keck for 8.6 hours (Tran et al. 1999). ² was observed with Keck (Donahue et al. 1999). ³ also known as RXJ1821.6+6827 was observed with CFHT, Keck and the 2.2 m telescope at the University of Hawaii (Gioia et al. 2004). ⁴ are all clusters taken from the XDCP survey and were observed with the VLT-FORS2 spectrograph (Nastasi et al. 2014). The references for the redshifts are as follows: 1. Nastasi et al. (2014) 2. Scharf et al. (1997) 3. Mehtens et al. (2012) 4. Adami et al. (2011) 5. Šuhada et al. (2011) 6. Bellagamba et al. (2011) 7. Gioia & Luppino (1994) 8. Basilakos et al. (2004) 9. Gioia et al. (2004) 10. Perlman et al. (2002)

Name	RA (J2000)	Dec (J2000)	z	z_{lit}	T (keV)	Members	σ_v (km s ⁻¹)	R_{200} (Mpc)
⁴ XMMXCS J000216.1-355633.8	00 ^h 02 ^m 16.1 ^s	-35°56′33.8″	0.7709 ± 0.0021	0.77 ¹	4.83 ^{+1.015} _{-0.76}	13	1100 ± 190	1.77
XMMXCS J005656.6-274031.9	00 ^h 56 ^m 56.6 ^s	-27°40′31.9″	0.5601 ± 0.0007	0.56 ²	3.30 ^{+0.94} _{-0.63}	15	380 ± 60	0.66
XMMXCS J015241.1-133855.9	01 ^h 52 ^m 41.1 ^s	-13°38′55.9″	0.8268 ± 0.0010	0.82 ³	3.23 ^{+0.38} _{-0.31}	29	840 ± 150	1.33
XMMXCS J021734.7-051326.9	02 ^h 17 ^m 34.7 ^s	-05°13′26.9″	0.6467 ± 0.0012	0.65 ⁴	2.23 ^{+0.90} _{-0.44}	12	620 ± 210	1.11
XMMXCS J025006.4-310400.8	02 ^h 50 ^m 06.4 ^s	-31°04′00.8″	0.9100 ± 0.0024	0.90 ²	4.50 ^{+1.33} _{-0.88}	13	1120 ± 260	1.66
XMMXCS J030205.1-000003.6	03 ^h 02 ^m 05.1 ^s	-00°00′03.6″	0.6450 ± 0.0007	0.65 ⁵	5.82 ^{+2.09} _{-1.32}	16	610 ± 180	1.04
⁴ XMMXCS J095417.1+173805.9	09 ^h 54 ^m 17.1 ^s	17°38′05.9″	0.8272 ± 0.0017	0.82 ¹	3.65 ^{+0.62} _{-0.51}	10	940 ± 310	1.42
XMMXCS J095940.7+023113.4	09 ^h 59 ^m 40.7 ^s	+02°31′13.4″	0.7291 ± 0.0005	0.72 ⁶	5.02 ^{+0.68} _{-0.55}	25	470 ± 90	0.88
¹ XMMXCS J105659.5-033728.0	10 ^h 56 ^m 59.5 ^s	-03°37′28.0″	0.8336 ± 0.0013	0.82 ⁷	7.57 ^{+0.43} _{-0.40}	29	1010 ± 120	1.57
XMMXCS J112349.4+052955.1	11 ^h 23 ^m 49.4 ^s	+05°29′55.1″	0.6550 ± 0.0007	0.65 ³	4.62 ^{+1.55} _{-0.95}	17	600 ± 210	1.05
XMMXCS J113602.9-032943.2	11 ^h 36 ^m 02.9 ^s	-03°29′43.2″	0.8297 ± 0.0011		3.32 ^{+1.20} _{-0.78}	21	700 ± 110	1.06
² XMMXCS J114023.0+660819.0	11 ^h 40 ^m 23.9 ^s	+66°08′19.0″	0.7855 ± 0.0015	0.78 ⁷	7.47 ^{+0.92} _{-0.77}	22	950 ± 100	1.51
⁴ XMMXCS J124312.2-131307.2	12 ^h 43 ^m 12.2 ^s	-13°13′07.2″	0.7910 ± 0.0014	0.80 ¹	4.92 ^{+2.93} _{-1.54}	11	790 ± 460	1.19
XMMXCS J134305.1-000056.8	13 ^h 43 ^m 05.1 ^s	-00°00′56.8″	0.6894 ± 0.0011	0.67 ⁸	4.49 ^{+0.72} _{-0.57}	23	920 ± 170	1.72
XMMXCS J145009.3+090428.8	14 ^h 50 ^m 09.3 ^s	+09°04′28.8″	0.6412 ± 0.0007	0.60 ³	3.84 ^{+0.66} _{-0.55}	22	630 ± 90	1.07
³ XMMXCS J182132.9+682755.0	18 ^h 21 ^m 32.9 ^s	+68°27′55.0″	0.8166 ± 0.0011	0.82 ⁹	4.49 ^{+0.79} _{-0.56}	19	860 ± 130	1.34
XMMXCS J215221.0-273022.6	21 ^h 52 ^m 21.0 ^s	-27°30′22.6″	0.8276 ± 0.0011	0.82 ³	2.18 ^{+0.67} _{-0.45}	15	530 ± 150	0.86
XMMXCS J230247.7+084355.9	23 ^h 02 ^m 47.7 ^s	+08°43′55.9″	0.7187 ± 0.0014	0.72 ¹⁰	5.29 ^{+0.59} _{-0.50}	22	1010 ± 130	1.60
⁴ XMMXCS J235616.4-344144.3	23 ^h 56 ^m 16.4 ^s	-34°41′44.3″	0.9391 ± 0.0012	0.94 ¹	4.57 ^{+0.48} _{-0.41}	10	670 ± 260	0.91

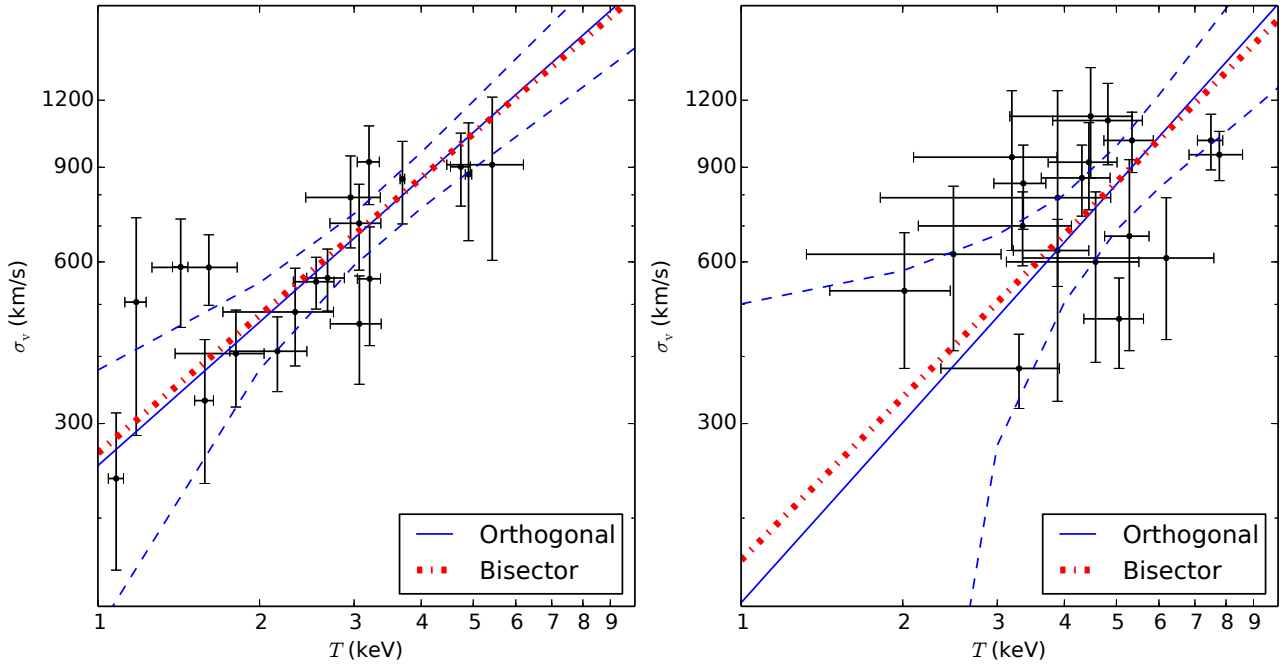


Figure 3. The σ_v – T relation assuming no evolution, i.e., $C = 0$ in Equation 3, for low (left - $0.0 < z < 0.5$) and high (right - $0.5 < z < 0.9$) redshift samples. The solid blue line shows an orthogonal regression fit to the data with the dashed line representing the 95 % confidence interval. The dot-dashed line shows a bisector regression fit to the data (see Section 3.2). A model of the form seen in Equation 3 was used in the Metropolis algorithm to determine a line of best-fit. (see Section 4.1). It is interesting to note that the two best-measured systems (XMMXCS J105659.5-033728.0 and XMMXCS J114023.0+660819.0) in the high-redshift subsample are relatively far off the best-fit relation, with a higher than predicted temperature. Our current observations do not provide good enough spatial resolution or deep enough multi-colour photometry to determine the exact reason for this and require further study and re-observations.

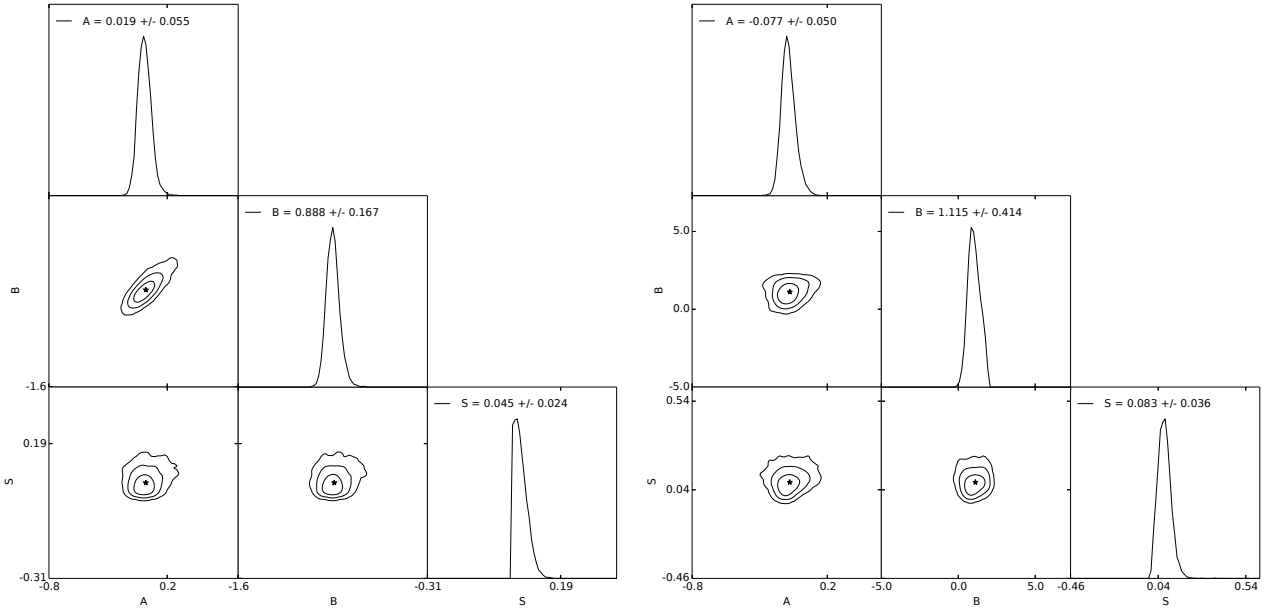


Figure 4. Corner plots for the low (left - $0.0 < z < 0.5$) and high (right- $0.5 < z < 0.9$) redshift sample showing all the one and two dimensional projections of the posterior probability distributions of the three parameters when using the orthogonal method. The values of each parameter are given in the top centre. The histograms show the one dimensional marginalised distribution for each parameter and the other plots show the 2 dimensional version, where the contours show 1,2 and 3 σ .

Table 5. Priors on $\sigma_v - T$ relation fit parameters

Parameter	Uniform Prior	Notes
A	(-5.0,5.0)	-
B	(0.0,2.0)	-
C	(-1.0,1.0)	-
S	(0.01,1.0)	Orthogonal method only
S_x	(0.01,1.0)	Bisector method only
S_y	(0.01,1.0)	Bisector method only

sample with the no evolution model the AIC value was -64.6 and when the fourth parameter for evolution (C) was included this increased to -62.1. Therefore, combining this with the results from the $\sigma_v - T$ relation fit, it can be concluded that the preferred model is the one with no evolution of the normalisation of the scaling relation.

5 DISCUSSION

5.1 Comparison with previous results

Table 6 and Figs.3–6 present the results of applying the orthogonal and bisector fitting methods to the low redshift, high redshift, and combined samples. We see that the bisector and orthogonal method give very similar results especially for our total sample without evolution. Hogg et al. (2010) suggests that the bisector method should be avoided, as by simply finding the difference between a forward and reverse fitting method large systematic errors will be introduced, but it has been widely used for scaling relation measurements in the past and is therefore included for completeness.

Results from previous studies of the $\sigma_v - T$ relation are collected in Table 1. All of these studies, except for Edge & Stewart

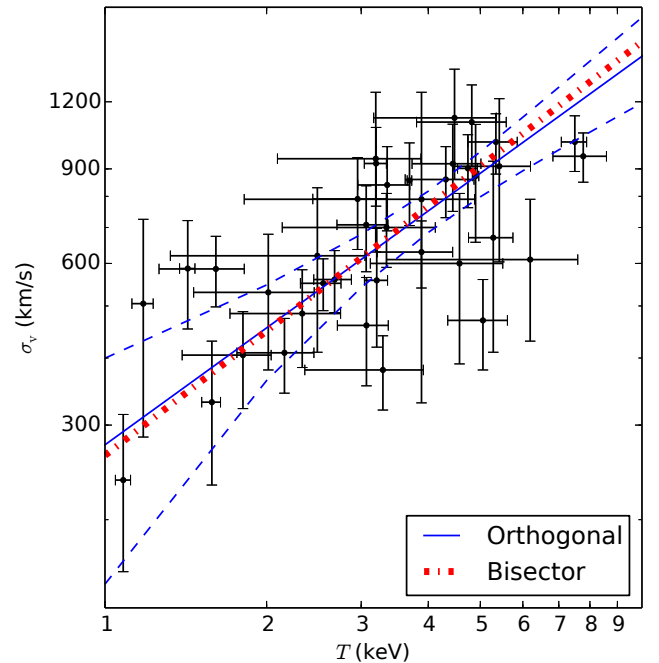
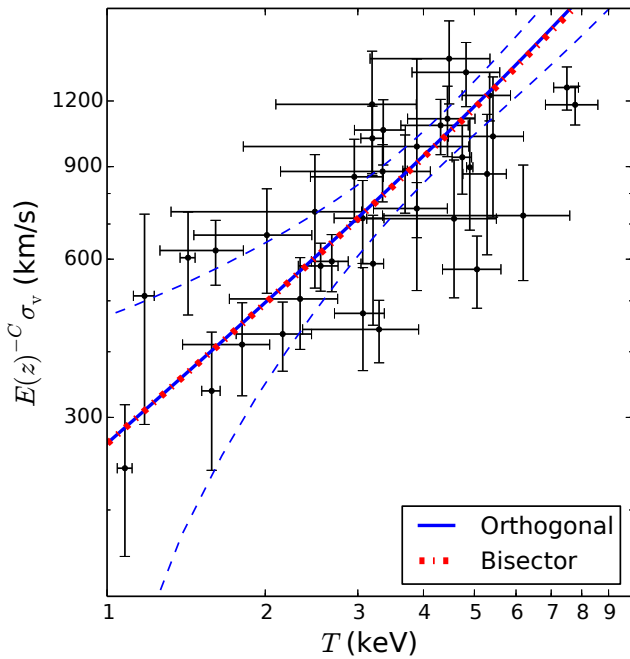


Figure 5. The $\sigma_v - T$ relation assuming no evolution, i.e. $C = 0$ in Equation 3, for the combined sample. All lines are as explained in Fig. 3.

(1991) and the low redshift sample of Wu et al. (1998), obtained a slope steeper than the expected self-similar slope of $\sigma_v \propto T^{0.5}$. We measured $B = 0.72 \pm 0.12$ using the orthogonal fitting method and $B = 0.77 \pm 0.08$ using the bisector fitting method for our combined sample. Therefore both the orthogonal and bisector slopes are in agreement with each other and the previous values in the literature,

Table 6. Best-fit σ_v - T scaling relation parameters using both the orthogonal and bisector regression methods (see Section 3.2).

Method	Parameter	Low Redshift	High Redshift	Combined (no evolution)	Combined (with evolution)
Orthogonal	A	0.02 ± 0.06	-0.08 ± 0.05	-0.05 ± 0.04	0.02 ± 0.05
	B	0.89 ± 0.16	1.12 ± 0.41	0.72 ± 0.12	0.86 ± 0.14
	S	0.05 ± 0.03	0.08 ± 0.04	0.06 ± 0.03	0.06 ± 0.03
	C	0	0	0	-0.37 ± 0.33
Bisector	A	0.02 ± 0.04	-0.07 ± 0.03	-0.04 ± 0.02	0.02 ± 0.04
	B	0.85 ± 0.11	1.01 ± 0.17	0.77 ± 0.08	0.86 ± 0.09
	S_x	0.15 ± 0.03	0.19 ± 0.03	0.15 ± 0.02	0.14 ± 0.02
	S_y	0.07 ± 0.03	0.12 ± 0.04	0.09 ± 0.02	0.09 ± 0.02
	C	0	0	0	-0.49 ± 0.25

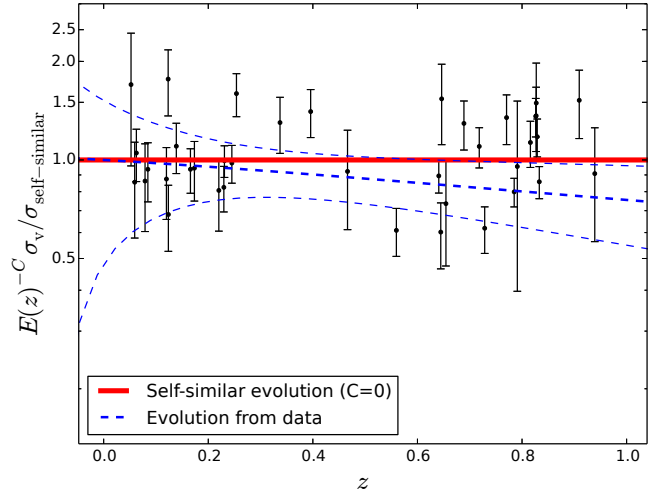
**Figure 6.** Plots showing the σ_v - T relation for the combined sample with varying evolution, i.e. C is a free parameter in Equation 3. The velocity dispersion is scaled to take into the account the evolution by multiplying by $E(z)^{-C}$. All lines are as explained in Fig. 3.

except for the result obtained by [Edge & Stewart \(1991\)](#) which is only consistent with the orthogonal result.

Except for work done by [Wu et al. \(1998\)](#) and [Nastasi et al. \(2014\)](#), all the previous results were obtained for low redshift samples and no test for evolution was performed. [Wu et al. \(1998\)](#) divided their sample into two groups, $z < 0.1$ and $z \geq 0.1$, and found no significant evolution, however their sample included only four clusters in the redshift range $0.5 < z < 1.0$. [Nastasi et al. \(2014\)](#) had a sample of 12 galaxy clusters and found a very large error of more than 50 per cent on their slope. They concluded that their sample size was too small to accurately measure evolution. We conclude that the data presented in this paper – a homogeneous cluster sample that is larger than those used in previous studies at $z > 0.5$ – are consistent with previous results.

5.2 Description of simulations

Comparison to simulations are important for two main reasons. Firstly, we can determine if there is any bias due to sample selection

**Figure 7.** Plot showing the evolution of the normalisation of the σ_v - T relation obtained for the data with the 95% confidence intervals in the dashed lines as compared to the self similar relation which predicts no evolution shown as the solid line. The black points show our sample data.

as the simulations provide both a bigger temperature and redshift range. It also allows us to compare different simulation models and learn about the nature of the non-gravitational physics through their effect on the gas temperature.

The Millennium Gas Project is a set of hydrodynamical simulations described in [Short et al. \(2010\)](#) which uses the same initial perturbations as the Millennium Simulation ([Springel et al. 2005](#)). These simulations include a variety of models, including gravity only; energy injection with radiative cooling; and feedback only. For comparison to the data presented in this paper, the feedback only model (FO) in a volume of $250 h^{-1} \text{Mpc}^3$ was used. This model includes supernova and AGN feedback using a semi-analytic galaxy formation model. Heating due to supernovae and AGN and the star formation rate are obtained using the model of [De Lucia & Blaizot \(2007\)](#). The AGN feedback model used is described in [Bower et al. \(2008\)](#), which is dependent on the matter accreted by the central black hole and the efficiency with which the matter is converted to energy near the event horizon, with the upper limit being at two per cent of the Eddington rate.

As a comparison to the velocity dispersion of the cluster, two proxies were considered, the velocity dispersion of the stars (σ_{stars}) and that obtained from the dark matter particles (σ_{DM}). The temperatures used from the simulation were spectroscopic-like temperatures (T_{S} ; [Mazzotta et al. 2004](#)). To ensure that only clusters similar to those in our sample were included we excluded all groups from

the simulation with a mass less than $10^{14} M_{\odot}$. We also included a temperature cut, $2 < T(\text{keV}) < 11$, and a redshift cut, $0 < z < 1$, to match our sample.

We also compared to the results of the BAHAMAS hydrodynamical simulation (McCarthy et al., in prep. and Caldwell et al., in prep.). Here, a $400 h^{-1} \text{Mpc}^3$ box is used, with initial conditions based on Planck 2013 cosmological parameters (Planck Collaboration et al. 2014), and both AGN and supernovae feedback models as described by Le Brun et al. (2014). A galaxy mass lower limit of $5 \times 10^9 M_{\odot}$ and a cluster mass lower limit of $10^{14} M_{\odot}$ were implemented. This simulation reproduces a large number of X-ray, SZ, and optical scaling relations of groups and clusters. However, unlike previous simulations, the new simulation also reproduces the observed galaxy stellar mass function remarkably well over a wide range of stellar masses. The velocity dispersion is traced by galaxies and is calculated using the gapper technique described by Beers et al. (1990). The temperatures used from the simulation were spectroscopic (T_S).

We note that spectroscopic-like temperatures, as used in both simulations, are most robust at $T > 2 \text{ keV}$, where the bremsstrahlung mechanism dominates (Short et al. 2010). Therefore, while we have applied mass, temperature, and redshift cuts to the simulated cluster catalogues that are a reasonable match to our observed sample, the correspondence is not exact, as 6 of the observed clusters have $T < 2 \text{ keV}$. This is a compromise aimed at limiting the potential impact of low mass clusters with less reliable temperature measurements in the simulations.

Matching the velocity dispersions to the simulations, however, is not as straight-forward, and is outside the scope of this paper, but for completeness we briefly discuss causes of bias identified in previous studies. Old et al. (2013) studied the recovery of velocity dispersions from simulation data and explored how sample selection can impact the measurements and cause a bias. They introduced *I*-band magnitude limits and found that the velocity dispersion recovered from the halos was systematically higher than that from the galaxies. When this sample was further limited to just the brightest galaxies, this discrepancy was enhanced. They suggest that the reason for this is that dynamical friction greatly affects the velocity of the galaxies, and therefore to reduce this bias a strictly magnitude-limited sample should be avoided.

Old et al. (2013) also calculated the velocity dispersion over different radial distances to see how it varied as a function of distance from the cluster centre. They found that the velocity dispersion was sensitive to the radius in which it was measured with a difference of 10 per cent in measurements being found between $0.5-1 R_{200}$. Sifón et al. (2016) also studied the impact of the choice of radius on velocity dispersion measurements, and found that the bias is negligible for measurements that sample beyond $0.7 R_{200}$ (see their Figure 4). Since our observations sample out to at least $0.7 R_{200}$ for all clusters, and beyond R_{200} for more than half the sample, we expect our velocity dispersion measurements to be unaffected by this source of bias.

We used these two sets of simulations to test our orthogonal fitting methods both with and without evolution.

5.3 Comparison with simulations - Fitting with no evolution

The orthogonal fitting method described in Section 3.2 was applied to both sets of simulations with $C = 0$. The parameters A , B and S for both the Millennium Gas Project and BAHAMAS simulations are shown in Table 7. The σ_v-T relation for the Millennium Gas Project with the two different σ_v proxies are shown in Fig. 8. The

slope is slightly steeper for the stars ($B=0.62 \pm 0.01$) than for the dark matter ($B=0.55 \pm 0.08$) but both are consistent with previous studies of the $\sigma_v - T$ relation and the results obtained from our data.

Fig. 9 shows that the orthogonal fit to the full BAHAMAS sample systematically overestimates the average velocity dispersion at $T > 5 \text{ keV}$. This may be due, in part, to the model not being a complete description of the data, as the scatter appears to vary with temperature. This is not captured in our orthogonal regression model (Equation 4), i.e., S is assumed to be constant with both T and z . A comparison was made to a fit performed by Caldwell et al. (in prep.) to the BAHAMAS data. In this method the $\sigma^2 - kT$ relation was derived by first parametrically determining the mean functions and redshift evolution of velocity dispersion and temperature, separately, with respect to mass (M_{500} critical). The velocity dispersion measurements are averaged in $0.25 \log_{10}(M_{500c})$ mass bins, to avoid biases from high cluster counts and the large scatter seen at low T (Fig. 9). These mean values of velocity dispersion and mass are fit with a power law, and the temperature relation is derived with the same method. This was converted into the $\sigma_v - T$ relation (with slope $B = 0.545$) that is plotted in Fig. 9. This method provides a better fit to BAHAMAS data over the full temperature range than the orthogonal method. We use the slope obtained using the Caldwell et al. method for further studies and comparisons. We examine the effect of bias in the recovered slope on our results in Section 5.4.

We note that there is no single method which gives the underlying ‘true’ scaling relation in the presence of errors on both variables and intrinsic scatter: the recovered slope and normalisation depend upon the details of the method used. The fitting of a scaling relation is also affected by the selection processes used when determining your sample and for this study this has not been corrected for. Since our clusters are selected on X-ray luminosity rather than temperature or velocity dispersion we believe that our values are not biased and therefore selection effects will not have as big an impact on our results.

5.4 The effect of biased slope measurements on the evolution of the normalisation

Having seen, using the BAHAMAS simulation, that the slope recovered using the orthogonal regression method may be biased high, we now discuss the potential impact of a biased slope measurement on our conclusions regarding the observed cluster sample in Section 5.1.

To investigate this, we generated 1000 mock samples (each containing 38 clusters) from the BAHAMAS simulation with the same temperature distribution as the observed sample, and applied the orthogonal regression method. Fig. 10 shows the distribution of recovered slope values. The average is $B = 0.69 \pm 0.13$, which is 2σ higher than the slope obtained from the fit performed by Caldwell et al. in prep (Section 5.2). Therefore, if the BAHAMAS sample is representative of the real cluster population, then we would conclude that the slope we have measured for the observed cluster sample is biased high.

To check if a biased slope estimate affects our conclusions regarding the lack of significant evidence for evolution of the normalisation of the relation (Section 4.2), we fixed the slope to $B = 0.545$ and re-ran the orthogonal fit for the observed cluster sample. We found $C = 0.15 \pm 0.28$, which is consistent with no evolution (Fig. 11). Therefore, even if the slope value of $B = 0.86 \pm 0.14$ that we measured was biased high for any reason, this does not affect

Table 7. Best fit values for the parameters in Equation 4 (slope, intercept and scatter) for the various models obtained from simulations without evolution. For the Millennium Gas Project we use dark matter (DM) and stars as the tracers for the velocity dispersion. The BAHAMAS simulation uses galaxies. The Millennium Gas simulations use spectroscopic like temperatures (T_{sl}) and the BAHAMAS simulation use spectroscopic temperatures (T_s). Caldwell et al. in prep present a different method for determining the $\sigma_v - T$ relation as discussed in Section 5.2, the results of which are also shown below.

Simulation	σ_{tracer}	T_{model}	A	B	S
Millennium Gas	DM	T_{sl}	-0.011 ± 0.002	0.553 ± 0.008	0.028 ± 0.001
Millennium Gas	Stars	T_{sl}	-0.034 ± 0.003	0.621 ± 0.010	0.034 ± 0.001
BAHAMAS	Galaxies	T_s	-0.055 ± 0.003	0.848 ± 0.012	0.055 ± 0.001
BAHAMAS (Caldwell et al., in prep)	Galaxies	T_s	-0.133	0.545	

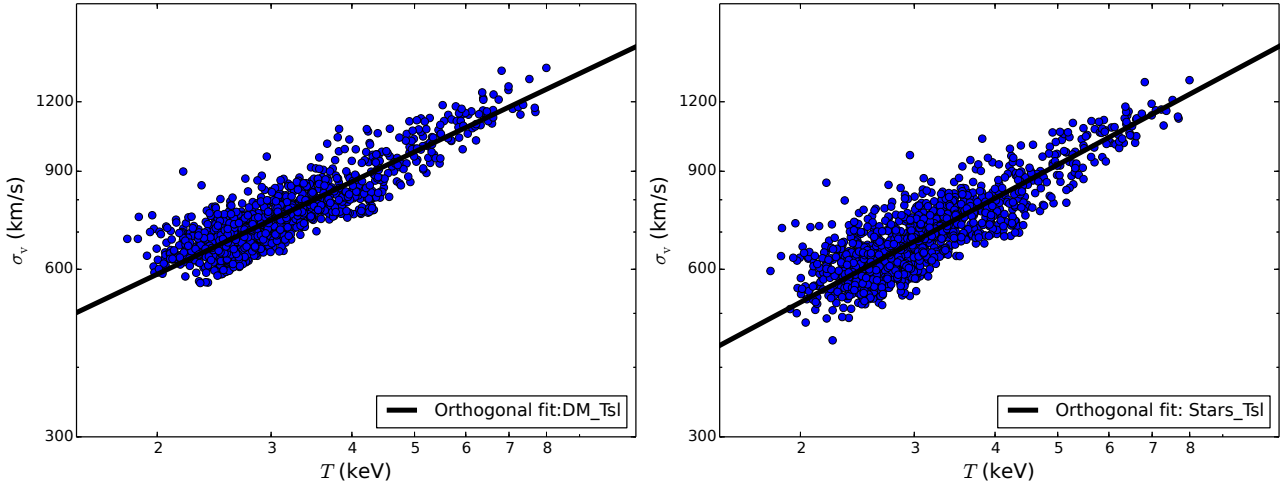


Figure 8. The $\sigma_v - T$ relation for the Millennium Gas Project simulations using dark matter and stars as proxies for the velocity dispersion. The blue dots are the data obtained from the simulation and the solid black line shows the fit using the orthogonal regression method. The slope is slightly steeper for the stars ($B=0.62 \pm 0.01$) than for the dark matter ($B=0.55 \pm 0.08$) but both are consistent with previous studies of the $\sigma_v - T$ relation and the results obtained from our data.

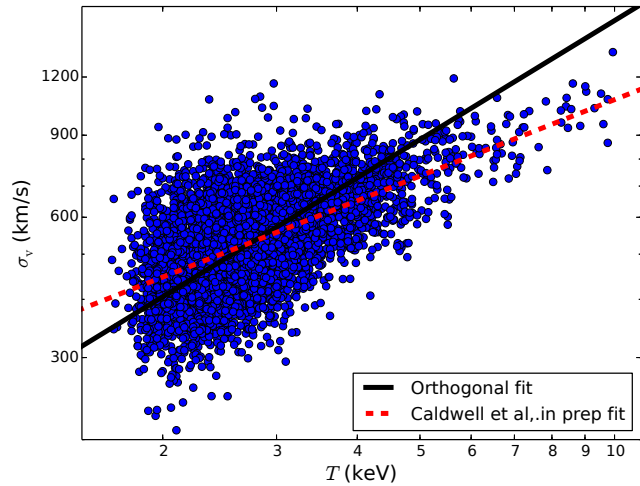


Figure 9. Plot showing the $\sigma_v - T$ relation for the BAHAMAS simulation data. The blue circles represent the data points from the simulation. The solid line is the fit obtained using the orthogonal method and the dashed line is the fit obtained using the method described in Section 5.2 and performed by Caldwell et al., in prep. From this it can be seen that the orthogonal fit over-estimates the velocity dispersion at $T_X > 5$ keV (see Section 5.2).

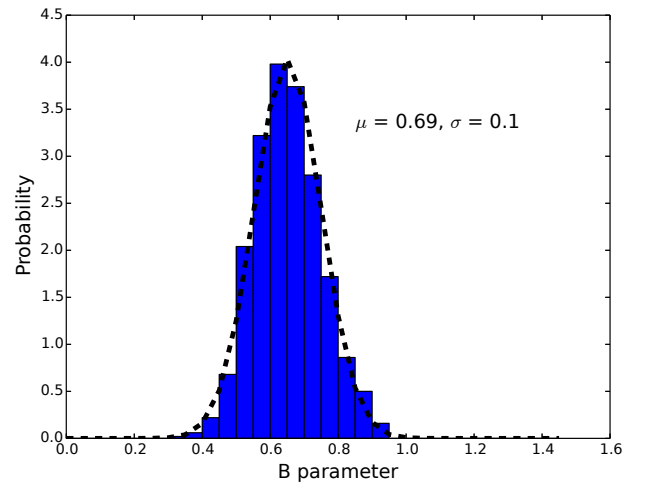


Figure 10. This histogram shows the probability of getting a specific value for the slope of the best-fit $\sigma - T$ relation given a set T distribution. We chose various subsamples from the BAHAMAS simulation which had the same T distribution as our sample and calculated the slope for each. The mean slope obtained is $B=0.69 \pm 0.13$, which is within 2 sigma of the value obtained from Caldwell et al, in prep, so there is a slight bias from the distribution of the sample.

our conclusion that we do not see significant evidence in favour of evolution.

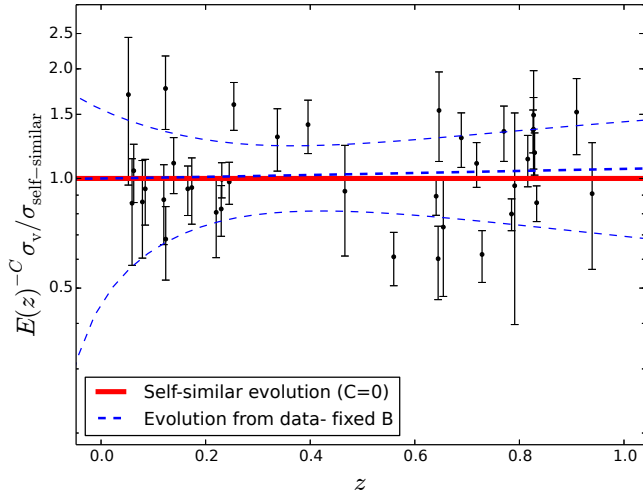


Figure 11. Plot showing the evolution of the normalisation of the $\sigma_v - T$ relation, with $B = 0.545$, obtained for the observed cluster sample with the 95% confidence intervals in the dashed lines, as compared to the self similar relation which predicts no evolution shown as the solid line. The black points show the measurements for the clusters in our sample.

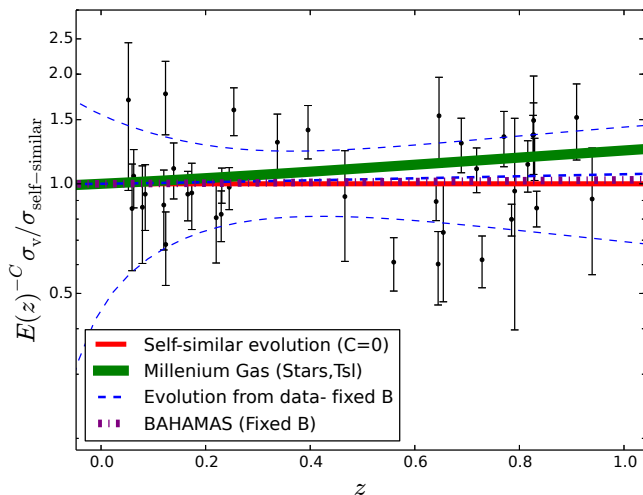


Figure 12. We compared the evolution of the normalisation of $\sigma_v - T$ relation of the Millennium Gas and BAHAMAS simulations with the self similar relation and that found from our data using a fixed slope. The solid line shows the line representing the self-similar relation i.e. $C = 0$, the dot-dashed line represents the BAHAMAS simulation results with a fixed $B = 0.545$ to avoid bias and the vertically dashed line represents the result from the Millennium Gas simulation. The blue dashed line and black points are our orthogonal fit and observed sample respectively.

5.5 Comparison with simulations - Fitting with evolution

We now investigate evolution in the normalisation of the $\sigma_v - T$ relation in the simulations by fitting for the value of C , as we did for the observed sample (see Section 4.2). The results are shown in Table 8 and graphically in Fig. 12. The BAHAMAS simulation was tested both with a slope that was allowed to vary and a fixed slope. Although, in Section 5.4 we showed that the over-estimated slope does not affect evolution, we included a fixed slope for further comparison. Both were found to be consistent with zero evolution, fur-

ther proving that the biased slope does not affect evolution. However, the simulations from the Millennium Gas Project show small but significant positive evolution ($C = 0.273 \pm 0.013$ for σ_{Stars} and T_{sl}). To see the reason for this, we can re-write the $\sigma_v - T$ relation in terms of the $\sigma_v - M$ and $T - M$ relations, where M is the cluster mass (see, e.g., Maughan 2014). We define

$$\sigma_v = 10^{A_{\sigma_v T}} \left(\frac{T}{5 \text{ keV}} \right)^{B_{\sigma_v T}} E(z)^{C_{\sigma_v T}}, \quad (9)$$

where

$$\begin{aligned} B_{\sigma_v T} &= B_{\sigma_v M} / B_{TM}, \\ A_{\sigma_v T} &= A_{\sigma_v M} - A_{TM} B_{\sigma_v T}, \text{ and} \\ C_{\sigma_v T} &= C_{\sigma_v M} - C_{TM} B_{\sigma_v T}. \end{aligned} \quad (10)$$

Here, A , B and C have the same meaning as before, and the subscripts indicate the corresponding relation (e.g., B_{TM} indicates the slope of the $T - M$ relation). If we set $C_{\sigma_v M} = 1/3$, $C_{TM} = 2/3$ and $B_{\sigma_v T} = 1/2$ as predicted by the self-similar relation, then we obtain $C_{\sigma_v T} = 0$ as expected. We performed fits to determine the values of $C_{\sigma_v M}$, C_{TM} and $B_{\sigma_v T}$ in the Millennium Gas simulation at $z = 0$ and $z = 0.5$. We found that $C_{\sigma_v M} = 1/3$ when using either σ_{Stars} or σ_{DM} as the measure of σ_v , and that $B_{\sigma_v T}$ varied from 0.55–0.6 (depending on whether spectroscopic-like or mass-weighted temperature estimates were used), which is slightly higher than the self-similar value, but not by enough to explain the positive evolution measured in the $\sigma_v - T$ relation. This leads to the conclusion that the evolution is driven by the value of C_{TM} , and it was found that the measured value for the dark matter was $C_{TM} = 2/3$ as expected, but that this decreased to values between 0–0.2 for the gas. Therefore in the Millennium Gas simulation, the lack of redshift evolution in the $T - M$ relation drives the positive evolution in the $\sigma_v - T$ relation.

The most likely explanation for the lack of redshift evolution in the $T - M$ relation in the Millennium Gas simulation is the absence of radiative cooling. When both cooling and feedback are included in simulations (as in BAHAMAS), the feedback acts as a regulation mechanism, heating the surrounding dense gas and expelling it from the cluster core. This in turn leads to higher-entropy gas flowing inwards. In the Millennium Gas simulation, the feedback model heats the gas and directly increases its entropy, which is eventually distributed throughout the cluster. This builds up over time as more and more energy is pumped into the gas from the growing black holes, and has the effect of slowing down the evolution of the $T - M$ relation (compared to the evolution expected due to the decreasing background density with redshift). This in turn leads to the positive evolution of the $\sigma_v - T$ relation. It is likely that the more sophisticated feedback model used in BAHAMAS, where the entropy evolution is driven by radiative cooling, is the more realistic of the two.

6 CONCLUSIONS

We have studied the evolution of the velocity dispersion–temperature ($\sigma_v - T$) relation using a cluster sample spanning the range $0.0 < z < 1.0$ drawn from XCS. This work improves upon previous studies in terms of the use of a homogeneous cluster sample and the number of $z > 0.5$ clusters included. We present new redshift and velocity dispersion measurements based on Gemini data for 12 such $z > 0.5$ XCS clusters.

We used an orthogonal regression method to measure the normalisation, slope and intrinsic scatter of the $\sigma_v - T$ relation for two subsamples: 19 clusters at $z < 0.5$, and 19 clusters with $z > 0.5$.

Table 8. Best fit values for the parameters in Equation 4 (slope, intercept, scatter and evolution) for the various models obtained from simulations. All abbreviations are as in Table 7.

Simulation	σ_{tracer}	T_{model}	A	B	S	C
Millennium Gas	DM	T_{sl}	-0.031 ± 0.002	0.551 ± 0.006	0.0220 ± 0.0010	0.371 ± 0.014
Millennium Gas	Stars	T_{sl}	-0.056 ± 0.002	0.619 ± 0.009	0.0295 ± 0.0010	0.397 ± 0.019
BAHAMAS (fixed B)	Galaxies	T_{s}	-0.135 ± 0.002	0.545	0.0390 ± 0.0010	0.046 ± 0.016
BAHAMAS (varying B)	Galaxies	T_{s}	-0.071 ± 0.005	0.779 ± 0.014	0.0570 ± 0.0010	-0.029 ± 0.024

In both cases, we found the slope of the relation to be consistent with the findings of previous studies, i.e., slightly steeper than expected from self-similarity. Under the assumption that the slope of the relation does not evolve with redshift, we measured the evolution of the normalisation of the relation using the complete sample of 38 clusters. We found this to be slightly negative but not significantly different from the self-similar solution ($\sigma_v \propto T^{0.86 \pm 0.14} E(z)^{-0.37 \pm 0.33}$). Moreover, a no evolution model is the preferred choice when considering the Akaike Information Criterion.

We applied the same scaling relation analysis methods to the BAHAMAS and Millennium Gas cosmological hydrodynamical simulations. The σ_v - T relation does not evolve in BAHAMAS, in agreement with our findings for the observed cluster sample. However, positive evolution is seen in the Millennium Gas simulation. The difference is most likely due to the inclusion of self-consistent modelling of radiative cooling in BAHAMAS, which is absent in the Millennium Gas simulation. This leads to a very slowly evolving T - M relation in the Millennium Gas simulation, which in turn drives the positive evolution of the σ_v - T relation. While this work has improved upon previous studies in terms of the number of high redshift clusters included, we note that the uncertainties on the scaling relation parameters are still rather large, and a combination of better measurements of individual cluster properties and a larger sample are required to make further progress. Future studies will look at implementing the Bayesian method described by Kelly (2007) to account for intrinsic scatter and measurement errors and looking at possible selection effects.

ACKNOWLEDGEMENTS

SW and MH acknowledge financial support from the National Research Foundation and SKA South Africa. This research has made use of the NASA/IPAC Extragalactic Database (NED) which is operated by the Jet Propulsion Laboratory, California Institute of Technology, under contract with the National Aeronautics and Space Administration. Based on observations obtained at the Gemini Observatory, which is operated by the Association of Universities for Research in Astronomy, Inc., under a cooperative agreement with the NSF on behalf of the Gemini partnership: the National Science Foundation (United States), the National Research Council (Canada), CONICYT (Chile), the Australian Research Council (Australia), Ministério da Ciência, Tecnologia e Inovação (Brazil) and Ministerio de Ciencia, Tecnología e Innovación Productiva (Argentina). PAT acknowledges support from the Science and Technology Facilities Council (grant number ST/L000652/1). JPS gratefully acknowledges support from a Hintze Research Fellowship. STK acknowledges support from STFC (grant number ST/L000768/1).

REFERENCES

- Abazajian K., et al., 2003, *AJ*, **126**, 2081
 Abazajian K., et al., 2004, *AJ*, **128**, 502
 Abazajian K., et al., 2005, *AJ*, **129**, 1755
 Abazajian K. N., et al., 2009, *ApJS*, **182**, 543
 Adami C., et al., 2011, *A&A*, **526**, A18
 Adelman-McCarthy J. K., et al., 2006, *ApJS*, **162**, 38
 Adelman-McCarthy J. K., et al., 2007, *ApJS*, **172**, 634
 Adelman-McCarthy J. K., et al., 2008, *ApJS*, **175**, 297
 Arnaud M., Pointecouteau E., Pratt G. W., 2005, *A&A*, **441**, 893
 Balogh M., Bower R. G., Smail I., Ziegler B. L., Davies R. L., Gaztelu A., Fritz A., 2002, *MNRAS*, **337**, 256
 Basilakos S., Plionis M., Georgakakis A., Georgantopoulos I., Gaga T., Kolokotronis V., Stewart G. C., 2004, *MNRAS*, **351**, 989
 Bayliss M. B., Hennawi J. F., Gladders M. D., Koester B. P., Sharon K., Dahle H., Oguri M., 2011, *ApJS*, **193**, 8
 Beers T. C., Flynn K., Gebhardt K., 1990, *AJ*, **100**, 32
 Bellagamba F., Maturi M., Hamana T., Meneghetti M., Miyazaki S., Moscardini L., 2011, *MNRAS*, **413**, 1145
 Berlind A. A., et al., 2006, *ApJS*, **167**, 1
 Bird C. M., Mushotzky R. F., Metzler C. A., 1995, *ApJ*, **453**, 40
 Bower R. G., 1997, *MNRAS*, **288**, 355
 Bower R. G., McCarthy I. G., Benson A. J., 2008, *MNRAS*, **390**, 1399
 Branchesi M., Gioia I. M., Fanti C., Fanti R., 2007, *A&A*, **472**, 739
 Brusa M., et al., 2010, *ApJ*, **716**, 348
 Bryan G. L., Norman M. L., 1998, *ApJ*, **495**, 80
 Burenin R. A., Vikhlinin A., Hornstrup A., Ebeling H., Quintana H., Meshcheryakov A., 2007, *ApJS*, **172**, 561
 Burnham K. P., Anderson D. R., 2002, *Model Selection and Multimodel Inference: A Practical Information-Theoretic Approach*, 2 edn. Springer-Verlag, New York
 Cappi A., Held E. V., Marano B., 1998, *A&AS*, **129**, 31
 Cash W., 1979, *ApJ*, **228**, 939
 Clerc N., Sadibekova T., Pierre M., Pacaud F., Le Fèvre J.-P., Adami C., Altieri B., Valtchanov I., 2012, *MNRAS*, **423**, 3561
 Clerc N., et al., 2014, *MNRAS*, **444**, 2723
 Cohn J. D., White M., 2005, *Astroparticle Physics*, **24**, 316
 Colless M., et al., 2003a, *ArXiv Astrophysics e-prints*,
 Colless M., et al., 2003b, *VizieR Online Data Catalog*, **7226**, 0
 Collins C. A., et al., 2009, *Nature*, **458**, 603
 Coziol R., Andernach H., Caretta C. A., Alamo-Martínez K. A., Tago E., 2009, *AJ*, **137**, 4795
 Crawford S. M., Wirth G. D., Bershady M. A., 2014, *ApJ*, **786**, 30
 De Lucia G., Blaizot J., 2007, *MNRAS*, **375**, 2
 De Propriis R., Couch W. J., Colless M., et al., 2002, *MNRAS*, **329**, 87
 Dickey J. M., 1990, in Thronson Jr. H. A., Shull J. M., eds, *Astrophysics and Space Science Library Vol. 161, The Interstellar Medium in Galaxies*. pp 473–481
 Donahue M., Voit G. M., Scharf C. A., Gioia I. M., Mullis C. R., Hughes J. P., Stocke J. T., 1999, *ApJ*, **527**, 525
 Edge A. C., Stewart G. C., 1991, *MNRAS*, **252**, 428
 Etti S., Tozzi P., Borgani S., Rosati P., 2004, *A&A*, **417**, 13
 Fadda D., Girardi M., Giuricin G., Mardirossian F., Mezzetti M., 1996, *ApJ*, **473**, 670
 Fassbender R., et al., 2011, *New Journal of Physics*, **13**, 125014
 Feruglio C., et al., 2008, *A&A*, **488**, 417
 Finn R. A., et al., 2005, *ApJ*, **630**, 206
 Finoguenov A., et al., 2007, *ApJS*, **172**, 182

- Freudling W., Haynes M. P., Giovanelli R., 1992, *ApJS*, **79**, 157
 Gioia I. M., Luppino G. A., 1994, *ApJS*, **94**, 583
 Gioia I. M., Wolter A., Mullis C. R., Henry J. P., Böhringer H., Briel U. G., 2004, *A&A*, **428**, 867
 Giovanelli R., Scodeggio M., Solanes J. M., Haynes M. P., Arce H., Sakai S., 1995, *AJ*, **109**, 1451
 Girardi M., Fadda D., Giuricin G., Mardirossian F., Mezzetti M., Biviano A., 1996, *ApJ*, **457**, 61
 Glazebrook K., Bland-Hawthorn J., 2001, *PASP*, **113**, 197
 Goto T., et al., 2003, *PASJ*, **55**, 771
 Guzzo L., et al., 2009, *A&A*, **499**, 357
 Hao J., et al., 2010, *ApJS*, **191**, 254
 Hasselfield M., et al., 2013, *J. Cosmology Astropart. Phys.*, **7**, 8
 Hennawi J. F., et al., 2008, *AJ*, **135**, 664
 Hilton M., et al., 2009, *ApJ*, **697**, 436
 Hilton M., et al., 2010, *ApJ*, **718**, 133
 Hilton M., et al., 2012, *MNRAS*, **424**, 2086
 Hoekstra H., Herbonnet R., Muzzin A., Babul A., Mahdavi A., Viola M., Cacciato M., 2015, *MNRAS*, **449**, 685
 Hogg D. W., Bovy J., Lang D., 2010, preprint, ([arXiv:1008.4686](https://arxiv.org/abs/1008.4686))
 Huchra J. P., et al., 2012, *ApJS*, **199**, 26
 Jeltama T. E., Mulchaey J. S., Lubin L. M., Fassnacht C. D., 2007, *ApJ*, **658**, 865
 Jones D. H., et al., 2009, *MNRAS*, **399**, 683
 Kaiser N., 1986, *MNRAS*, **222**, 323
 Kay S. T., da Silva A. C., Aghanim N., Blanchard A., Liddle A. R., Puget J.-L., Sadat R., Thomas P. A., 2007, *MNRAS*, **377**, 317
 Kelly B. C., 2007, *ApJ*, **665**, 1489
 Koester B. P., et al., 2007, *ApJ*, **660**, 239
 Kravtsov A. V., Borgani S., 2012, *ARA&A*, **50**, 353
 Kurtz M. J., Mink D. J., 1998, *PASP*, **110**, 934
 Le Brun A. M. C., McCarthy I. G., Schaye J., Ponman T. J., 2014, *MNRAS*, **441**, 1270
 Le Fevre O., Crampton D., Lilly S. J., Hammer F., Tresse L., 1995, *ApJ*, **455**, 60
 Lilly S. J., et al., 2007, *ApJS*, **172**, 70
 Lloyd-Davies E. J., et al., 2011, *MNRAS*, **418**, 14
 Lubin L. M., Bahcall N. A., 1993, *ApJ*, **415**, L17
 Lumb D. H., et al., 2004, *A&A*, **420**, 853
 Magnelli B., Elbaz D., Chary R. R., Dickinson M., Le Borgne D., Frayer D. T., Willmer C. N. A., 2009, *A&A*, **496**, 57
 Mann A. W., Ebeling H., 2012, *MNRAS*, **420**, 2120
 Maughan B. J., 2014, *MNRAS*, **437**, 1171
 Maughan B. J., Jones L. R., Ebeling H., Scharf C., 2006, *MNRAS*, **365**, 509
 Maughan B. J., Giles P. A., Randall S. W., Jones C., Forman W. R., 2012, *MNRAS*, **421**, 1583
 Mazzotta P., Rasia E., Moscardini L., Tormen G., 2004, *MNRAS*, **354**, 10
 Mehrrens N., et al., 2012, *MNRAS*, **423**, 1024
 Mewe R., Schrijver C. J., 1986, *A&A*, **169**, 178
 Miller C. J., Krughoff K. S., Batuski D. J., Hill J. M., 2002, *AJ*, **124**, 1918
 Mulchaey J. S., Lubin L. M., Fassnacht C., Rosati P., Jeltama T. E., 2006, *ApJ*, **646**, 133
 Mullis C. R., et al., 2003, *ApJ*, **594**, 154
 Nastasi A., et al., 2014, *A&A*, **564**, A17
 Ofek E. O., Oguri M., Jackson N., Inada N., Kayo I., 2007, *MNRAS*, **382**, 412
 Old L., Gray M. E., Pearce F. R., 2013, *MNRAS*, **434**, 2606
 Ortiz-Gil A., Guzzo L., Schuecker P., Böhringer H., Collins C. A., 2004, *MNRAS*, **348**, 325
 Perlman E. S., Horner D. J., Jones L. R., Scharf C. A., Ebeling H., Wegner G., Malkan M., 2002, *ApJS*, **140**, 265
 Pinkney J., Rhee G., Burns J. O., Hill J. M., Oegerle W., Batuski D., Hintzen P., 1993, *ApJ*, **416**, 36
 Planck Collaboration et al., 2014, *A&A*, **571**, A16
 Planck Collaboration et al., 2015, preprint, ([arXiv:1502.01597](https://arxiv.org/abs/1502.01597))
 Ponman T. J., Bourner P. D. J., Ebeling H., Böhringer H., 1996, *MNRAS*, **283**, 690
 Poole G. B., Babul A., McCarthy I. G., Fardal M. A., Bildfell C. J., Quinn T., Mahdavi A., 2007, *MNRAS*, **380**, 437
 Quintana H., Melnick J., 1982, *AJ*, **87**, 972
 Randall S. W., Sarazin C. L., Ricker P. M., 2002, *ApJ*, **577**, 579
 Reichardt C. L., et al., 2013, *ApJ*, **763**, 127
 Ritchie B. W., Thomas P. A., 2002, *MNRAS*, **329**, 675
 Roza E., et al., 2009, *ApJ*, **699**, 768
 Sacchi N., et al., 2009, *ApJ*, **703**, 1778
 Sahlén M., et al., 2009, *MNRAS*, **397**, 577
 Sakelliou I., Merrifield M. R., 1998, *MNRAS*, **293**, 489
 Sánchez Almeida J., Aguerri J. A. L., Muñoz-Tuñón C., Huertas-Company M., 2011, *ApJ*, **735**, 125
 Schaerer D., Contini T., Pindao M., 1999, *A&AS*, **136**, 35
 Schafer R. A., 1991, XSPEC, an x-ray spectral fitting package : version 2 of the user's guide
 Scharf C. A., Ebeling H., Perlman E., Malkan M., Wegner G., 1997, *ApJ*, **477**, 79
 Schweizer F., 1996, *AJ*, **111**, 109
 Scodeggio M., Solanes J. M., Giovanelli R., Haynes M. P., 1995, *ApJ*, **444**, 41
 Short C. J., Thomas P. A., Young O. E., Pearce F. R., Jenkins A., Muanwong O., 2010, *MNRAS*, **408**, 2213
 Sifón C., et al., 2013, *ApJ*, **772**, 25
 Sifón C., et al., 2016, *MNRAS*,
 Silverman J. D., et al., 2005, *ApJ*, **618**, 123
 Smith R. J., et al., 2004, *AJ*, **128**, 1558
 Springel V., et al., 2005, *Nature*, **435**, 629
 Stott J. P., et al., 2010, *ApJ*, **718**, 23
 Stoughton C., et al., 2002, *AJ*, **123**, 485
 Struble M. F., Rood H. J., 1999, *ApJS*, **125**, 35
 Takey A., Schwobe A., Lamer G., 2011, *A&A*, **534**, A120
 Takey A., Schwobe A., Lamer G., 2013, *A&A*, **558**, A75
 Tonry J., Davis M., 1979, *AJ*, **84**, 1511
 Tran K.-V. H., Kelson D. D., van Dokkum P., Franx M., Illingworth G. D., Magee D., 1999, *ApJ*, **522**, 39
 Trichas M., et al., 2010, *MNRAS*, **405**, 2243
 Trump J. R., et al., 2007, *ApJS*, **172**, 383
 Verdugo M., Ziegler B. L., Gerken B., 2008, *A&A*, **486**, 9
 Vikhlinin A., McNamara B. R., Forman W., Jones C., Quintana H., Hornstrup A., 1998, *ApJ*, **502**, 558
 Vikhlinin A., van Speybroeck L., Markevitch M., Forman W. R., Grego L., 2002, *ApJ*, **578**, L107
 Vikhlinin A., Kravtsov A., Forman W., Jones C., Markevitch M., Murray S. S., Van Speybroeck L., 2006, *ApJ*, **640**, 691
 Vikhlinin A., et al., 2009, *ApJ*, **692**, 1060
 Voit G. M., 2005, *Reviews of Modern Physics*, **77**, 207
 Wegner G. A., 2011, *MNRAS*, **413**, 1333
 White D. A., Jones C., Forman W., 1997, *MNRAS*, **292**, 419
 Wu X.-P., Fang L.-Z., Xu W., 1998, *A&A*, **338**, 813
 Wu X.-P., Xue Y.-J., Fang L.-Z., 1999, *ApJ*, **524**, 22
 Xue Y.-J., Wu X.-P., 2000, *ApJ*, **538**, 65
 Yoon J. H., Schawinski K., Sheen Y.-K., Ree C. H., Yi S. K., 2008, *ApJS*, **176**, 414
 Šuhada R., et al., 2011, *A&A*, **530**, A110
 von der Linden A., et al., 2014, *MNRAS*, **439**, 2

APPENDIX A: OBSERVATIONS LOG

Table A1. Spectroscopic observations log. For all observations the R400 grating and the OG515 filter was used.

Cluster Name	Mask	Slits	Airmass Range	Observation Date	Frames(s)	Seeing (")
XMMXCS J005656.6-274031.9	GS2012B-Q-011-03	33	1.22	2012-10-19	1 x 1830	
"	"		1.48 - 1.76	2012-10-16	2 x 1830	
"	"		1.01 - 1.04	2012-10-15	3 x 1830	0.76 - 0.80
"	GS2012B-Q-011-04	35	1.05 - 1.35	2012-11-14	4 x 1830	
XMMXCS J015241.1-133855.9	GS2011B-Q-050-01	33	1.05 - 1.21	2011-12-02	6 x 1830	
"	GS2011B-Q-050-02	34	1.05 - 1.65	2011-12-03	6 x 1830	
XMMXCS J021734.7-051326.9	GS2012B-Q-011-06	34	1.14 - 1.48	2012-12-05	4 x 1830	
XMMXCS J025006.4-310400.8	GS2012B-Q-011-09	32	1.11 - 1.20	2012-11-24	2 x 1830	
"	"		1.01 - 1.19	2012-11-21	4 x 1830	
"	GS2010B-Q-046-06	35	1.06 - 1.12	2010-11-14	2 x 1830	0.50 - 0.60
"	"		1.06 - 1.44	2010-11-13	5 x 1830, 1 x 762	1
XMMXCS J030205.1-000003.6	GS2011B-Q-050-03	32	1.17	2011-12-01	1 x 1830	
"	"		1.18	2011-11-20	1 x 1098	
"	"		1.17 - 1.45	2011-11-18	4 x 1830	
"	GS2011B-Q-050-04	32	1.32	2011-12-31	1 x 1098	
"	"		1.23 - 1.74	2011-12-30	4 x 1830	0.85 - 1.40
"	GS2011B-Q-050-05	33	1.27 - 1.57	2012-01-17	2 x 1830	0.7
XMMXCS J095940.7+023113.4	GS2010B-Q-046-02	35	1.19 - 1.23	2011-01-09	3 x 1830	
"	"		1.19 - 1.25	2011-01-08	4 x 1830	
"	GS-2012A-Q-46-01	35	1.19 - 1.29	2012-03-18	4 x 1830	
"	"		1.19 - 1.23	2012-03-02	2 x 1830	
"	GS-2012A-Q-46-02	34	1.20 - 1.35	2012-03-27	3 x 1830	
"	"		1.23 - 1.46	2012-03-23	3 x 1830	0.8
"	GS-2012A-Q-46-03	34	1.21 - 1.54	2012-03-22	6 x 1830	0.65 - 0.70
XMMXCS J112349.3+052956.8	GS-2012A-Q-46-05	33	1.23 - 1.33	2012-04-22	5 x 1830	
"	"		1.47	2012-04-21	1 x 1830	
"	GS-2012A-Q-46-06	32	1.25 - 1.65	2012-05-15	4 x 1830	0.63 - 0.76
"	"		1.45 - 1.66	2012-04-22	2 x 1830	
"	GS2010B-Q-046-03	33	1.26	2011-01-31	1 x 1830	
"	"		1.35 - 1.64	2011-01-29	2 x 1525, 1 x 975	
"	"		1.23 - 1.24	2011-01-27	2 x 1830	
XMMXCS J113602.9-032943.2	GS-2012A-Q-46-07	36	1.14	2012-05-24	1 x 1830	
"	"		1.12	2012-05-23	1 x 1830	
"	"		1.12 - 1.16	2012-05-20	3 x 1830	
"	"		1.12	2012-05-19	1 x 1830	
"	GS-2012A-Q-46-08	33	1.48 - 1.76	2012-07-15	2 x 1830	
"	"		1.41 - 1.80	2012-07-11	3 x 1830	0.50 - 0.70
"	"		1.5	2012-07-10	1 x 1830	
XMMXCS J134305.1-000056.8	GS-2012A-Q-46-10	36	1.16 - 1.23	2012-05-24	4 x 1830	
"	"		1.24	2012-05-21	1 x 1830	
"	GS-2012A-Q-46-11	34	1.25	2012-07-10	1 x 1830	
"	"		1.16 - 1.19	2012-07-09	2 x 1830	
"	"		1.2	2012-07-06	1 x 1830	
"	"		1.54 - 1.84	2012-06-22	2 x 1830	
XMMXCS J145009.3+090428.8	GN2012A-Q-070-05	32	1.02 - 1.05	2012-07-09	2 x 1800	1.15
"	"		1.11 - 1.62	2012-06-26	4 x 1800	0.84 - 0.98
"	GN2012A-Q-070-06	34	1.02 - 1.04	2012-07-07	2 x 1800	
"	"		1.09 - 1.17	2012-07-06	2 x 1800	
"	"		1.48 - 1.79	2012-06-27	2 x 1800	
"	GN2012A-Q-070-07	33	1.22 - 1.59	2012-07-22	3 x 1800	
"	"		1.04 - 1.16	2012-07-08	3 x 1800	1
XMMXCS J215221.0-273022.6	GS2010B-Q-046-04	36	1.14 - 1.24	2010-11-12	2 x 1830	
"	"		1.02 - 1.21	2010-09-14	4 x 1830	
"	GS2011B-Q-050-06	34	1.07 - 1.15	2011-10-05	2 x 1830	
"	"		1.12 - 1.56	2011-09-18	4 x 1830	0.60 - 1.00
"	GS2011B-Q-050-07	34	1.00 - 1.10	2011-10-24	4 x 1830	
"	"		1.05 - 1.12	2011-10-16	2 x 1830	
XMMXCS J230247.7+084355.9	GN2012A-Q-070-10	34	1.37	2012-08-08	1 x 1800	0.60 - 0.68
"	"		1.02 - 1.11	2012-07-30	5 x 1800	0.43 - 0.86
"	GN2012A-Q-070-11	33	1.18 - 1.31	2012-08-13	2 x 1800	
"	"		1.02 - 1.08	2012-08-09	3 x 1800	0.60 - 0.68
"	"		1.19	2012-08-08	1 x 1800	1

APPENDIX B: REDSHIFT CATALOGUE

Tables of galaxy redshifts measured in each cluster to appear in the online version of the article.

Name	RA(J2000)	Dec(J2000)	z	Reference
GALEXASC J000046.26-251058.3	00 ^h 00 ^m 46.26 ^s	-25°10'59.9''	0.0821	Colless et al. (2003a)
GALEXASC J000057.30-250623.9	00 ^h 00 ^m 57.23 ^s	-25°06'25.9''	0.0821	Colless et al. (2003a)
2dFGRS S134Z161	23 ^h 59 ^m 32.60 ^s	-25°13'02.2''	0.0823	Colless et al. (2003a)
GALEXASC J235957.50-250120.7	23 ^h 59 ^m 57.51 ^s	-25°01'20.5''	0.0823	Colless et al. (2003a)
2dFGRS S134Z139	00 ^h 00 ^m 25.25 ^s	-25°20'48.2''	0.0834	Colless et al. (2003a)
2MASX J00002408-2510371	00 ^h 00 ^m 24.10 ^s	-25°10'38.0''	0.0837	Colless et al. (2003a)
2MASX J00004212-2512080	00 ^h 00 ^m 42.12 ^s	-25°12'08.1''	0.0837	Jones et al. (2009)
2MASX J00002446-2516181	00 ^h 00 ^m 24.45 ^s	-25°16'18.3''	0.0839	Colless et al. (2003a)
AM 2357-252 NED01	00 ^h 00 ^m 13.28 ^s	-25°11'08.1''	0.0841	Coziol et al. (2009)
2dFGRS S134Z105	00 ^h 01 ^m 02.68 ^s	-25°08'59.4''	0.0844	Colless et al. (2003a)
2MASX J00000684-2515021	00 ^h 00 ^m 06.85 ^s	-25°15'02.0''	0.0847	Colless et al. (2003a)
2MASX J00001841-2510051	00 ^h 00 ^m 18.43 ^s	-25°10'04.9''	0.0847	Colless et al. (2003a)
AM 2357-252	00 ^h 00 ^m 13.70 ^s	-25°11'10.0''	0.0847	Colless et al. (2003a)
2MASX J00000093-2521313	00 ^h 00 ^m 00.94 ^s	-25°21'31.8''	0.0848	Colless et al. (2003a)
AM 2357-252	00 ^h 00 ^m 14.06 ^s	-25°11'12.6''	0.0851	Jones et al. (2009)
2dFGRS S134Z131	00 ^h 00 ^m 28.86 ^s	-25°07'11.2''	0.0854	Colless et al. (2003a)
2MASX J00003358-2509120	00 ^h 00 ^m 33.59 ^s	-25°09'12.1''	0.0857	Colless et al. (2003a)
2MASX J00000817-2512181	00 ^h 00 ^m 08.16 ^s	-25°12'18.1''	0.0864	Colless et al. (2003a)
2MASX J00004617-2515090	00 ^h 00 ^m 46.18 ^s	-25°15'09.3''	0.0869	Colless et al. (2003a)

Table B1. XMMXCSJ000013.9-251052.1: Column 1 gives the name of the galaxy, column 2 and 3 give the right ascension and declination respectively, and column 4 gives the redshift of the galaxy. Column 5 gives the reference from which the redshift was taken.

Name	RA(J2000)	Dec(J2000)	z	Reference
GALEXMSC J003407.05-432228.7	00 ^h 34 ^m 06.97 ^s	-43°22'30.2''	0.3877	Feruglio et al. (2008)
SWIRE3 J003407.30-432152.8	00 ^h 34 ^m 07.29 ^s	-43°21'52.9''	0.3880	Sacchi et al. (2009)
SWIRE3 J003400.83-432122.5	00 ^h 34 ^m 00.77 ^s	-43°21'22.5''	0.3890	Sacchi et al. (2009)
SWIRE3 J003408.87-432244.6	00 ^h 34 ^m 08.87 ^s	-43°22'44.7''	0.3890	Sacchi et al. (2009)
SWIRE3 J003405.07-431742.3	00 ^h 34 ^m 05.06 ^s	-43°17'42.3''	0.3910	Sacchi et al. (2009)
IRAC 236852	00 ^h 34 ^m 27.40 ^s	-43°18'59.6''	0.3925	Feruglio et al. (2008)
SWIRE3 J003425.16-431912.1	00 ^h 34 ^m 25.15 ^s	-43°19'12.2''	0.3930	Sacchi et al. (2009)
SWIRE3 J003422.50-431550.8	00 ^h 34 ^m 22.49 ^s	-43°15'51.0''	0.3940	Sacchi et al. (2009)
SWIRE3 J003428.37-431704.2	00 ^h 34 ^m 28.36 ^s	-43°17'04.4''	0.3940	Sacchi et al. (2009)
SWIRE3 J003444.36-431806.2	00 ^h 34 ^m 44.37 ^s	-43°18'06.4''	0.3940	Sacchi et al. (2009)
SWIRE3 J003413.21-431727.4	00 ^h 34 ^m 13.20 ^s	-43°17'27.5''	0.3960	Sacchi et al. (2009)
SWIRE3 J003417.67-431909.8	00 ^h 34 ^m 17.67 ^s	-43°19'09.9''	0.3960	Sacchi et al. (2009)
SWIRE3 J003424.77-432117.8	00 ^h 34 ^m 24.78 ^s	-43°21'18.2''	0.3960	Sacchi et al. (2009)
SWIRE3 J003430.66-431956.6	00 ^h 34 ^m 30.65 ^s	-43°19'56.8''	0.3960	Sacchi et al. (2009)
SWIRE3 J003419.36-432157.4	00 ^h 34 ^m 19.35 ^s	-43°21'57.6''	0.3970	Sacchi et al. (2009)
SWIRE3 J003426.75-431854.7	00 ^h 34 ^m 26.74 ^s	-43°18'54.6''	0.3970	Sacchi et al. (2009)
SWIRE3 J003407.33-432141.6	00 ^h 34 ^m 07.33 ^s	-43°21'41.7''	0.3980	Sacchi et al. (2009)
SWIRE3 J003417.78-431928.4	00 ^h 34 ^m 17.77 ^s	-43°19'28.5''	0.3980	Sacchi et al. (2009)
ESIS J003412.63-431705.5	00 ^h 34 ^m 12.63 ^s	-43°17'05.5''	0.3990	Sacchi et al. (2009)
SWIRE3 J003425.85-432057.8	00 ^h 34 ^m 25.86 ^s	-43°20'58.0''	0.3990	Sacchi et al. (2009)
SWIRE3 J003424.03-431914.9	00 ^h 34 ^m 24.02 ^s	-43°19'15.0''	0.4010	Sacchi et al. (2009)
SWIRE3 J003442.95-431727.6	00 ^h 34 ^m 42.94 ^s	-43°17'27.2''	0.4020	Sacchi et al. (2009)

Table B2. XMMXCSJ003430.1-431905.6: All columns are as explained in Table B1.

Name	RA(J2000)	Dec(J2000)	z	Reference
CI 0053-37:[CHM98] 12	00 ^h 55 ^m 55.56 ^s	-37°32'19.7''	0.1613	Guzzo et al. (2009)
CI 0053-37:[CHM98] 14	00 ^h 55 ^m 57.74 ^s	-37°32'22.6''	0.1613	Guzzo et al. (2009)
CI 0053-37:[CHM98] 08	00 ^h 55 ^m 58.90 ^s	-37°33'00.7''	0.1617	Cappi et al. (1998)
(GSB2009) J005552.68-373143.0	00 ^h 55 ^m 52.68 ^s	-37°31'43.0''	0.1626	Guzzo et al. (2009)
2MASX J00555916-3732186	00 ^h 55 ^m 59.11 ^s	-37°32'18.2''	0.1631	Cappi et al. (1998)
APMUKS(BJ) B005339.96-374945.2	00 ^h 56 ^m 01.56 ^s	-37°33'32.0''	0.1633	Guzzo et al. (2009)
CI 0053-37:[CHM98] 15	00 ^h 55 ^m 59.32 ^s	-37°32'35.2''	0.1636	Cappi et al. (1998)
APMUKS(BJ) B005340.88-374818.8	00 ^h 56 ^m 02.42 ^s	-37°32'04.6''	0.1638	Cappi et al. (1998)
CI 0053-37:[CHM98] 20	00 ^h 55 ^m 56.26 ^s	-37°31'48.0''	0.1649	Cappi et al. (1998)
2XMM J005557.1-373237	00 ^h 55 ^m 56.74 ^s	-37°32'35.4''	0.1653	Cappi et al. (1998)
CI 0053-37:[CHM98] 09	00 ^h 56 ^m 02.76 ^s	-37°33'03.9''	0.1654	Cappi et al. (1998)
2MASX J00560639-3733176	00 ^h 56 ^m 06.41 ^s	-37°33'17.6''	0.1661	Guzzo et al. (2009)
CI 0053-37:[CHM98] 21	00 ^h 56 ^m 09.54 ^s	-37°31'49.0''	0.1663	Cappi et al. (1998)
(GSB2009) J005559.52-373343.2	00 ^h 55 ^m 59.52 ^s	-37°33'43.2''	0.1665	Guzzo et al. (2009)
APMUKS(BJ) B005339.81-374854.8	00 ^h 56 ^m 01.34 ^s	-37°32'40.9''	0.1673	Cappi et al. (1998)
APMUKS(BJ) B005343.30-374914.5	00 ^h 56 ^m 04.82 ^s	-37°33'00.0''	0.1682	Guzzo et al. (2009)
(GSB2009) J005552.42-373131.8	00 ^h 55 ^m 52.42 ^s	-37°31'31.8''	0.1686	Guzzo et al. (2009)
CI 0053-37:[CHM98] 04	00 ^h 56 ^m 09.71 ^s	-37°33'39.9''	0.1691	Cappi et al. (1998)
2MASX J00560925-3733595	00 ^h 56 ^m 09.28 ^s	-37°33'59.3''	0.1694	Cappi et al. (1998)
APMUKS(BJ) B005348.77-375021.3	00 ^h 56 ^m 10.23 ^s	-37°34'07.9''	0.1720	Cappi et al. (1998)
CI 0053-37:[CHM98] 11	00 ^h 56 ^m 04.75 ^s	-37°32'51.0''	0.1721	Cappi et al. (1998)
CI 0053-37:[CHM98] 03	00 ^h 56 ^m 07.07 ^s	-37°33'49.4''	0.1722	Cappi et al. (1998)

Table B3. XMMXCSJ005603.0-373248.0: All columns are as explained in Table B1.

Name	RA(J2000)	Dec(J2000)	z	Reference
2MASX J01530967+0102002	01 ^h 53 ^m 09.69 ^s	+01°02'00.3''	0.0579	Berlind et al. (2006)
2MASX J01531414+0103443	01 ^h 53 ^m 14.16 ^s	+01°03'44.4''	0.0579	Abazajian et al. (2003)
2MASX J01531014+0101302	01 ^h 53 ^m 10.13 ^s	+01°01'30.5''	0.0586	Abazajian et al. (2003)
2MASX J01530528+0059092	01 ^h 53 ^m 05.29 ^s	+00°59'09.2''	0.0588	Stoughton et al. (2002)
2MASX J01531034+0105562	01 ^h 53 ^m 10.37 ^s	+01°05'56.7''	0.0590	Abazajian et al. (2003)
2MASX J01530827+0101502	01 ^h 53 ^m 08.29 ^s	+01°01'50.7''	0.0594	Berlind et al. (2006)
SDSS J015251.27+010705.4	01 ^h 52 ^m 51.28 ^s	+01°07'05.4''	0.0595	Stoughton et al. (2002)
SDSS J015316.74+010139.4	01 ^h 53 ^m 16.75 ^s	+01°01'39.5''	0.0596	Berlind et al. (2006)
2MASX J01530347+0101232	01 ^h 53 ^m 03.49 ^s	+01°01'23.0''	0.0596	Abazajian et al. (2003)
2MASX J01531521+0102203	01 ^h 53 ^m 15.24 ^s	+01°02'20.7''	0.0598	Abazajian et al. (2003)
SDSS J015249.63+010023.3	01 ^h 52 ^m 49.61 ^s	+01°00'22.6''	0.0600	Goto et al. (2003)
2MASX J01532128+0055143	01 ^h 53 ^m 21.27 ^s	+00°55'14.6''	0.0607	Stoughton et al. (2002)

Table B4. XMMXCSJ015315.0+010214.2: All columns are as explained in Table B1.

Name	RA(J2000)	Dec(J2000)	z	Reference
(MLF2006) J072049.93+710856.6	07 ^h 20 ^m 49.93 ^s	+71°08'56.6''	0.2270	Mulchaey et al. (2006)
1RXS J072049.0+710724	07 ^h 20 ^m 47.35 ^s	+71°07'15.4''	0.2274	Jeltema et al. (2007)
(MLF2006) J072103.45+710906.0	07 ^h 21 ^m 03.45 ^s	+71°09'06.0''	0.2274	Mulchaey et al. (2006)
(MLF2006) J072044.89+710845.5	07 ^h 20 ^m 44.89 ^s	+71°08'45.5''	0.2275	Mulchaey et al. (2006)
(MLF2006) J072039.75+710950.8	07 ^h 20 ^m 39.75 ^s	+71°09'50.8''	0.2277	Mulchaey et al. (2006)
(MLF2006) J072046.96+710922.8	07 ^h 20 ^m 46.96 ^s	+71°09'22.8''	0.2285	Jeltema et al. (2007)
(MLF2006) J072059.93+710932.2	07 ^h 20 ^m 59.93 ^s	+71°09'32.2''	0.2288	Mulchaey et al. (2006)
(JML2007) J072044.89+710930.9	07 ^h 20 ^m 44.89 ^s	+71°09'30.9''	0.2294	Jeltema et al. (2007)
(JML2007) J072048.69+711123.2	07 ^h 20 ^m 48.69 ^s	+71°11'23.2''	0.2299	Jeltema et al. (2007)
GALEXASC J072040.85+711127.4	07 ^h 20 ^m 40.46 ^s	+71°11'27.9''	0.2300	Jeltema et al. (2007)
(MLF2006) J072053.73+710859.6	07 ^h 20 ^m 53.73 ^s	+71°08'59.6''	0.2300	Jeltema et al. (2007)
(MLF2006) J072114.17+7111028.0	07 ^h 21 ^m 14.17 ^s	+71°10'28.0''	0.2304	Mulchaey et al. (2006)
(MLF2006) J072054.47+710857.4	07 ^h 20 ^m 54.47 ^s	+71°08'57.4''	0.2305	Mulchaey et al. (2006)
(JML2007) J072045.08+711118.1	07 ^h 20 ^m 45.08 ^s	+71°11'18.1''	0.2306	Jeltema et al. (2007)
(JML2007) J072046.39+711005.0	07 ^h 20 ^m 46.39 ^s	+71°10'05.0''	0.2307	Jeltema et al. (2007)
(MLF2006) J072103.43+710917.7	07 ^h 21 ^m 03.43 ^s	+71°09'17.7''	0.2308	Mulchaey et al. (2006)
GALEXMSC J072113.65+710952.5	07 ^h 21 ^m 13.26 ^s	+71°09'49.8''	0.2314	Mulchaey et al. (2006)
(MLF2006) J072109.63+710903.3	07 ^h 21 ^m 09.63 ^s	+71°09'03.3''	0.2315	Mulchaey et al. (2006)
(MLF2006) J072109.09+710922.1	07 ^h 21 ^m 09.09 ^s	+71°09'22.1''	0.2320	Mulchaey et al. (2006)
(JML2007) J072039.35+710730.9	07 ^h 20 ^m 39.35 ^s	+71°07'30.9''	0.2323	Jeltema et al. (2007)
GALEXASC J072111.89+710857.1	07 ^h 21 ^m 11.40 ^s	+71°08'57.2''	0.2325	Mulchaey et al. (2006)
(MLF2006) J072048.06+711037.5	07 ^h 20 ^m 48.06 ^s	+71°10'37.5''	0.2326	Jeltema et al. (2007)
(MLF2006) J072058.02+710916.2	07 ^h 20 ^m 58.02 ^s	+71°09'16.2''	0.2328	Jeltema et al. (2007)
(MLF2006) J072050.33+710925.7	07 ^h 20 ^m 50.33 ^s	+71°09'25.7''	0.2329	Jeltema et al. (2007)
(JML2007) J072056.17+711105.1	07 ^h 20 ^m 56.17 ^s	+71°11'05.1''	0.2331	Jeltema et al. (2007)
(JML2007) J072055.02+710815.0	07 ^h 20 ^m 55.02 ^s	+71°08'15.0''	0.2335	Jeltema et al. (2007)
(MLF2006) J072046.75+710904.4	07 ^h 20 ^m 46.75 ^s	+71°09'04.4''	0.2337	Jeltema et al. (2007)
GALEXMSC J072016.54+710943.2	07 ^h 20 ^m 16.53 ^s	+71°09'42.6''	0.2340	Mulchaey et al. (2006)
(MLF2006) J072044.19+710854.1	07 ^h 20 ^m 44.19 ^s	+71°08'54.1''	0.2347	Mulchaey et al. (2006)

Table B5. XMMXCSJ072054.3+710900.5: All columns are as explained in Table B1.

Name	RA(J2000)	Dec(J2000)	z	Reference
(VMF98) 049:[BBS2002] 021	08 ^h 19 ^m 42.12 ^s	+70°54'32.1''	0.2272	Balogh et al. (2002)
(VMF98) 049:[BBS2002] 040	08 ^h 19 ^m 11.99 ^s	+70°55'43.8''	0.2274	Balogh et al. (2002)
(VMF98) 049:[BBS2002] 027	08 ^h 19 ^m 01.38 ^s	+70°54'51.6''	0.2277	Balogh et al. (2002)
(VMF98) 049:[BBS2002] 002	08 ^h 18 ^m 48.72 ^s	+70°52'55.8''	0.2278	Balogh et al. (2002)
(VMF98) 049:[BBS2002] 026	08 ^h 19 ^m 22.86 ^s	+70°54'44.9''	0.2280	Balogh et al. (2002)
(VMF98) 049:[BBS2002] 033	08 ^h 19 ^m 17.75 ^s	+70°55'01.0''	0.2289	Balogh et al. (2002)
(VMF98) 049:[BBS2002] 013	08 ^h 19 ^m 46.92 ^s	+70°53'53.9''	0.2294	Balogh et al. (2002)
(VMF98) 049:[BBS2002] 025	08 ^h 18 ^m 56.12 ^s	+70°54'39.4''	0.2296	Balogh et al. (2002)
(VMF98) 049:[BBS2002] 029	08 ^h 18 ^m 54.03 ^s	+70°54'52.6''	0.2297	Balogh et al. (2002)
(VMF98) 049:[BBS2002] 011	08 ^h 19 ^m 07.76 ^s	+70°53'37.7''	0.2304	Balogh et al. (2002)
2MASX J08191836+7055042	08 ^h 19 ^m 18.31 ^s	+70°55'04.2''	0.2304	Balogh et al. (2002)
(VMF98) 049:[BBS2002] 036	08 ^h 19 ^m 23.75 ^s	+70°55'24.3''	0.2304	Balogh et al. (2002)
(VMF98) 049:[BBS2002] 015	08 ^h 19 ^m 35.25 ^s	+70°54'02.4''	0.2305	Balogh et al. (2002)
(VMF98) 049:[BBS2002] 047	08 ^h 19 ^m 23.60 ^s	+70°56'30.8''	0.2306	Balogh et al. (2002)
(VMF98) 049:[BBS2002] 012	08 ^h 19 ^m 37.97 ^s	+70°53'49.5''	0.2309	Balogh et al. (2002)
(VMF98) 049:[BBS2002] 037	08 ^h 19 ^m 05.95 ^s	+70°55'34.5''	0.2310	Balogh et al. (2002)
(VMF98) 049:[BBS2002] 043	08 ^h 19 ^m 12.64 ^s	+70°56'05.8''	0.2313	Balogh et al. (2002)
(VMF98) 049:[BBS2002] 006	08 ^h 19 ^m 06.49 ^s	+70°53'04.1''	0.2319	Balogh et al. (2002)
(VMF98) 049:[BBS2002] 016	08 ^h 19 ^m 04.37 ^s	+70°53'55.0''	0.2320	Balogh et al. (2002)

Table B6. XMMXCSJ081918.6+705457.5: All columns are as explained in Table B1.

Name	RA(J2000)	Dec(J2000)	z	Reference
SDSS J094400.28+164011.1	09 ^h 44 ^m 00.29 ^s	+16°40′11.2″	0.2487	Verdugo et al. (2008)
SDSS J094334.06+164035.7	09 ^h 43 ^m 34.06 ^s	+16°40′35.7″	0.2500	Verdugo et al. (2008)
SDSS J094353.35+163958.8	09 ^h 43 ^m 53.35 ^s	+16°39′58.8″	0.2511	Verdugo et al. (2008)
SDSS J094345.51+164130.4	09 ^h 43 ^m 45.52 ^s	+16°41′30.5″	0.2514	Verdugo et al. (2008)
SDSS J094353.48+164022.7	09 ^h 43 ^m 53.49 ^s	+16°40′22.7″	0.2516	Verdugo et al. (2008)
SDSS J094358.03+164116.5	09 ^h 43 ^m 58.03 ^s	+16°41′16.6″	0.2520	Verdugo et al. (2008)
2MASX J09435839+1641091	09 ^h 43 ^m 58.33 ^s	+16°41′09.1″	0.2527	Verdugo et al. (2008)
SDSS J094351.68+164144.7	09 ^h 43 ^m 51.68 ^s	+16°41′44.7″	0.2529	Verdugo et al. (2008)
SDSS J094353.53+164142.6	09 ^h 43 ^m 53.53 ^s	+16°41′42.7″	0.2529	Verdugo et al. (2008)
SDSS J094333.62+163906.3	09 ^h 43 ^m 33.62 ^s	+16°39′06.3″	0.2530	Verdugo et al. (2008)
SDSS J094338.73+163854.9	09 ^h 43 ^m 38.74 ^s	+16°38′55.0″	0.2533	Verdugo et al. (2008)
SDSS J094401.36+163800.9	09 ^h 44 ^m 01.37 ^s	+16°38′01.0″	0.2536	Verdugo et al. (2008)
SDSS J094352.54+164439.4	09 ^h 43 ^m 52.54 ^s	+16°44′39.5″	0.2538	Verdugo et al. (2008)
SDSS J094358.77+164001.9	09 ^h 43 ^m 58.78 ^s	+16°40′01.9″	0.2538	Verdugo et al. (2008)
SDSS J094332.40+164000.5	09 ^h 43 ^m 32.41 ^s	+16°40′00.6″	0.2539	Verdugo et al. (2008)
SDSS J094359.68+163729.9	09 ^h 43 ^m 59.69 ^s	+16°37′29.9″	0.2542	Verdugo et al. (2008)
SDSS J094348.66+164038.8	09 ^h 43 ^m 48.67 ^s	+16°40′38.8″	0.2546	Verdugo et al. (2008)
SDSS J094355.86+164035.5	09 ^h 43 ^m 55.86 ^s	+16°40′35.6″	0.2551	Verdugo et al. (2008)
SDSS J094336.77+164102.3	09 ^h 43 ^m 36.78 ^s	+16°41′02.3″	0.2552	Verdugo et al. (2008)
SDSS J094356.38+163650.7	09 ^h 43 ^m 56.38 ^s	+16°36′50.8″	0.2552	Verdugo et al. (2008)
SDSS J094358.90+163921.7	09 ^h 43 ^m 58.90 ^s	+16°39′21.7″	0.2561	Verdugo et al. (2008)
SDSS J094405.00+163834.3	09 ^h 44 ^m 05.00 ^s	+16°38′34.4″	0.2561	Verdugo et al. (2008)
SDSS J094359.32+164109.4	09 ^h 43 ^m 59.33 ^s	+16°41′09.4″	0.2570	Verdugo et al. (2008)
SDSS J094342.95+164034.1	09 ^h 43 ^m 42.96 ^s	+16°40′34.1″	0.2573	Verdugo et al. (2008)
SDSS J094403.16+163948.1	09 ^h 44 ^m 03.17 ^s	+16°39′48.1″	0.2574	Verdugo et al. (2008)
SDSS J094337.95+163932.2	09 ^h 43 ^m 37.95 ^s	+16°39′32.3″	0.2574	Verdugo et al. (2008)
SDSS J094340.06+163923.2	09 ^h 43 ^m 40.06 ^s	+16°39′23.3″	0.2578	Verdugo et al. (2008)

Table B7. XMMXCSJ094358.2+164120.7: All columns are as explained in Table B1.

Name	RA(J2000)	Dec(J2000)	z	Reference
SDSS J100027.86+251750.9	10 ^h 00 ^m 27.87 ^s	+25°17′51.0″	0.0495	Le Fevre et al. (1995)
2MASX J09590595+2512006	09 ^h 59 ^m 05.97 ^s	+25°12′01.0″	0.0511	Adelman-McCarthy et al. (2008)
2MASX J09585969+2518276	09 ^h 58 ^m 59.70 ^s	+25°18′27.8″	0.0518	Adelman-McCarthy et al. (2008)
SDSS J095848.25+251116.9	09 ^h 58 ^m 48.25 ^s	+25°11′16.9″	0.0518	Adelman-McCarthy et al. (2008)
2MASX J09594076+2459301	09 ^h 59 ^m 40.76 ^s	+24°59′30.5″	0.0519	Adelman-McCarthy et al. (2008)
2MASX J10001346+2450242	10 ^h 00 ^m 13.49 ^s	+24°50′24.1″	0.0519	Adelman-McCarthy et al. (2008)
UGC 05361	09 ^h 59 ^m 00.86 ^s	+25°12′08.2″	0.0519	Huchra et al. (2012)
2MASX J09590450+2527176	09 ^h 59 ^m 04.50 ^s	+25°27′18.2″	0.0519	Adelman-McCarthy et al. (2008)
SDSS J100144.49+250159.3	10 ^h 01 ^m 44.49 ^s	+25°01′59.3″	0.0526	Adelman-McCarthy et al. (2008)
2MASX J09591647+2509482	09 ^h 59 ^m 16.44 ^s	+25°09′48.8″	0.0528	Adelman-McCarthy et al. (2008)
SDSS J095900.71+251134.6	09 ^h 59 ^m 00.72 ^s	+25°11′34.7″	0.0529	Adelman-McCarthy et al. (2008)
2MASX J10010959+2520030	10 ^h 01 ^m 09.60 ^s	+25°20′03.3″	0.0542	Adelman-McCarthy et al. (2008)
SDSS J100105.06+245810.3	10 ^h 01 ^m 05.06 ^s	+24°58′10.4″	0.0549	Adelman-McCarthy et al. (2008)
SDSS J095938.75+251010.8	09 ^h 59 ^m 38.75 ^s	+25°10′10.9″	0.0555	Adelman-McCarthy et al. (2008)
2MASX J10000767+2514162	10 ^h 00 ^m 07.65 ^s	+25°14′16.4″	0.0556	Adelman-McCarthy et al. (2008)

Table B8. XMMXCSJ095957.6+251629.0: All columns are as explained in Table B1.

Name	RA(J2000)	Dec(J2000)	z	Reference
SDSS J100052.66+013941.1	10 ^h 00 ^m 52.67 ^s	+01°39'41.2''	0.2166	Lilly et al. (2007)
zCOSMOS 805589	10 ^h 00 ^m 33.07 ^s	+01°41'04.8''	0.2179	Lilly et al. (2007)
SDSS J100057.84+013637.1	10 ^h 00 ^m 57.84 ^s	+01°36'37.2''	0.2190	Lilly et al. (2007)
2MASX J10004852+0139137	10 ^h 00 ^m 48.54 ^s	+01°39'13.9''	0.2190	Colless et al. (2003b)
SDSS J100037.77+014013.9	10 ^h 00 ^m 37.77 ^s	+01°40'14.0''	0.2194	Lilly et al. (2007)
SDSS J100057.85+013752.1	10 ^h 00 ^m 57.85 ^s	+01°37'52.2''	0.2195	Lilly et al. (2007)
SDSS J100045.29+013847.4	10 ^h 00 ^m 45.30 ^s	+01°38'47.4''	0.2205	Abazajian et al. (2004)
2MASX J10004552+0139267	10 ^h 00 ^m 45.54 ^s	+01°39'26.5''	0.2207	Abazajian et al. (2003)
zCOSMOS 805608	10 ^h 00 ^m 32.16 ^s	+01°38'43.5''	0.2212	Lilly et al. (2007)
SDSS J100044.55+013942.0	10 ^h 00 ^m 44.55 ^s	+01°39'42.2''	0.2214	Trump et al. (2007)
SDSS J100038.81+013827.6	10 ^h 00 ^m 38.81 ^s	+01°38'27.6''	0.2219	Lilly et al. (2007)
SDSS J100049.03+013526.8	10 ^h 00 ^m 49.03 ^s	+01°35'26.9''	0.2220	Brusa et al. (2010)
SDSS J100103.45+014413.1	10 ^h 01 ^m 03.45 ^s	+01°44'13.1''	0.2220	Lilly et al. (2007)
zCOSMOS 805183	10 ^h 00 ^m 50.21 ^s	+01°43'20.6''	0.2224	Lilly et al. (2007)
zCOSMOS 805250	10 ^h 00 ^m 47.36 ^s	+01°37'41.6''	0.2235	Lilly et al. (2007)
SDSS J100108.66+013935.2	10 ^h 01 ^m 08.67 ^s	+01°39'35.2''	0.2278	Abazajian et al. (2004)

Table B9. XMMXCSJ100047.4+013926.9: All columns are as explained in Table B1.

Name	RA(J2000)	Dec(J2000)	z	Reference
SDSS J100125.41+023145.1	10 ^h 01 ^m 25.42 ^s	+02°31'45.2''	0.1210	Abazajian et al. (2004)
SDSS J100131.47+022556.7	10 ^h 01 ^m 31.48 ^s	+02°25'56.7''	0.1211	Trump et al. (2007)
SDSS J100157.95+022746.1	10 ^h 01 ^m 57.96 ^s	+02°27'46.1''	0.1213	Lilly et al. (2007)
SDSS J100120.63+022601.5	10 ^h 01 ^m 20.63 ^s	+02°26'01.6''	0.1216	Lilly et al. (2007)
GALEXMSC J100120.08+022019.9	10 ^h 01 ^m 20.07 ^s	+02°20'20.0''	0.1224	Lilly et al. (2007)
SDSS J100131.65+022001.3	10 ^h 01 ^m 31.66 ^s	+02°20'01.3''	0.1224	Lilly et al. (2007)
SDSS J100135.32+022831.2	10 ^h 01 ^m 35.33 ^s	+02°28'31.2''	0.1225	Lilly et al. (2007)
SDSS J100138.98+022607.8	10 ^h 01 ^m 38.99 ^s	+02°26'07.8''	0.1228	Lilly et al. (2007)
SDSS J100130.65+022624.2	10 ^h 01 ^m 30.65 ^s	+02°26'24.2''	0.1228	Abazajian et al. (2004)
SDSS J100117.12+022919.1	10 ^h 01 ^m 17.13 ^s	+02°29'19.2''	0.1230	Lilly et al. (2007)
SDSS J100141.85+022519.5	10 ^h 01 ^m 41.86 ^s	+02°25'19.5''	0.1232	Abazajian et al. (2004)
2MASX J10013646+0226418	10 ^h 01 ^m 36.46 ^s	+02°26'42.2''	0.1234	Abazajian et al. (2003)
2MASX J10013692+0230318	10 ^h 01 ^m 36.93 ^s	+02°30'31.9''	0.1237	Abazajian et al. (2003)
SDSS J100119.77+022756.1	10 ^h 01 ^m 19.77 ^s	+02°27'56.1''	0.1237	Lilly et al. (2007)
zCOSMOS 830563	10 ^h 01 ^m 20.30 ^s	+02°27'14.6''	0.1237	Lilly et al. (2007)
2MASX J10013974+0225487	10 ^h 01 ^m 39.76 ^s	+02°25'48.8''	0.1242	Abazajian et al. (2003)
SDSS J100143.45+022409.8	10 ^h 01 ^m 43.45 ^s	+02°24'09.9''	0.1245	Abazajian et al. (2004)
SDSS J100115.65+022423.0	10 ^h 01 ^m 15.66 ^s	+02°24'23.1''	0.1245	Lilly et al. (2007)
SDSS J100144.43+022654.0	10 ^h 01 ^m 44.43 ^s	+02°26'54.0''	0.1246	Trump et al. (2007)
SDSS J100132.33+023306.1	10 ^h 01 ^m 32.33 ^s	+02°33'06.2''	0.1253	Lilly et al. (2007)
SDSS J100123.59+022416.8	10 ^h 01 ^m 23.59 ^s	+02°24'16.8''	0.1264	Lilly et al. (2007)
SDSS J100135.42+022246.8	10 ^h 01 ^m 35.42 ^s	+02°22'46.8''	0.1265	Lilly et al. (2007)
SDSS J100147.06+022257.6	10 ^h 01 ^m 47.07 ^s	+02°22'57.7''	0.1269	Lilly et al. (2007)
SDSS J100123.20+022414.9	10 ^h 01 ^m 23.20 ^s	+02°24'14.9''	0.1273	Lilly et al. (2007)
SDSS J100154.07+021935.8	10 ^h 01 ^m 54.07 ^s	+02°19'35.9''	0.1281	Lilly et al. (2007)
SDSS J100127.72+023126.4	10 ^h 01 ^m 27.73 ^s	+02°31'26.5''	0.1298	Lilly et al. (2007)

Table B10. XMMXCSJ100141.7+022539.8: All columns are as explained in Table B1.

Name	RA(J2000)	Dec(J2000)	z	Reference
2MASX J10403601+4002107	10 ^h 40 ^m 35.98 ^s	+40°02′10.8″	0.1331	Adelman-McCarthy et al. (2006)
SDSS J104045.34+395448.5	10 ^h 40 ^m 45.35 ^s	+39°54′48.6″	0.1341	Sánchez Almeida et al. (2011)
B3 1037+401	10 ^h 40 ^m 44.45 ^s	+39°54′54.9″	0.1341	Adelman-McCarthy et al. (2006)
SDSS J104126.57+395845.5	10 ^h 41 ^m 26.58 ^s	+39°58′45.5″	0.1352	Miller et al. (2002)
SDSS J104043.44+395705.3	10 ^h 40 ^m 43.44 ^s	+39°57′05.3″	0.1357	Adelman-McCarthy et al. (2006)
2MASX J10403391+4003497	10 ^h 40 ^m 33.96 ^s	+40°03′49.5″	0.1369	Miller et al. (2002)
2MASX J10405360+4001417	10 ^h 40 ^m 53.62 ^s	+40°01′42.0″	0.1374	Adelman-McCarthy et al. (2006)
SDSS J104044.49+395711.2	10 ^h 40 ^m 44.50 ^s	+39°57′11.3″	0.1380	Ofek et al. (2007)
SDSS J103943.42+400435.2	10 ^h 39 ^m 43.42 ^s	+40°04′35.2″	0.1384	Adelman-McCarthy et al. (2006)
2MASX J10414241+4000453	10 ^h 41 ^m 42.43 ^s	+40°00′45.8″	0.1385	Adelman-McCarthy et al. (2006)
2MASX J10404446+3957117	10 ^h 40 ^m 44.50 ^s	+39°57′11.3″	0.1386	Schaerer et al. (1999)
SDSS J104047.01+395551.8	10 ^h 40 ^m 47.01 ^s	+39°55′51.8″	0.1386	Adelman-McCarthy et al. (2006)
SDSS J104114.47+395901.6	10 ^h 41 ^m 14.48 ^s	+39°59′01.6″	0.1401	Adelman-McCarthy et al. (2006)
SDSS J104027.21+400459.3	10 ^h 40 ^m 27.22 ^s	+40°04′59.4″	0.1416	Adelman-McCarthy et al. (2006)
SDSS J104006.83+395356.8	10 ^h 40 ^m 06.84 ^s	+39°53′56.9″	0.1420	Adelman-McCarthy et al. (2006)
2MASX J10412053+3947284	10 ^h 41 ^m 20.49 ^s	+39°47′29.3″	0.1433	Adelman-McCarthy et al. (2006)
SDSS J103945.82+400047.0	10 ^h 39 ^m 45.83 ^s	+40°00′47.1″	0.1441	Adelman-McCarthy et al. (2006)

Table B11. XMMXCSJ104044.4+395710.4: All columns are as explained in Table B1.

Name	RA(J2000)	Dec(J2000)	z	Reference
SDSS J111512.70+531930.5	11 ^h 15 ^m 12.71 ^s	+53°19′30.6″	0.4586	Bayliss et al. (2011)
SDSS J111520.84+532100.9	11 ^h 15 ^m 20.84 ^s	+53°21′01.0″	0.4601	Bayliss et al. (2011)
SDSS J111517.30+532115.2	11 ^h 15 ^m 17.30 ^s	+53°21′15.3″	0.4639	Bayliss et al. (2011)
SDSS J111517.85+531949.3	11 ^h 15 ^m 17.85 ^s	+53°19′49.4″	0.4640	Bayliss et al. (2011)
SDSS J111507.37+531955.7	11 ^h 15 ^m 07.38 ^s	+53°19′55.8″	0.4642	Bayliss et al. (2011)
SDSS J111505.53+532042.4	11 ^h 15 ^m 05.54 ^s	+53°20′42.4″	0.4654	Bayliss et al. (2011)
SDSS J111514.49+531948.8	11 ^h 15 ^m 14.49 ^s	+53°19′48.9″	0.4654	Bayliss et al. (2011)
SDSS J111514.51+531853.1	11 ^h 15 ^m 14.51 ^s	+53°18′53.1″	0.4660	Bayliss et al. (2011)
SDSS J111514.84+531954.3	11 ^h 15 ^m 14.85 ^s	+53°19′54.3″	0.4664	Abazajian et al. (2005)
SDSS J111519.70+531837.9	11 ^h 15 ^m 19.71 ^s	+53°18′37.9″	0.4670	Bayliss et al. (2011)
SDSS J111504.19+532100.4	11 ^h 15 ^m 04.20 ^s	+53°21′00.5″	0.4671	Bayliss et al. (2011)
SDSS J111518.75+531948.3	11 ^h 15 ^m 18.76 ^s	+53°19′48.4″	0.4686	Abazajian et al. (2005)
SDSS J111509.79+531925.2	11 ^h 15 ^m 09.79 ^s	+53°19′25.3″	0.4702	Bayliss et al. (2011)
SDSS J111515.10+532002.8	11 ^h 15 ^m 15.10 ^s	+53°20′02.8″	0.4708	Bayliss et al. (2011)
SDSS J111512.25+531830.8	11 ^h 15 ^m 12.26 ^s	+53°18′30.9″	0.4745	Bayliss et al. (2011)
(BHG2011) J111510.10+531939.9	11 ^h 15 ^m 10.11 ^s	+53°19′39.9″	0.4759	Bayliss et al. (2011)

Table B12. XMMXCSJ111515.6+531949.5: All columns are as explained in Table B1.

Name	RA(J2000)	Dec(J2000)	z	Reference
2MASX J11511361+5507364	11 ^h 51 ^m 13.65 ^s	+55°07′36.5″	0.0757	Abazajian et al. (2005)
2MASX J11513633+5505433	11 ^h 51 ^m 36.33 ^s	+55°05′43.3″	0.0781	Abazajian et al. (2005)
SDSS J115109.52+550645.0	11 ^h 51 ^m 09.52 ^s	+55°06′45.1″	0.0782	Abazajian et al. (2005)
SDSS J115107.14+550839.1	11 ^h 51 ^m 07.14 ^s	+55°08′39.3″	0.0783	Abazajian et al. (2005)
2MASX J11510461+5510363	11 ^h 51 ^m 04.57 ^s	+55°10′36.0″	0.0787	Abazajian et al. (2005)
2MASX J11505351+5512012	11 ^h 50 ^m 53.45 ^s	+55°12′01.3″	0.0793	Abazajian et al. (2005)
2MASX J11511349+5506594	11 ^h 51 ^m 13.47 ^s	+55°06′59.2″	0.0794	Abazajian et al. (2005)
(KK81) 1	11 ^h 51 ^m 25.80 ^s	+55°06′19.0″	0.0794	Schweizer (1996)
SDSS J115146.44+550644.2	11 ^h 51 ^m 46.45 ^s	+55°06′44.2″	0.0796	Abazajian et al. (2005)
2MASX J11515770+5508085	11 ^h 51 ^m 57.70 ^s	+55°08′08.4″	0.0797	Abazajian et al. (2005)
2MASX J11512829+5504483	11 ^h 51 ^m 28.30 ^s	+55°04′48.2″	0.0797	Abazajian et al. (2005)
SDSS J115132.91+550757.0	11 ^h 51 ^m 32.92 ^s	+55°07′57.1″	0.0798	Abazajian et al. (2005)
SDSS J115213.62+551312.7	11 ^h 52 ^m 13.62 ^s	+55°13′12.7″	0.0803	Abazajian et al. (2005)
2MASX J11512340+5506563	11 ^h 51 ^m 23.38 ^s	+55°06′56.0″	0.0806	Abazajian et al. (2005)
2MASX J11511641+5509594	11 ^h 51 ^m 16.45 ^s	+55°09′59.0″	0.0811	Abazajian et al. (2005)
SDSS J115201.62+550414.1	11 ^h 52 ^m 01.63 ^s	+55°04′14.2″	0.0814	Abazajian et al. (2005)

Table B13. XMMXCSJ115112.0+550655.5: All columns are as explained in Table B1.

Name	RA(J2000)	Dec(J2000)	z	Reference
SDSS J123140.79+413626.3	12:31 ^m 40.80 ^s	+41°36′26.4″	0.1708	Adelman-McCarthy et al. (2006)
2MASX J12320414+4133324	12:32 ^m 04.12 ^s	+41°33′32.4″	0.1713	Adelman-McCarthy et al. (2006)
2MASX J12315661+4133582	12:31 ^m 56.59 ^s	+41°33′58.5″	0.1719	Adelman-McCarthy et al. (2006)
2MASX J12320054+4133322	12:32 ^m 00.56 ^s	+41°33′31.9″	0.1727	Adelman-McCarthy et al. (2006)
2MASX J12320463+4133362	12:32 ^m 04.68 ^s	+41°33′36.0″	0.1732	Adelman-McCarthy et al. (2007)
2MASX J12315296+4133182	12:31 ^m 52.98 ^s	+41°33′18.7″	0.1739	Adelman-McCarthy et al. (2006)
2MASX J12314144+4139361	12:31 ^m 41.46 ^s	+41°39′35.9″	0.1750	Adelman-McCarthy et al. (2006)
SDSS J123151.89+413434.7	12:31 ^m 51.90 ^s	+41°34′34.7″	0.1750	Adelman-McCarthy et al. (2006)
2MASX J12314386+4137341	12:31 ^m 43.90 ^s	+41°37′33.9″	0.1757	Adelman-McCarthy et al. (2006)
SDSS J123136.04+414314.0	12:31 ^m 36.05 ^s	+41°43′14.0″	0.1763	Adelman-McCarthy et al. (2006)

Table B14. XMMXCSJ123144.4+413732.0: All columns are as explained in Table B1.

Name	RA(J2000)	Dec(J2000)	z	Reference
SDSS J151623.79+000156.4	15 ^h 16 ^m 23.79 ^s	+00°01′56.5″	0.1126	Stoughton et al. (2002)
SDSS J151626.35-000228.8	15 ^h 16 ^m 26.35 ^s	-00°02′28.9″	0.1142	Stoughton et al. (2002)
2MASX J15161900+0005067	15 ^h 16 ^m 19.00 ^s	+00°05′06.6″	0.1147	Abazajian et al. (2003)
2MASX J15162348+0006093	15 ^h 16 ^m 23.49 ^s	+00°06′09.1″	0.1154	Abazajian et al. (2003)
2MASX J15161563+0005291	15 ^h 16 ^m 15.63 ^s	+00°05′29.0″	0.1158	Abazajian et al. (2003)
2MASX J15162547+0003377	15 ^h 16 ^m 25.45 ^s	+00°03′37.6″	0.1167	Abazajian et al. (2003)
SDSS J151626.17+000707.4	15 ^h 16 ^m 26.18 ^s	+00°07′07.5″	0.1167	Stoughton et al. (2002)
2MASX J15161988+0003343	15 ^h 16 ^m 19.92 ^s	+00°03′34.5″	0.1174	Abazajian et al. (2003)
SDSS J151602.71+001518.3	15 ^h 16 ^m 02.71 ^s	+00°15′18.4″	0.1178	Abazajian et al. (2003)
2MASX J15160423+0002561	15 ^h 16 ^m 04.21 ^s	+00°02′56.4″	0.1183	Abazajian et al. (2003)
2MASX J15171323+0009193	15 ^h 17 ^m 13.25 ^s	+00°09′19.7″	0.1186	Abazajian et al. (2003)
SDSS J151640.19-000404.8	15 ^h 16 ^m 40.19 ^s	-00°04′04.8″	0.1188	Stoughton et al. (2002)
2MASX J15160950+0014541	15 ^h 16 ^m 09.53 ^s	+00°14′54.2″	0.1189	Abazajian et al. (2003)
2MASX J15170956+0007443	15 ^h 17 ^m 09.57 ^s	+00°07′44.7″	0.1190	Abazajian et al. (2003)
SDSS J151614.81+000022.5	15 ^h 16 ^m 14.81 ^s	+00°02′22.5″	0.1196	Abazajian et al. (2003)
SDSS J151615.10+000429.5	15 ^h 16 ^m 15.11 ^s	+00°04′29.6″	0.1201	Abazajian et al. (2003)
2MASX J15162640+0017507	15 ^h 16 ^m 26.38 ^s	+00°17′51.1″	0.1202	Abazajian et al. (2003)
SDSS J151629.25+000835.5	15 ^h 16 ^m 29.26 ^s	+00°08′35.6″	0.1203	Abazajian et al. (2003)
2MASX J15161210+0017401	15 ^h 16 ^m 12.12 ^s	+00°17′40.0″	0.1204	Abazajian et al. (2003)
2MASX J15160737+0020071	15 ^h 16 ^m 07.37 ^s	+00°20′07.1″	0.1206	Abazajian et al. (2003)
SDSS J151637.99+000718.7	15 ^h 16 ^m 38.00 ^s	+00°07′18.7″	0.1207	Abazajian et al. (2003)
2MASX J15161794+0005203	15 ^h 16 ^m 17.93 ^s	+00°05′20.5″	0.1208	Guzzo et al. (2009)
SDSS J151559.04-000323.8	15 ^h 15 ^m 59.04 ^s	-00°03′23.9″	0.1208	Stoughton et al. (2002)
SDSS J151709.75+001224.0	15 ^h 17 ^m 09.75 ^s	+00°12′24.1″	0.1210	Abazajian et al. (2003)
SDSS J151615.30-000325.4	15 ^h 16 ^m 15.3 ^s	-00°03′25.4″	0.1211	Abazajian et al. (2003)
SDSS J151649.45-000135.0	15 ^h 16 ^m 49.46 ^s	-00°01′35.0″	0.1215	Abazajian et al. (2003)
2MASX J15160803+0002011	15 ^h 16 ^m 08.06 ^s	+00°02′01.1″	0.1215	Abazajian et al. (2003)
SDSS J151624.58-000923.7	15 ^h 16 ^m 24.58 ^s	-00°09′23.7″	0.1216	Abazajian et al. (2003)
SDSS J151604.14+001024.8	15 ^h 16 ^m 04.15 ^s	+00°01′24.9″	0.1218	Abazajian et al. (2003)
2MASX J15160330+0008271	15 ^h 16 ^m 03.33 ^s	+00°08′27.5″	0.1223	Abazajian et al. (2003)
SDSS J151614.44+000508.3	15 ^h 16 ^m 14.45 ^s	+00°05′08.4″	0.1229	Guzzo et al. (2009)
SDSS J151613.19+000509.1	15 ^h 16 ^m 13.19 ^s	+00°05′09.1″	0.1239	Guzzo et al. (2009)
SDSS J151631.54+000648.1	15 ^h 16 ^m 31.54 ^s	+00°06′48.2″	0.1260	Abazajian et al. (2003)
2MASX J15155460+0002127	15 ^h 15 ^m 54.63 ^s	+00°02′13.0″	0.1266	Abazajian et al. (2003)
2MASX J15163414-0004296	15 ^h 16 ^m 34.14 ^s	-00°04′29.7″	0.1266	Jones et al. (2009)

Table B15. XMMXCSJ151618.6+000531.3: All columns are as explained in Table B1.

Name	RA(J2000)	Dec(J2000)	z	Reference
SDSS J161126.49+541619.2	16 ^h 11 ^m 26.49 ^s	+54°16′19.2″	0.3310	Trichas et al. (2010)
SDSS J161131.39+541333.1	16 ^h 11 ^m 31.39 ^s	+54°13′33.2″	0.3330	Trichas et al. (2010)
SDSS J161147.78+541132.2	16 ^h 11 ^m 47.78 ^s	+54°11′32.3″	0.3340	Trichas et al. (2010)
ELAIS06S(R) J161127.5+541422	16 ^h 11 ^m 27.53 ^s	+54°14′22.7″	0.3350	Trichas et al. (2010)
SDSS J161122.54+541706.5	16 ^h 11 ^m 22.54 ^s	+54°17′06.6″	0.3360	Trichas et al. (2010)
SDSS J161134.91+541404.6	16 ^h 11 ^m 34.92 ^s	+54°14′04.7″	0.3360	Trichas et al. (2010)
SDSS J161135.93+541634.5	16 ^h 11 ^m 35.94 ^s	+54°16′34.5″	0.3380	Trichas et al. (2010)
SDSS J161138.50+541922.0	16 ^h 11 ^m 38.50 ^s	+54°19′22.1″	0.3390	Trichas et al. (2010)
SDSS J161128.25+541720.8	16 ^h 11 ^m 28.26 ^s	+54°17′20.8″	0.3400	Trichas et al. (2010)
SDSS J161140.23+541741.1	16 ^h 11 ^m 40.24 ^s	+54°17′41.1″	0.3410	Trichas et al. (2010)
SDSS J161143.52+541628.5	16 ^h 11 ^m 43.53 ^s	+54°16′28.5″	0.3410	Trichas et al. (2010)
SDSS J161115.41+541627.4	16 ^h 11 ^m 15.42 ^s	+54°16′27.4″	0.3420	Trichas et al. (2010)

Table B16. XMMXCSJ161132.7+541628.3: All columns are as explained in Table B1.

Name	RA(J2000)	Dec(J2000)	z	Reference
SDSS J163057.87+243412.6	16 ^h 30 ^m 57.88 ^s	+24°34'12.7''	0.0560	Adelman-McCarthy et al. (2006)
CGCG 138-016	16 ^h 28 ^m 36.04 ^s	+24°33'19.8''	0.0571	Freudling et al. (1992)
SDSS J162854.19+243138.5	16 ^h 28 ^m 54.20 ^s	+24°31'38.6''	0.0574	Adelman-McCarthy et al. (2006)
2MASX J16305968+2437076	16 ^h 30 ^m 59.72 ^s	+24°37'08.0''	0.0579	Adelman-McCarthy et al. (2007)
SDSS J163039.80+243938.2	16 ^h 30 ^m 39.80 ^s	+24°39'38.3''	0.0580	Adelman-McCarthy et al. (2006)
2MASX J16310298+2442456	16 ^h 31 ^m 03.00 ^s	+24°42'45.6''	0.0581	Adelman-McCarthy et al. (2006)
2MASX J16311876+2442442	16 ^h 31 ^m 18.75 ^s	+24°42'44.2''	0.0582	Adelman-McCarthy et al. (2006)
2MASX J16310320+2442586	16 ^h 31 ^m 03.26 ^s	+24°42'58.5''	0.0586	Adelman-McCarthy et al. (2007)
SDSS J163056.45+243816.4	16 ^h 30 ^m 56.45 ^s	+24°38'16.4''	0.0589	Adelman-McCarthy et al. (2006)
2MASX J16293963+2408563	16 ^h 29 ^m 39.59 ^s	+24°08'56.0''	0.0591	Adelman-McCarthy et al. (2007)
SDSS J163021.72+245911.6	16 ^h 30 ^m 21.73 ^s	+24°59'11.6''	0.0607	Adelman-McCarthy et al. (2006)
SDSS J163020.55+243457.6	16 ^h 30 ^m 20.56 ^s	+24°34'57.6''	0.0611	Adelman-McCarthy et al. (2006)
SDSS J163022.47+243215.9	16 ^h 30 ^m 22.48 ^s	+24°32'16.0''	0.0613	Adelman-McCarthy et al. (2006)
2MASX J16301853+2430424	16 ^h 30 ^m 18.54 ^s	+24°30'42.0''	0.0614	Adelman-McCarthy et al. (2007)
2MASX J16303722+2440374	16 ^h 30 ^m 37.21 ^s	+24°40'37.8''	0.0616	Adelman-McCarthy et al. (2006)
SDSS J163031.89+242519.5	16 ^h 30 ^m 31.89 ^s	+24°25'19.6''	0.0617	Adelman-McCarthy et al. (2006)
2MASX J16300229+2434054	16 ^h 30 ^m 02.28 ^s	+24°34'05.3''	0.0618	Adelman-McCarthy et al. (2007)
SDSS J163026.85+243652.1	16 ^h 30 ^m 26.86 ^s	+24°36'52.2''	0.0619	Adelman-McCarthy et al. (2006)
2MASX J16295863+2440084	16 ^h 29 ^m 58.65 ^s	+24°40'08.3''	0.0620	Adelman-McCarthy et al. (2006)
SDSS J163025.22+243517.2	16 ^h 30 ^m 25.23 ^s	+24°35'17.3''	0.0622	Adelman-McCarthy et al. (2006)
2MASX J16302666+2436404	16 ^h 30 ^m 26.65 ^s	+24°36'40.3''	0.0623	Adelman-McCarthy et al. (2006)
SDSS J163110.03+243637.9	16 ^h 31 ^m 10.04 ^s	+24°36'38.0''	0.0623	Adelman-McCarthy et al. (2006)
MCG +04-39-010 NED01	16 ^h 30 ^m 14.56 ^s	+24°34'38.0''	0.0626	Adelman-McCarthy et al. (2006)
SDSS J163046.39+245653.0	16 ^h 30 ^m 46.40 ^s	+24°56'53.1''	0.0629	Adelman-McCarthy et al. (2006)
2MASX J16300112+2432064	16 ^h 30 ^m 01.12 ^s	+24°32'06.8''	0.0630	Adelman-McCarthy et al. (2007)
CGCG 138-030	16 ^h 30 ^m 53.84 ^s	+24°33'43.6''	0.0632	Huchra et al. (2012)
SDSS J162854.70+244050.7	16 ^h 28 ^m 54.71 ^s	+24°40'50.8''	0.0632	Adelman-McCarthy et al. (2006)
SDSS J163042.59+242611.3	16 ^h 30 ^m 42.60 ^s	+24°26'11.3''	0.0633	Adelman-McCarthy et al. (2006)
2MASX J16314233+2445531	16 ^h 31 ^m 42.33 ^s	+24°45'53.1''	0.0634	Adelman-McCarthy et al. (2007)
MCG +04-39-010 NED07	16 ^h 30 ^m 16.11 ^s	+24°34'16.3''	0.0634	Adelman-McCarthy et al. (2007)
2MASX J16292467+2452082	16 ^h 29 ^m 24.69 ^s	+24°52'08.2''	0.0634	Adelman-McCarthy et al. (2007)
SDSS J163053.84+243147.2	16 ^h 30 ^m 53.84 ^s	+24°31'47.3''	0.0635	Adelman-McCarthy et al. (2006)
SDSS J163019.67+243330.0	16 ^h 30 ^m 19.68 ^s	+24°33'30.1''	0.0635	Adelman-McCarthy et al. (2006)
2MASX J16313042+2449302	16 ^h 31 ^m 30.39 ^s	+24°49'30.1''	0.0636	Adelman-McCarthy et al. (2007)
2MASX J16284192+2446279	16 ^h 28 ^m 41.91 ^s	+24°46'27.8''	0.0638	Adelman-McCarthy et al. (2006)
SDSS J163104.62+245719.8	16 ^h 31 ^m 04.62 ^s	+24°57'19.9''	0.0639	Adelman-McCarthy et al. (2006)
IC 4607	16 ^h 30 ^m 15.87 ^s	+24°34'27.7''	0.0639	Huchra et al. (2012)
SDSS J163106.44+241248.7	16 ^h 31 ^m 06.45 ^s	+24°12'48.7''	0.0639	Adelman-McCarthy et al. (2006)
SDSS J163110.30+245853.6	16 ^h 31 ^m 10.31 ^s	+24°58'53.7''	0.0641	Adelman-McCarthy et al. (2006)
SDSS J163109.43+242202.7	16 ^h 31 ^m 09.43 ^s	+24°22'02.8''	0.0642	Adelman-McCarthy et al. (2006)
2MASX J16301543+2442443	16 ^h 30 ^m 15.43 ^s	+24°42'44.1''	0.0643	Adelman-McCarthy et al. (2007)
2MASX J16303890+2430594	16 ^h 30 ^m 38.89 ^s	+24°30'59.2''	0.0643	Adelman-McCarthy et al. (2006)
MCG +04-39-010 NED03	16 ^h 30 ^m 14.59 ^s	+24°35'13.2''	0.0643	Adelman-McCarthy et al. (2007)
SDSS J163041.54+245853.0	16 ^h 30 ^m 41.55 ^s	+24°58'53.0''	0.0644	Adelman-McCarthy et al. (2006)
SDSS J162836.55+244752.4	16 ^h 28 ^m 36.56 ^s	+24°47'52.4''	0.0644	Adelman-McCarthy et al. (2006)
2MASX J16315966+2428552	16 ^h 31 ^m 59.69 ^s	+24°28'55.4''	0.0645	Adelman-McCarthy et al. (2007)
2MASX J16301449+2437063	16 ^h 30 ^m 14.50 ^s	+24°37'06.4''	0.0646	Adelman-McCarthy et al. (2006)
2MASX J16305028+2455226	16 ^h 30 ^m 50.28 ^s	+24°55'22.7''	0.0647	Adelman-McCarthy et al. (2006)
2MASX J16302886+2433164	16 ^h 30 ^m 28.83 ^s	+24°33'16.3''	0.0647	Adelman-McCarthy et al. (2006)
2MASX J16301215+2433473	16 ^h 30 ^m 12.17 ^s	+24°33'47.7''	0.0649	Adelman-McCarthy et al. (2006)
SDSS J163004.88+240409.2	16 ^h 30 ^m 04.89 ^s	+24°04'09.3''	0.0650	Adelman-McCarthy et al. (2006)
2MASX J16300743+2440363	16 ^h 30 ^m 07.44 ^s	+24°40'36.3''	0.0651	Adelman-McCarthy et al. (2006)
2MASX J16304317+2440386	16 ^h 30 ^m 43.18 ^s	+24°40'39.1''	0.0653	Adelman-McCarthy et al. (2006)
2MASX J16303509+2435324	16 ^h 30 ^m 35.09 ^s	+24°35'32.3''	0.0654	Adelman-McCarthy et al. (2007)
SDSS J162911.44+243413.9	16 ^h 29 ^m 11.45 ^s	+24°34'14.0''	0.0655	Adelman-McCarthy et al. (2006)
2MASX J16294712+2434194	16 ^h 29 ^m 47.10 ^s	+24°34'19.4''	0.0656	Adelman-McCarthy et al. (2007)
2MASX J16303981+2434546	16 ^h 30 ^m 39.85 ^s	+24°34'55.2''	0.0659	Adelman-McCarthy et al. (2007)
2MASX J16303606+2455434	16 ^h 30 ^m 36.06 ^s	+24°55'43.2''	0.0659	Adelman-McCarthy et al. (2006)
SDSS J163002.23+244721.6	16 ^h 30 ^m 02.24 ^s	+24°47'21.7''	0.0660	Adelman-McCarthy et al. (2006)
2MASX J16303737+2440154	16 ^h 30 ^m 37.41 ^s	+24°40'15.2''	0.0663	Adelman-McCarthy et al. (2007)
2MASX J16311982+2424422	16 ^h 31 ^m 19.80 ^s	+24°24'41.9''	0.0665	Adelman-McCarthy et al. (2006)
SDSS J163025.16+243528.7	16 ^h 30 ^m 25.17 ^s	+24°35'28.7''	0.0670	Adelman-McCarthy et al. (2006)

Table B17. XMMXCSJ163015.6+243423.2: All columns are as explained in Table B1.

Name	RA(J2000)	Dec(J2000)	z	Reference
(W2011) J339.86728-05.76581	22 ^h 39 ^m 28.15 ^s	-05°45′56.9″	0.2402	Wegner (2011)
(W2011) J339.85526-05.78358	22 ^h 39 ^m 25.26 ^s	-05°47′00.9″	0.2405	Wegner (2011)
(W2011) J339.85416-05.78444	22 ^h 39 ^m 25.00 ^s	-05°47′04.0″	0.2410	Wegner (2011)
(W2011) J339.84311-05.75219	22 ^h 39 ^m 22.35 ^s	-05°45′07.9″	0.2414	Wegner (2011)
(W2011) J339.85796-05.66972	22 ^h 39 ^m 25.91 ^s	-05°40′11.0″	0.2421	Wegner (2011)
(W2011) J339.91522-05.73214	22 ^h 39 ^m 39.65 ^s	-05°43′55.7″	0.2421	Wegner (2011)
(W2011) J339.92899-05.70703	22 ^h 39 ^m 42.96 ^s	-05°42′25.3″	0.2424	Wegner (2011)
APMUKS(BJ) B223649.45-060121.8	22 ^h 39 ^m 25.61 ^s	-05°45′43.1″	0.2425	Wegner (2011)
(W2011) J339.88293-05.68617	22 ^h 39 ^m 31.91 ^s	-05°41′10.2″	0.2425	Wegner (2011)
(W2011) J339.93253-05.72194	22 ^h 39 ^m 43.81 ^s	-05°43′19.0″	0.2427	Wegner (2011)
(W2011) J339.85922-05.77811	22 ^h 39 ^m 26.21 ^s	-05°46′41.2″	0.2434	Wegner (2011)
APMUKS(BJ) B223704.30-055906.2	22 ^h 39 ^m 40.49 ^s	-05°43′26.7″	0.2436	Wegner (2011)
(W2011) J339.91388-05.73789	22 ^h 39 ^m 39.33 ^s	-05°44′16.4″	0.2437	Wegner (2011)
(W2011) J339.93896-05.75525	22 ^h 39 ^m 45.35 ^s	-05°45′18.9″	0.2437	Wegner (2011)
APMUKS(BJ) B223702.94-060320.8	22 ^h 39 ^m 39.10 ^s	-05°47′41.7″	0.2441	Wegner (2011)
(W2011) J339.92871-05.74033	22 ^h 39 ^m 42.89 ^s	-05°44′25.2″	0.2441	Wegner (2011)
(W2011) J339.87462-05.69311	22 ^h 39 ^m 29.91 ^s	-05°41′35.2″	0.2441	Wegner (2011)
(W2011) J339.91187-05.63333	22 ^h 39 ^m 38.85 ^s	-05°43′00.0″	0.2442	Wegner (2011)
GALEXASC J223938.36-054401.5	22 ^h 39 ^m 38.36 ^s	-05°44′03.8″	0.2442	Wegner (2011)
(W2011) J339.82141-05.70861	22 ^h 39 ^m 17.14 ^s	-05°42′31.0″	0.2443	Wegner (2011)
APMUKS(BJ) B223656.20-055649.6	22 ^h 39 ^m 32.31 ^s	-05°41′10.7″	0.2443	Wegner (2011)
(W2011) J339.90479-05.74742	22 ^h 39 ^m 37.15 ^s	-05°44′50.7″	0.2445	Wegner (2011)
GALEXASC J223932.33-054544.9	22 ^h 39 ^m 32.36 ^s	-05°45′46.5″	0.2445	Wegner (2011)
(W2011) J339.90805-05.72461	22 ^h 39 ^m 37.93 ^s	-05°43′28.6″	0.2445	Wegner (2011)
(W2011) J339.88004-05.67217	22 ^h 39 ^m 31.21 ^s	-05°40′19.8″	0.2446	Wegner (2011)
(W2011) J339.88586-05.68911	22 ^h 39 ^m 32.61 ^s	-05°41′20.8″	0.2446	Wegner (2011)
(W2011) J339.91403-05.73167	22 ^h 39 ^m 39.37 ^s	-05°43′54.0″	0.2447	Wegner (2011)
(W2011) J339.89958-05.70617	22 ^h 39 ^m 35.90 ^s	-05°42′22.2″	0.2448	Wegner (2011)
(W2011) J339.90379-05.73611	22 ^h 39 ^m 36.91 ^s	-05°45′22.0″	0.2448	Wegner (2011)
(W2011) J339.89209-05.80678	22 ^h 39 ^m 34.10 ^s	-05°48′24.4″	0.2448	Wegner (2011)
(W2011) J339.85654-05.78022	22 ^h 39 ^m 25.57 ^s	-05°46′48.8″	0.2449	Wegner (2011)
(W2011) J339.93542-05.67039	22 ^h 39 ^m 44.50 ^s	-05°40′13.4″	0.2451	Wegner (2011)
(W2011) J339.83524-05.75508	22 ^h 39 ^m 20.46 ^s	-05°45′18.3″	0.2452	Wegner (2011)
(W2011) J339.85291-05.78672	22 ^h 39 ^m 24.70 ^s	-05°47′12.2″	0.2452	Wegner (2011)
(W2011) J340.00000-05.73803	22 ^h 40 ^m 00.00 ^s	-05°44′16.9″	0.2453	Wegner (2011)
2MASX J22392454-0547173	22 ^h 39 ^m 24.57 ^s	-05°47′17.4″	0.2453	Wegner (2011)
APMUKS(BJ) B223715.80-060103.5	22 ^h 39 ^m 51.98 ^s	-05°45′23.8″	0.2454	Wegner (2011)
(W2011) J339.85626-05.78508	22 ^h 39 ^m 25.50 ^s	-05°47′06.3″	0.2454	Wegner (2011)
(W2011) J339.95475-05.79149	22 ^h 39 ^m 49.14 ^s	-05°47′29.4″	0.2454	Wegner (2011)
(W2011) J339.85004-05.74921	22 ^h 39 ^m 24.01 ^s	-05°44′57.2″	0.2454	Wegner (2011)
APMUKS(BJ) B223651.70-060319.5	22 ^h 39 ^m 27.86 ^s	-05°47′40.2″	0.2455	Wegner (2011)
(W2011) J339.88324-05.68225	22 ^h 39 ^m 31.98 ^s	-05°40′56.1″	0.2457	Wegner (2011)
(W2011) J339.84662-05.75625	22 ^h 39 ^m 23.19 ^s	-05°45′22.5″	0.2457	Wegner (2011)
(W2011) J339.90917-05.77036	22 ^h 39 ^m 38.20 ^s	-05°46′13.3″	0.2458	Wegner (2011)
(W2011) J339.89420-05.81267	22 ^h 39 ^m 34.61 ^s	-05°48′45.6″	0.2460	Wegner (2011)
(W2011) J339.94089-05.71742	22 ^h 39 ^m 45.81 ^s	-05°43′02.7″	0.2462	Wegner (2011)
(W2011) J339.94528-05.76256	22 ^h 39 ^m 46.87 ^s	-05°45′45.2″	0.2463	Wegner (2011)
(W2011) J339.90976-05.75339	22 ^h 39 ^m 38.34 ^s	-05°45′12.2″	0.2464	Wegner (2011)
(W2011) J339.87332-05.80614	22 ^h 39 ^m 29.60 ^s	-05°48′22.1″	0.2466	Wegner (2011)
(W2011) J339.89771-05.80597	22 ^h 39 ^m 35.45 ^s	-05°48′21.5″	0.2469	Wegner (2011)
2MASX J22392032-0544233	22 ^h 39 ^m 20.40 ^s	-05°44′23.1″	0.2469	Wegner (2011)
(W2011) J339.87396-05.76278	22 ^h 39 ^m 29.75 ^s	-05°45′46.0″	0.2470	Wegner (2011)
APMUKS(BJ) B223704.44-055858.1	22 ^h 39 ^m 40.60 ^s	-05°43′18.5″	0.2470	Wegner (2011)
(W2011) J339.90925-05.77828	22 ^h 39 ^m 38.22 ^s	-05°46′41.8″	0.2471	Wegner (2011)
(W2011) J339.94589-05.64414	22 ^h 39 ^m 47.01 ^s	-05°38′38.9″	0.2472	Wegner (2011)
(W2011) J339.84738-05.74164	22 ^h 39 ^m 23.37 ^s	-05°44′29.9″	0.2473	Wegner (2011)
APMUKS(BJ) B223710.40-055450.0	22 ^h 39 ^m 46.57 ^s	-05°39′11.1″	0.2475	Wegner (2011)
(W2011) J339.82697-05.74289	22 ^h 39 ^m 18.47 ^s	-05°44′34.4″	0.2475	Wegner (2011)
(W2011) J339.82428-05.74400	22 ^h 39 ^m 17.83 ^s	-05°44′38.4″	0.2475	Wegner (2011)
(W2011) J339.88842-05.80075	22 ^h 39 ^m 33.23 ^s	-05°48′02.7″	0.2478	Wegner (2011)
(W2011) J339.88092-05.75026	22 ^h 39 ^m 31.42 ^s	-05°45′00.9″	0.2489	Wegner (2011)
(W2011) J339.91043-05.69272	22 ^h 39 ^m 38.50 ^s	-05°41′33.8″	0.2490	Wegner (2011)
(W2011) J339.90521-05.68931	22 ^h 39 ^m 37.25 ^s	-05°41′21.5″	0.2492	Wegner (2011)
(W2011) J339.92203-05.73417	22 ^h 39 ^m 41.29 ^s	-05°44′03.0″	0.2492	Wegner (2011)
(W2011) J339.92083-05.73192	22 ^h 39 ^m 41.00 ^s	-05°43′54.8″	0.2497	Wegner (2011)
(W2011) J339.91183-05.68417	22 ^h 39 ^m 38.84 ^s	-05°41′03.0″	0.2500	Wegner (2011)
APMUKS(BJ) B223659.52-055721.9	22 ^h 39 ^m 35.71 ^s	-05°41′42.4″	0.2502	Wegner (2011)
(W2011) J339.90482-05.67711	22 ^h 39 ^m 37.16 ^s	-05°40′37.6″	0.2509	Wegner (2011)

Name	RA(J2000)	Dec(J2000)	z	Reference
AGC 331543	23 ^h 38 ^m 31.41 ^s	+27°13'48.2''	0.1218	Scodeggio et al. (1995)
AGC 331535	23 ^h 37 ^m 55.52 ^s	+27°08'25.8''	0.1222	Scodeggio et al. (1995)
2MASX J23380720+2715028	23 ^h 38 ^m 07.24 ^s	+27°15'02.9''	0.1222	Scodeggio et al. (1995)
AGC 331529	23 ^h 37 ^m 41.99 ^s	+27°04'37.4''	0.1226	Scodeggio et al. (1995)
AGC 331531	23 ^h 37 ^m 47.13 ^s	+27°09'29.5''	0.1226	Scodeggio et al. (1995)
2MASX J23375415+2718448	23 ^h 37 ^m 54.16 ^s	+27°18'44.8''	0.1238	Scodeggio et al. (1995)
2MASX J23375559+2711128	23 ^h 37 ^m 55.59 ^s	+27°11'13.1''	0.1245	Giovanelli et al. (1995)
AGC 331526	23 ^h 37 ^m 22.51 ^s	+27°06'32.6''	0.1246	Scodeggio et al. (1995)
2MASX J23380218+2712088	23 ^h 38 ^m 02.18 ^s	+27°12'09.1''	0.1246	Smith et al. (2004)
2MASX J23382282+2717516	23 ^h 38 ^m 22.83 ^s	+27°17'51.6''	0.1263	Scodeggio et al. (1995)
2MASX J23372726+2707408	23 ^h 37 ^m 27.26 ^s	+27°07'41.0''	0.1264	Scodeggio et al. (1995)
BATC J233724.29+271434.14	23 ^h 37 ^m 24.10 ^s	+27°14'32.8''	0.1265	Pinkney et al. (1993)

Table B19. XMMXCSJ233757.0+271121.0: All columns are as explained in Table B1.

ID	RA(J2000)	Dec(J2000)	z	Reference	Member
1	10 ^h 57 ^m 03.77 ^s	-03°37'37.3''	0.8312	Nastasi et al. (2014) Tran et al. (1999)	✓
2	10 ^h 56 ^m 50.84 ^s	-03°37'37.4''	0.8390	Nastasi et al. (2014) Tran et al. (1999)	✓
3	10 ^h 57 ^m 04.10 ^s	-03°37'37.3''	0.8329	Nastasi et al. (2014) Tran et al. (1999)	✓
4	10 ^h 56 ^m 54.31 ^s	-03°37'37.4''	0.8380	Nastasi et al. (2014) Tran et al. (1999)	✓
5	10 ^h 56 ^m 51.77 ^s	-03°37'37.4''	0.8371	Nastasi et al. (2014) Tran et al. (1999)	✓
6	10 ^h 56 ^m 58.44 ^s	-03°37'37.4''	0.8353	Nastasi et al. (2014) Tran et al. (1999)	✓
7	10 ^h 56 ^m 56.37 ^s	-03°37'37.4''	0.8317	Nastasi et al. (2014) Tran et al. (1999)	✓
8	10 ^h 57 ^m 01.50 ^s	-03°37'37.3''	0.8346	Nastasi et al. (2014) Tran et al. (1999)	✓
9	10 ^h 56 ^m 56.90 ^s	-03°37'37.4''	0.8403	Nastasi et al. (2014) Tran et al. (1999)	✓
10	10 ^h 56 ^m 57.31 ^s	-03°37'37.4''	0.8175	Nastasi et al. (2014) Tran et al. (1999)	✓
11	10 ^h 57 ^m 02.97 ^s	-03°37'37.3''	0.8367	Nastasi et al. (2014) Tran et al. (1999)	✓
12	10 ^h 57 ^m 01.64 ^s	-03°37'37.3''	0.8239	Nastasi et al. (2014) Tran et al. (1999)	✓
13	10 ^h 57 ^m 01.04 ^s	-03°37'37.3''	0.8420	Nastasi et al. (2014) Tran et al. (1999)	✓
14	10 ^h 56 ^m 59.51 ^s	-03°37'37.4''	0.8454	Nastasi et al. (2014) Tran et al. (1999)	✓
15	10 ^h 56 ^m 59.90 ^s	-03°37'37.4''	0.8314	Nastasi et al. (2014) Tran et al. (1999)	✓
16	10 ^h 57 ^m 04.64 ^s	-03°37'37.3''	0.8282	Nastasi et al. (2014) Tran et al. (1999)	✓
17	10 ^h 57 ^m 03.37 ^s	-03°37'37.3''	0.8259	Nastasi et al. (2014) Tran et al. (1999)	✓
18	10 ^h 57 ^m 02.44 ^s	-03°37'37.3''	0.8397	Nastasi et al. (2014) Tran et al. (1999)	✓
19	10 ^h 57 ^m 02.44 ^s	-03°37'37.3''	0.8224	Nastasi et al. (2014) Tran et al. (1999)	✓
20	10 ^h 57 ^m 02.84 ^s	-03°37'37.3''	0.8314	Nastasi et al. (2014) Tran et al. (1999)	✓
21	10 ^h 57 ^m 02.17 ^s	-03°37'37.3''	0.8249	Nastasi et al. (2014) Tran et al. (1999)	✓
22	10 ^h 57 ^m 03.77 ^s	-03°37'37.3''	0.8392	Nastasi et al. (2014) Tran et al. (1999)	✓
23	10 ^h 57 ^m 03.84 ^s	-03°37'37.3''	0.8308	Nastasi et al. (2014) Tran et al. (1999)	✓
24	10 ^h 57 ^m 08.84 ^s	-03°37'37.3''	0.8250	Nastasi et al. (2014) Tran et al. (1999)	✓
25	10 ^h 57 ^m 01.97 ^s	-03°37'37.3''	0.8127	Nastasi et al. (2014) Tran et al. (1999)	✓
26	10 ^h 57 ^m 01.31 ^s	-03°37'37.3''	0.8213	Nastasi et al. (2014) Tran et al. (1999)	✓
27	10 ^h 56 ^m 57.97 ^s	-03°37'37.4''	0.8209	Nastasi et al. (2014) Tran et al. (1999)	✓
28	10 ^h 56 ^m 57.77 ^s	-03°37'37.4''	0.8286	Nastasi et al. (2014) Tran et al. (1999)	✓
29	10 ^h 56 ^m 57.37 ^s	-03°37'37.4''	0.8353	Nastasi et al. (2014) Tran et al. (1999)	✓
30	10 ^h 56 ^m 56.97 ^s	-03°37'37.4''	0.8332	Nastasi et al. (2014) Tran et al. (1999)	✓
31	10 ^h 56 ^m 54.44 ^s	-03°37'37.4''	0.8378	Nastasi et al. (2014) Tran et al. (1999)	✓
32	10 ^h 56 ^m 53.30 ^s	-03°37'37.4''	0.8319	Nastasi et al. (2014) Tran et al. (1999)	✓

Table B20. XMMXCSJ105659.5-033728.0: Columns 2 - 5 are as explained in Table B1. Column 1 gives an arbitrary ID for each galaxy and column 6 shows whether or not the galaxy was included as a member for the determination of the velocity dispersion.

ID	RA(J2000)	Dec(J2000)	z	Reference	Member
1	11 ^h 40 ^m 22.31 ^s	66°08'15.1''	0.7844	Nastasi et al. (2014) Donahue et al. (1999)	✓
2	11 ^h 40 ^m 22.01 ^s	66°08'12.1''	0.7903	Nastasi et al. (2014) Donahue et al. (1999)	✓
3	11 ^h 40 ^m 22.61 ^s	66°08'17.1''	0.7844	Nastasi et al. (2014) Donahue et al. (1999)	✓
4	11 ^h 40 ^m 22.01 ^s	66°08'19.0''	0.7927	Nastasi et al. (2014) Donahue et al. (1999)	✓
5	11 ^h 40 ^m 21.41 ^s	66°08'20.1''	0.7826	Nastasi et al. (2014) Donahue et al. (1999)	✓
6	11 ^h 40 ^m 17.70 ^s	66°08'23.0''	0.7808	Nastasi et al. (2014) Donahue et al. (1999)	✓
7	11 ^h 40 ^m 16.91 ^s	66°08'25.1''	0.7909	Nastasi et al. (2014) Donahue et al. (1999)	✓
8	11 ^h 40 ^m 17.21 ^s	66°08'29.1''	0.7916	Nastasi et al. (2014) Donahue et al. (1999)	✓
9	11 ^h 40 ^m 27.41 ^s	66°08'23.0''	0.7761	Nastasi et al. (2014) Donahue et al. (1999)	✓
10	11 ^h 40 ^m 27.01 ^s	66°08'09.0''	0.7760	Nastasi et al. (2014) Donahue et al. (1999)	✓
11	11 ^h 40 ^m 29.30 ^s	66°08'02.1''	0.7831	Nastasi et al. (2014) Donahue et al. (1999)	✓
12	11 ^h 40 ^m 24.50 ^s	66°07'26.1''	0.7823	Nastasi et al. (2014) Donahue et al. (1999)	✓
13	11 ^h 40 ^m 14.81 ^s	66°07'32.1''	0.7824	Nastasi et al. (2014) Donahue et al. (1999)	✓
14	11 ^h 40 ^m 30.80 ^s	66°09'03.0''	0.7900	Nastasi et al. (2014) Donahue et al. (1999)	✓
15	11 ^h 40 ^m 15.11 ^s	66°09'22.0''	0.7773	Nastasi et al. (2014) Donahue et al. (1999)	✓
16	11 ^h 40 ^m 17.40 ^s	66°09'14.1''	0.7909	Nastasi et al. (2014) Donahue et al. (1999)	✓
17	11 ^h 40 ^m 42.80 ^s	66°10'19.0''	0.7814	Nastasi et al. (2014) Donahue et al. (1999)	✓
18	11 ^h 40 ^m 40.40 ^s	66°07'52.0''	0.7889	Nastasi et al. (2014) Donahue et al. (1999)	✓
19	11 ^h 40 ^m 37.10 ^s	66°07'25.0''	0.7902	Nastasi et al. (2014) Donahue et al. (1999)	✓
20	11 ^h 40 ^m 10.31 ^s	66°07'18.1''	0.7898	Nastasi et al. (2014) Donahue et al. (1999)	✓
21	11 ^h 40 ^m 05.90 ^s	66°08'05.0''	0.7790	Nastasi et al. (2014) Donahue et al. (1999)	✓
22	11 ^h 39 ^m 58.91 ^s	66°07'60.0''	0.7792	Nastasi et al. (2014) Donahue et al. (1999)	✓
23	11 ^h 40 ^m 06.00 ^s	66°08'18.0''	0.7714	Nastasi et al. (2014) Donahue et al. (1999)	✓

Table B21. XMMXCSJ114023.0+660819.0: All columns are as explained in Table B20.

ID	RA(J2000)	Dec(J2000)	z	Reference	Member
1	18 ^h 21 ^m 16.61 ^s	68°30'25.0''	0.8151	Nastasi et al. (2014) Gioia et al. (2004)	✓
2	18 ^h 21 ^m 21.50 ^s	68°29'57.1''	0.8225	Nastasi et al. (2014) Gioia et al. (2004)	✓
3	18 ^h 21 ^m 26.21 ^s	68°29'31.0''	0.8206	Nastasi et al. (2014) Gioia et al. (2004)	✓
4	18 ^h 21 ^m 30.80 ^s	68°29'29.1''	0.8204	Nastasi et al. (2014) Gioia et al. (2004)	✓
5	18 ^h 21 ^m 27.90 ^s	68°28'43.0''	0.8229	Nastasi et al. (2014) Gioia et al. (2004)	✓
6	18 ^h 21 ^m 33.80 ^s	68°28'40.1''	0.8235	Nastasi et al. (2014) Gioia et al. (2004)	✓
7	18 ^h 21 ^m 32.60 ^s	68°27'54.1''	0.8167	Nastasi et al. (2014) Gioia et al. (2004)	✓
8	18 ^h 21 ^m 34.91 ^s	68°27'53.0''	0.8099	Nastasi et al. (2014) Gioia et al. (2004)	✓
9	18 ^h 21 ^m 37.20 ^s	68°27'51.1''	0.8153	Nastasi et al. (2014) Gioia et al. (2004)	✓
10	18 ^h 21 ^m 33.60 ^s	68°27'50.1''	0.8161	Nastasi et al. (2014) Gioia et al. (2004)	✓
11	18 ^h 21 ^m 35.21 ^s	68°27'34.0''	0.8115	Nastasi et al. (2014) Gioia et al. (2004)	✓
12	18 ^h 21 ^m 36.60 ^s	68°27'21.0''	0.8172	Nastasi et al. (2014) Gioia et al. (2004)	✓
13	18 ^h 21 ^m 37.50 ^s	68°27'07.0''	0.8231	Nastasi et al. (2014) Gioia et al. (2004)	✓
14	18 ^h 21 ^m 37.91 ^s	68°27'00.1''	0.8159	Nastasi et al. (2014) Gioia et al. (2004)	✓
15	18 ^h 21 ^m 18.20 ^s	68°27'00.1''	0.7942	Nastasi et al. (2014) Gioia et al. (2004)	✓
16	18 ^h 21 ^m 47.71 ^s	68°27'06.1''	0.8089	Nastasi et al. (2014) Gioia et al. (2004)	✓
17	18 ^h 21 ^m 51.11 ^s	68°27'17.0''	0.8060	Nastasi et al. (2014) Gioia et al. (2004)	✓
18	18 ^h 21 ^m 57.71 ^s	68°27'25.0''	0.8118	Nastasi et al. (2014) Gioia et al. (2004)	✓
19	18 ^h 21 ^m 50.81 ^s	68°26'09.0''	0.8152	Nastasi et al. (2014) Gioia et al. (2004)	✓
20	18 ^h 21 ^m 47.81 ^s	68°25'18.1''	0.8122	Nastasi et al. (2014) Gioia et al. (2004)	✓

Table B22. XMMXCSJ182132.9+682755.0: All columns are as explained in Table B20.

ID	Mask	RA(J2000)	Dec(J2000)	z	Quality	Identification	Member
1	GS-2012B-Q-011-03	00 ^h 56 ^m 46.52 ^s	-27°41'57.9"	0.6625	3	X	
2	GS-2012B-Q-011-03	00 ^h 56 ^m 47.54 ^s	-27°41'53.6"	0.6294	2	X	
3	GS-2012B-Q-011-03	00 ^h 56 ^m 47.56 ^s	-27°41'03.2"	0.5864	3	X	
5	GS-2012B-Q-011-03	00 ^h 56 ^m 47.54 ^s	-27°41'19.7"	0.5604	3	X	
6	GS-2012B-Q-011-03	00 ^h 56 ^m 54.47 ^s	-27°41'52.9"	0.5604	3	X	✓
7	GS-2012B-Q-011-03	00 ^h 56 ^m 52.73 ^s	-27°41'46.0"	0.5744	3	X	
9	GS-2012B-Q-011-03	00 ^h 56 ^m 53.45 ^s	-27°41'28.0"	0.5754	3	X	
11	GS-2012B-Q-011-03	00 ^h 56 ^m 53.03 ^s	-27°40'44.8"	0.5574	3	X	✓
12	GS-2012B-Q-011-03	00 ^h 56 ^m 57.06 ^s	-27°40'12.4"	0.8196	2	X	
13	GS-2012B-Q-011-03	00 ^h 56 ^m 58.95 ^s	-27°40'28.2"	0.5604	3	X	✓
14	GS-2012B-Q-011-03	00 ^h 56 ^m 55.93 ^s	-27°40'29.9"	0.5584	3	X	✓
16	GS-2012B-Q-011-03	00 ^h 56 ^m 54.31 ^s	-27°40'29.3"	0.5614	3	X	✓
17	GS-2012B-Q-011-03	00 ^h 56 ^m 57.48 ^s	-27°41'01.7"	0.5584	3	X	✓
18	GS-2012B-Q-011-03	00 ^h 56 ^m 59.35 ^s	-27°40'52.0"	0.5974	3	X	
19	GS-2012B-Q-011-03	00 ^h 56 ^m 57.03 ^s	-27°40'30.4"	0.5584	3	X	✓
20	GS-2012B-Q-011-03	00 ^h 56 ^m 56.80 ^s	-27°39'34.3"	0.6014	3	X	
23	GS-2012B-Q-011-03	00 ^h 56 ^m 59.28 ^s	-27°39'39.9"	0.8326	3	X	
25	GS-2012B-Q-011-03	00 ^h 57 ^m 02.36 ^s	-27°39'29.9"	0.6284	2	X	
26	GS-2012B-Q-011-03	00 ^h 57 ^m 01.73 ^s	-27°39'34.3"	0.5694	3	X	
27	GS-2012B-Q-011-03	00 ^h 57 ^m 00.36 ^s	-27°39'24.9"	0.8646	3	X	
28	GS-2012B-Q-011-03	00 ^h 57 ^m 02.35 ^s	-27°38'51.1"	0.5574	3	X	
29	GS-2012B-Q-011-03	00 ^h 57 ^m 03.56 ^s	-27°39'31.0"	0.5604	3	X	
31	GS-2012B-Q-011-03	00 ^h 57 ^m 04.76 ^s	-27°39'09.0"	0.6294	3	X	
32	GS-2012B-Q-011-03	00 ^h 57 ^m 03.51 ^s	-27°38'27.3"	0.2472	3	X	
1	GS-2012B-Q-011-04	00 ^h 56 ^m 46.96 ^s	-27°41'44.6"	1.0127	2	X	
2	GS-2012B-Q-011-04	00 ^h 56 ^m 46.52 ^s	-27°41'57.9"	0.6625	3	X	
3	GS-2012B-Q-011-04	00 ^h 56 ^m 49.75 ^s	-27°42'31.4"	0.8336	3	X	
4	GS-2012B-Q-011-04	00 ^h 56 ^m 44.95 ^s	-27°40'56.3"	0.7956	2	X	
5	GS-2012B-Q-011-04	00 ^h 56 ^m 46.64 ^s	-27°41'05.7"	0.5874	3	X	
6	GS-2012B-Q-011-04	00 ^h 56 ^m 47.56 ^s	-27°41'03.2"	0.5844	3	X	
7	GS-2012B-Q-011-04	00 ^h 56 ^m 48.10 ^s	-27°41'00.3"	0.8126	3	X	
8	GS-2012B-Q-011-04	00 ^h 56 ^m 52.46 ^s	-27°41'45.7"	0.2121	3	X	
10	GS-2012B-Q-011-04	00 ^h 56 ^m 54.96 ^s	-27°41'47.8"	0.5614	3	X	✓
11	GS-2012B-Q-011-04	00 ^h 56 ^m 50.57 ^s	-27°40'27.9"	0.5634	3	X	✓
12	GS-2012B-Q-011-04	00 ^h 56 ^m 53.08 ^s	-27°41'09.5"	0.8586	3	X	
13	GS-2012B-Q-011-04	00 ^h 56 ^m 58.35 ^s	-27°41'49.6"	0.6785	2	X	
14	GS-2012B-Q-011-04	00 ^h 56 ^m 52.88 ^s	-27°40'14.6"	0.7365	2	X	
15	GS-2012B-Q-011-04	00 ^h 56 ^m 54.90 ^s	-27°39'55.1"	0.5584	3	X	✓
16	GS-2012B-Q-011-04	00 ^h 56 ^m 54.76 ^s	-27°40'12.1"	0.5594	3	X	✓
17	GS-2012B-Q-011-04	00 ^h 56 ^m 54.76 ^s	-27°40'51.7"	0.5614	3	X	✓
18	GS-2012B-Q-011-04	00 ^h 56 ^m 56.82 ^s	-27°40'30.8"	0.5994	3	X	
19	GS-2012B-Q-011-04	00 ^h 56 ^m 59.12 ^s	-27°40'41.9"	0.5964	3	X	
20	GS-2012B-Q-011-04	00 ^h 56 ^m 56.89 ^s	-27°40'02.0"	1.1908	2	X	
23	GS-2012B-Q-011-04	00 ^h 56 ^m 58.05 ^s	-27°37'52.0"	0.7795	3	X	
24	GS-2012B-Q-011-04	00 ^h 56 ^m 59.04 ^s	-27°37'40.1"	0.6515	3	X	
25	GS-2012B-Q-011-04	00 ^h 56 ^m 57.22 ^s	-27°39'34.6"	0.6314	3	X	
26	GS-2012B-Q-011-04	00 ^h 56 ^m 59.03 ^s	-27°39'15.2"	0.6294	3	X	
27	GS-2012B-Q-011-04	00 ^h 57 ^m 07.97 ^s	-27°39'28.5"	0.6525	3	X	
28	GS-2012B-Q-011-04	00 ^h 57 ^m 04.24 ^s	-27°39'23.8"	0.5614	3	X	
29	GS-2012B-Q-011-04	00 ^h 57 ^m 04.76 ^s	-27°39'09.0"	0.6294	3	X	
30	GS-2012B-Q-011-04	00 ^h 57 ^m 03.46 ^s	-27°39'29.6"	0.4123	3	X	
31	GS-2012B-Q-011-04	00 ^h 57 ^m 02.17 ^s	-27°40'29.0"	0.5574	3	X	✓
32	GS-2012B-Q-011-04	00 ^h 57 ^m 02.74 ^s	-27°40'15.3"	0.5614	3	X	✓
33	GS-2012B-Q-011-04	00 ^h 57 ^m 01.02 ^s	-27°39'31.7"	0.3893	3	X	
35	GS-2012B-Q-011-04	00 ^h 57 ^m 02.94 ^s	-27°40'29.7"	0.5614	3	X	✓

Table B23. XMMXCSJ005656.6-274031.9: Column 1 gives an ID for each galaxy in the mask given in column 2. Column 3 and 4 give the right ascension and declination respectively. Column 5 gives the redshift, column 6 gives the quality of the redshift according to the following scheme: $Q = 3$ corresponds to two or more strongly detected features; $Q = 2$ refers to one strongly detected or two weakly detected features; $Q = 1$ one weakly detected feature and $Q = 0$ when no features could be identified. Column 7 shows whether the redshift was found via visible inspection (V) or cross-correlation (X). Column 8 shows whether or not the galaxy was classified as a member and used in the calculation of the velocity dispersion.

ID	Mask	RA(J2000)	Dec(J2000)	z	Quality	Identification	Member
1	Nastasi et al. (2014)	01 ^h 52 ^m 41.30 ^s	-13°38'55.0''	0.8307	2		✓
3	Nastasi et al. (2014)	01 ^h 52 ^m 41.11 ^s	-13°39'07.9''	0.8303	3		✓
4	Nastasi et al. (2014)	01 ^h 52 ^m 42.71 ^s	-13°38'59.1''	0.8261	4		✓
5	Nastasi et al. (2014)	01 ^h 52 ^m 39.41 ^s	-13°38'55.8''	0.8233	3		✓
6	Nastasi et al. (2014)	01 ^h 52 ^m 40.70 ^s	-13°39'21.0''	0.8261	2		
7	Nastasi et al. (2014)	01 ^h 52 ^m 40.21 ^s	-13°39'24.1''	0.8307	3		✓
8	Nastasi et al. (2014)	01 ^h 52 ^m 43.20 ^s	-13°38'29.5''	0.8268	3		✓
9	Nastasi et al. (2014)	01 ^h 52 ^m 35.81 ^s	-13°39'15.0''	0.8326	2		✓
11	Nastasi et al. (2014)	01 ^h 52 ^m 47.21 ^s	-13°38'00.1''	0.8256	3		✓
13	Nastasi et al. (2014)	01 ^h 52 ^m 37.01 ^s	-13°40'15.0''	0.8324	2		✓
14	Nastasi et al. (2014)	01 ^h 52 ^m 36.00 ^s	-13°40'15.9''	0.8295	3		✓
15	Nastasi et al. (2014)	01 ^h 52 ^m 32.90 ^s	-13°40'01.9''	0.8279	3		✓
1	GS-2011B-Q-050-01	01 ^h 52 ^m 47.02 ^s	-13°41'18.3''	0.3772	2	X	
2	GS-2011B-Q-050-01	01 ^h 52 ^m 50.28 ^s	-13°39'20.2''	0.8277	3	X	
7	GS-2011B-Q-050-01	01 ^h 52 ^m 46.56 ^s	-13°39'37.1''	0.6377	2	X	
9	GS-2011B-Q-050-01	01 ^h 52 ^m 41.85 ^s	-13°40'19.6''	0.8149	2	X	✓
11	GS-2011B-Q-050-01	01 ^h 52 ^m 42.62 ^s	-13°39'50.4''	0.6160	2	X	
12	GS-2011B-Q-050-01	01 ^h 52 ^m 40.75 ^s	-13°39'20.9''	0.8250	3	X	✓
13	GS-2011B-Q-050-01	01 ^h 52 ^m 41.35 ^s	-13°38'56.1''	0.8290	3	X	✓
14	GS-2011B-Q-050-01	01 ^h 52 ^m 38.16 ^s	-13°38'54.3''	0.2460	3	X	
15	GS-2011B-Q-050-01	01 ^h 52 ^m 45.36 ^s	-13°38'38.5''	0.3533	3	X	
19	GS-2011B-Q-050-01	01 ^h 52 ^m 38.81 ^s	-13°38'28.0''	0.8211	3	X	✓
20	GS-2011B-Q-050-01	01 ^h 52 ^m 45.02 ^s	-13°39'26.0''	0.2756	3	X	
23	GS-2011B-Q-050-01	01 ^h 52 ^m 39.42 ^s	-13°38'02.8''	0.8211	2	X	✓
25	GS-2011B-Q-050-01	01 ^h 52 ^m 33.99 ^s	-13°38'48.2''	0.7724	3	X	
28	GS-2011B-Q-050-01	01 ^h 52 ^m 33.31 ^s	-13°38'45.3''	0.6357	3	X	
29	GS-2011B-Q-050-01	01 ^h 52 ^m 32.11 ^s	-13°38'28.7''	0.6345	3	X	
30	GS-2011B-Q-050-01	01 ^h 52 ^m 34.76 ^s	-13°37'58.5''	0.3948	3	X	
32	GS-2011B-Q-050-01	01 ^h 52 ^m 32.62 ^s	-13°37'44.1''	0.4942	2	X	
4	GS-2011B-Q-050-02	01 ^h 52 ^m 50.28 ^s	-13°39'20.2''	0.8276	2	X	✓
6	GS-2011B-Q-050-02	01 ^h 52 ^m 44.86 ^s	-13°40'14.2''	0.4947	2	V	
8	GS-2011B-Q-050-02	01 ^h 52 ^m 48.15 ^s	-13°38'53.9''	0.7398	2	X	
9	GS-2011B-Q-050-02	01 ^h 52 ^m 41.65 ^s	-13°39'42.5''	0.5290	3	X	
10	GS-2011B-Q-050-02	01 ^h 52 ^m 39.98 ^s	-13°39'22.4''	0.8294	3	X	✓
11	GS-2011B-Q-050-02	01 ^h 52 ^m 45.13 ^s	-13°39'09.0''	0.8313	2	X	✓
16	GS-2011B-Q-050-02	01 ^h 52 ^m 44.84 ^s	-13°38'24.8''	0.5340	2	X	
17	GS-2011B-Q-050-02	01 ^h 52 ^m 43.17 ^s	-13°38'29.5''	0.8258	3	X	
19	GS-2011B-Q-050-02	01 ^h 52 ^m 38.37 ^s	-13°39'22.7''	0.8290	2	X	✓
21	GS-2011B-Q-050-02	01 ^h 52 ^m 40.24 ^s	-13°39'00.4''	0.8193	3	X	✓
22	GS-2011B-Q-050-02	01 ^h 52 ^m 37.62 ^s	-13°38'30.5''	0.8202	2	X	✓
23	GS-2011B-Q-050-02	01 ^h 52 ^m 38.75 ^s	-13°38'24.1''	0.2813	3	X	
26	GS-2011B-Q-050-02	01 ^h 52 ^m 36.40 ^s	-13°36'50.5''	0.7283	3	X	
28	GS-2011B-Q-050-02	01 ^h 52 ^m 32.62 ^s	-13°37'44.1''	0.4941	2	X	
31	GS-2011B-Q-050-02	01 ^h 52 ^m 36.01 ^s	-13°37'45.2''	0.7848	2	X	
32	GS-2011B-Q-050-02	01 ^h 52 ^m 37.42 ^s	-13°37'45.5''	0.7858	2	X	
5606	KECK	01 ^h 52 ^m 44.13 ^s	-13°34'11.9''	0.8140			
5612	KECK	01 ^h 52 ^m 44.19 ^s	-13°34'49.9''	0.8209			
5638	KECK	01 ^h 52 ^m 42.02 ^s	-13°38'40.8''	0.8300			✓
5655	KECK	01 ^h 52 ^m 43.40 ^s	-13°38'24.1''	0.8348			✓
5688	KECK	01 ^h 52 ^m 42.88 ^s	-13°38'25.1''	0.8300			✓
5853	KECK	01 ^h 52 ^m 40.42 ^s	-13°38'20.7''	0.8297			✓
5900	KECK	01 ^h 52 ^m 39.78 ^s	-13°38'44.0''	0.8222			✓
5909	KECK	01 ^h 52 ^m 39.15 ^s	-13°40'35.3''	0.8213			✓
5922	KECK	01 ^h 52 ^m 39.52 ^s	-13°39'50.9''	0.8211			✓

Table B24. XMMXCSJ015241.1-133855.9: All columns are as explained in Table B23.

ID	Mask	RA(J2000)	Dec(J2000)	z	Quality	Identification	Member
2	GS-2012B-Q-011-06	02 ^h 17 ^m 30.50 ^s	-05°11'31.4''	0.5674	3	X	
3	GS-2012B-Q-011-06	02 ^h 17 ^m 28.40 ^s	-05°12'03.6''	0.9216	3	X	
6	GS-2012B-Q-011-06	02 ^h 17 ^m 27.60 ^s	-05°13'60.0''	0.6424	3	X	✓
8	GS-2012B-Q-011-06	02 ^h 17 ^m 34.35 ^s	-05°12'43.8''	0.6474	3	X	✓
10	GS-2012B-Q-011-06	02 ^h 17 ^m 33.72 ^s	-05°12'51.6''	0.6408	3	X	✓
11	GS-2012B-Q-011-06	02 ^h 17 ^m 35.84 ^s	-05°12'58.9''	0.8246	3	X	
12	GS-2012B-Q-011-06	02 ^h 17 ^m 30.52 ^s	-05°13'21.4''	0.8336	2	X	
13	GS-2012B-Q-011-06	02 ^h 17 ^m 35.79 ^s	-05°14'20.1''	0.6454	3	X	✓
15	GS-2012B-Q-011-06	02 ^h 17 ^m 32.55 ^s	-05°12'59.2''	0.6414	3	X	✓
16	GS-2012B-Q-011-06	02 ^h 17 ^m 33.02 ^s	-05°13'13.4''	0.6494	3	V	✓
17	GS-2012B-Q-011-06	02 ^h 17 ^m 34.18 ^s	-05°13'38.8''	0.4443	3	X	
18	GS-2012B-Q-011-06	02 ^h 17 ^m 34.97 ^s	-05°13'28.6''	0.6494	3	X	✓
19	GS-2012B-Q-011-06	02 ^h 17 ^m 35.92 ^s	-05°13'28.8''	1.0958	3	X	
20	GS-2012B-Q-011-06	02 ^h 17 ^m 41.81 ^s	-05°11'32.9''	0.4963	3	X	
22	GS-2012B-Q-011-06	02 ^h 17 ^m 38.72 ^s	-05°13'00.8''	0.6484	3	X	✓
23	GS-2012B-Q-011-06	02 ^h 17 ^m 39.37 ^s	-05°13'32.3''	0.7515	3	X	
24	GS-2012B-Q-011-06	02 ^h 17 ^m 37.16 ^s	-05°13'29.0''	0.6444	3	X	✓
25	GS-2012B-Q-011-06	02 ^h 17 ^m 38.01 ^s	-05°13'09.3''	0.6494	3	X	✓
26	GS-2012B-Q-011-06	02 ^h 17 ^m 40.15 ^s	-05°13'13.4''	0.7445	3	X	
27	GS-2012B-Q-011-06	02 ^h 17 ^m 43.39 ^s	-05°12'32.3''	0.6504	2	V	✓
28	GS-2012B-Q-011-06	02 ^h 17 ^m 42.49 ^s	-05°12'52.5''	0.4893	3	X	
29	GS-2012B-Q-011-06	02 ^h 17 ^m 41.00 ^s	-05°14'03.2''	0.6805	3	X	
30	GS-2012B-Q-011-06	02 ^h 17 ^m 44.89 ^s	-05°12'58.0''	0.4233	3	X	
31	GS-2012B-Q-011-06	02 ^h 17 ^m 45.25 ^s	-05°13'11.1''	0.2892	3	X	
32	GS-2012B-Q-011-06	02 ^h 17 ^m 43.79 ^s	-05°13'47.5''	0.6484	3	V	✓
33	GS-2012B-Q-011-06	02 ^h 17 ^m 46.73 ^s	-05°13'34.3''	0.6454	3	V	
34	GS-2012B-Q-011-06	02 ^h 17 ^m 46.01 ^s	-05°13'32.0''	0.5804	3	X	

Table B25. XMMXCSJ021734.7-051326.9: All columns are as explained in Table B23.

ID	Mask	RA(J2000)	Dec(J2000)	z	Quality	Identification	Member
1	GS-2010B-Q-46-06	02 ^h 50 ^m 22.92 ^s	-31°03′53.0″	0.8337	3	X	
8	GS-2010B-Q-46-06	02 ^h 50 ^m 15.25 ^s	-31°03′33.5″	0.7263	3	X	
9	GS-2010B-Q-46-06	02 ^h 50 ^m 13.27 ^s	-31°03′35.7″	0.6168	3	X	
10	GS-2010B-Q-46-06	02 ^h 50 ^m 12.05 ^s	-31°03′08.0″	0.7146	3	X	
14	GS-2010B-Q-46-06	02 ^h 50 ^m 06.63 ^s	-31°03′13.7″	0.8496	3	X	
15	GS-2010B-Q-46-06	02 ^h 50 ^m 08.70 ^s	-31°03′49.7″	0.9052	3	X	✓
16	GS-2010B-Q-46-06	02 ^h 50 ^m 03.78 ^s	-31°03′51.5″	0.3533	3	X	
17	GS-2010B-Q-46-06	02 ^h 50 ^m 06.89 ^s	-31°03′51.5″	0.9217	3	X	✓
18	GS-2010B-Q-46-06	02 ^h 50 ^m 05.48 ^s	-31°03′53.0″	0.6972	3	X	
19	GS-2010B-Q-46-06	02 ^h 50 ^m 04.50 ^s	-31°03′51.5″	0.9149	3	X	✓
21	GS-2010B-Q-46-06	02 ^h 50 ^m 02.79 ^s	-31°04′04.9″	0.9831	3	X	
22	GS-2010B-Q-46-06	02 ^h 50 ^m 06.48 ^s	-31°03′56.9″	0.9069	3	X	✓
23	GS-2010B-Q-46-06	02 ^h 50 ^m 09.04 ^s	-31°04′06.3″	0.7567	3	X	
25	GS-2010B-Q-46-06	02 ^h 50 ^m 03.83 ^s	-31°04′34.0″	0.8988	3	X	✓
26	GS-2010B-Q-46-06	02 ^h 50 ^m 04.24 ^s	-31°04′50.6″	0.9095	3	X	✓
28	GS-2010B-Q-46-06	02 ^h 50 ^m 04.59 ^s	-31°05′41.7″	0.6197	3	X	
34	GS-2010B-Q-46-06	02 ^h 50 ^m 04.26 ^s	-31°07′05.2″	0.1261	3	X	
1	GS-2012B-Q-011-09	02 ^h 50 ^m 22.92 ^s	-31°03′53.0″	0.5924	2	X	
2	GS-2012B-Q-011-09	02 ^h 50 ^m 18.11 ^s	-31°03′10.5″	0.9326	2	X	
4	GS-2012B-Q-011-09	02 ^h 50 ^m 16.05 ^s	-31°03′23.1″	1.0077	2	X	
5	GS-2012B-Q-011-09	02 ^h 50 ^m 14.89 ^s	-31°03′32.1″	0.7245	3	X	
6	GS-2012B-Q-011-09	02 ^h 50 ^m 14.94 ^s	-31°02′56.8″	0.9927	2	X	
9	GS-2012B-Q-011-09	02 ^h 50 ^m 08.98 ^s	-31°03′01.1″	0.9086	3	X	✓
10	GS-2012B-Q-011-09	02 ^h 50 ^m 10.24 ^s	-31°03′27.8″	0.9056	3	X	✓
11	GS-2012B-Q-011-09	02 ^h 50 ^m 07.01 ^s	-31°01′00.9″	0.5204	3	X	
13	GS-2012B-Q-011-09	02 ^h 50 ^m 06.54 ^s	-31°03′44.7″	0.9126	3	X	✓
17	GS-2012B-Q-011-09	02 ^h 50 ^m 03.99 ^s	-31°03′53.0″	0.9176	3	X	✓
18	GS-2012B-Q-011-09	02 ^h 50 ^m 07.33 ^s	-31°04′10.6″	0.9106	3	X	✓
19	GS-2012B-Q-011-09	02 ^h 50 ^m 02.67 ^s	-31°03′26.0″	0.9797	3	X	
20	GS-2012B-Q-011-09	02 ^h 50 ^m 07.38 ^s	-31°05′28.7″	0.6494	2	X	
21	GS-2012B-Q-011-09	02 ^h 49 ^m 58.10 ^s	-31°03′39.6″	0.8696	3	X	✓
22	GS-2012B-Q-011-09	02 ^h 50 ^m 05.48 ^s	-31°04′40.5″	0.9026	2	X	
27	GS-2012B-Q-011-09	02 ^h 49 ^m 58.68 ^s	-31°05′25.8″	0.6274	3	X	
28	GS-2012B-Q-011-09	02 ^h 49 ^m 59.99 ^s	-31°05′07.8″	0.8816	2	X	
29	GS-2012B-Q-011-09	02 ^h 49 ^m 58.60 ^s	-31°04′59.2″	0.9216	3	X	
30	GS-2012B-Q-011-09	02 ^h 50 ^m 00.51 ^s	-31°04′44.5″	0.5654	3	X	✓
31	GS-2012B-Q-011-09	02 ^h 50 ^m 04.26 ^s	-31°07′05.2″	0.9827	3	X	

Table B26. XMMXCSJ025006.4-310400.8: All columns are as explained in Table B23.

ID	Mask	RA(J2000)	Dec(J2000)	z	Quality	Identification	Member
1	GS-2011B-Q-050-03	03 ^h 02 ^m 13.84 ^s	-00°00'41.6''	0.4988	3	X	
7	GS-2011B-Q-050-03	03 ^h 02 ^m 13.04 ^s	00°00'41.5''	0.5958	3	X	
9	GS-2011B-Q-050-03	03 ^h 02 ^m 06.74 ^s	-00°00'06.1''	0.6432	3	X	✓
11	GS-2011B-Q-050-03	03 ^h 02 ^m 07.86 ^s	00°00'21.2''	0.6425	3	X	✓
12	GS-2011B-Q-050-03	03 ^h 02 ^m 06.20 ^s	-00°00'04.0''	0.6451	3	X	✓
13	GS-2011B-Q-050-03	03 ^h 02 ^m 08.78 ^s	00°00'39.9''	0.6486	3	X	✓
15	GS-2011B-Q-050-03	03 ^h 02 ^m 05.64 ^s	-00°00'00.5''	0.6452	3	X	✓
17	GS-2011B-Q-050-03	03 ^h 02 ^m 02.94 ^s	-00°00'53.1''	0.6503	3	X	✓
19	GS-2011B-Q-050-03	03 ^h 02 ^m 04.94 ^s	-00°00'33.0''	0.6477	2	X	✓
21	GS-2011B-Q-050-03	03 ^h 02 ^m 02.12 ^s	00°00'04.2''	0.6368	3	X	✓
22	GS-2011B-Q-050-03	03 ^h 02 ^m 00.91 ^s	-00°00'53.0''	0.4075	3	X	
23	GS-2011B-Q-050-03	03 ^h 02 ^m 00.40 ^s	-00°00'49.9''	0.6482	2	X	✓
25	GS-2011B-Q-050-03	03 ^h 01 ^m 59.56 ^s	00°00'31.0''	0.4688	2	X	
28	GS-2011B-Q-050-03	03 ^h 01 ^m 56.38 ^s	00°00'59.2''	0.4070	2	X	
31	GS-2011B-Q-050-03	03 ^h 01 ^m 55.80 ^s	-00°00'20.3''	0.7886	3	X	
5	GS-2011B-Q-050-04	03 ^h 02 ^m 11.53 ^s	00°00'46.1''	0.4094	2	X	
9	GS-2011B-Q-050-04	03 ^h 02 ^m 09.28 ^s	-00°01'04.8''	0.6700	3	X	
11	GS-2011B-Q-050-04	03 ^h 02 ^m 04.69 ^s	-00°00'32.1''	0.6435	2	X	✓
14	GS-2011B-Q-050-04	03 ^h 02 ^m 08.70 ^s	00°01'05.4''	0.6450	2	X	✓
15	GS-2011B-Q-050-04	03 ^h 02 ^m 07.94 ^s	00°00'30.1''	0.4770	3	X	
16	GS-2011B-Q-050-04	03 ^h 02 ^m 05.73 ^s	00°00'02.0''	0.6390	2	X	✓
17	GS-2011B-Q-050-04	03 ^h 02 ^m 05.26 ^s	00°00'09.0''	0.6454	2	X	✓
18	GS-2011B-Q-050-04	03 ^h 02 ^m 06.46 ^s	00°00'00.8''	0.6457	2	X	✓
23	GS-2011B-Q-050-04	03 ^h 02 ^m 00.18 ^s	-00°00'40.1''	0.4694	2	X	
24	GS-2011B-Q-050-04	03 ^h 02 ^m 00.65 ^s	00°00'21.3''	0.4051	3	X	
27	GS-2011B-Q-050-04	03 ^h 01 ^m 57.71 ^s	-00°00'34.4''	0.4944	2	X	
29	GS-2011B-Q-050-04	03 ^h 01 ^m 56.13 ^s	-00°00'20.8''	0.7888	3	X	
30	GS-2011B-Q-050-04	03 ^h 01 ^m 56.63 ^s	00°00'47.0''	0.9857	3	X	
17	GS-2011B-Q-050-05	03 ^h 02 ^m 06.06 ^s	-00°00'53.1''	0.6431	2	X	✓
18	GS-2011B-Q-050-05	03 ^h 02 ^m 02.64 ^s	-00°00'47.7''	0.6609	2	X	
20	GS-2011B-Q-050-05	03 ^h 02 ^m 04.82 ^s	-00°00'43.3''	0.6477	2	X	✓
21	GS-2011B-Q-050-05	03 ^h 02 ^m 06.50 ^s	-00°00'27.7''	0.4945	2	X	
26	GS-2011B-Q-050-05	03 ^h 01 ^m 59.29 ^s	00°00'43.5''	0.4070	3	X	
27	GS-2011B-Q-050-05	03 ^h 02 ^m 00.34 ^s	00°00'36.2''	0.4072	3	X	
28	GS-2011B-Q-050-05	03 ^h 01 ^m 57.26 ^s	-00°00'31.2''	0.5948	3	X	

Table B27. XMMXCSJ030205.1-000003.6: All columns are as explained in Table B23.

ID	Mask	RA(J2000)	Dec(J2000)	z	Quality	Identification	Member
2	GS-2010B-Q-046-01	09 ^h 59 ^m 41.78 ^s	02°33'39.1"	0.6964	3	X	
3	GS-2010B-Q-046-01	09 ^h 59 ^m 34.47 ^s	02°33'47.0"	0.6766	3	X	
4	GS-2010B-Q-046-01	09 ^h 59 ^m 43.01 ^s	02°32'32.0"	0.6963	3	X	
5	GS-2010B-Q-046-01	09 ^h 59 ^m 42.91 ^s	02°31'49.7"	0.7268	3	X	✓
7	GS-2010B-Q-046-01	09 ^h 59 ^m 39.41 ^s	02°33'00.1"	0.4701	3	X	
8	GS-2010B-Q-046-01	09 ^h 59 ^m 39.35 ^s	02°32'39.2"	0.6778	3	X	
9	GS-2010B-Q-046-01	09 ^h 59 ^m 38.13 ^s	02°32'11.0"	0.7296	3	X	✓
10	GS-2010B-Q-046-01	09 ^h 59 ^m 39.29 ^s	02°32'04.1"	0.7317	3	X	✓
11	GS-2010B-Q-046-01	09 ^h 59 ^m 35.47 ^s	02°31'56.0"	0.3317	3	X	
15	GS-2010B-Q-046-01	09 ^h 59 ^m 43.71 ^s	02°31'01.9"	0.2455	3	X	
16	GS-2010B-Q-046-01	09 ^h 59 ^m 43.04 ^s	02°31'08.7"	0.7314	3	X	✓
17	GS-2010B-Q-046-01	09 ^h 59 ^m 42.96 ^s	02°31'16.7"	0.7285	3	X	✓
18	GS-2010B-Q-046-01	09 ^h 59 ^m 40.88 ^s	02°30'34.2"	0.8369	3	X	
20	GS-2010B-Q-046-01	09 ^h 59 ^m 40.58 ^s	02°31'41.2"	0.7248	3	X	✓
21	GS-2010B-Q-046-01	09 ^h 59 ^m 41.64 ^s	02°31'29.9"	0.7307	3	X	✓
23	GS-2010B-Q-046-01	09 ^h 59 ^m 40.98 ^s	02°30'40.5"	0.8360	3	X	
24	GS-2010B-Q-046-01	09 ^h 59 ^m 40.40 ^s	02°30'54.6"	0.7169	3	X	
25	GS-2010B-Q-046-01	09 ^h 59 ^m 44.35 ^s	02°29'54.1"	0.7303	3	X	✓
27	GS-2010B-Q-046-01	09 ^h 59 ^m 41.46 ^s	02°30'18.2"	0.8352	3	X	
28	GS-2010B-Q-046-01	09 ^h 59 ^m 41.05 ^s	02°30'09.9"	0.7156	3	X	
30	GS-2010B-Q-046-01	09 ^h 59 ^m 35.91 ^s	02°29'13.4"	0.7149	3	X	
35	GS-2010B-Q-046-01	09 ^h 59 ^m 40.98 ^s	02°28'49.6"	0.4095	3	X	
6	GS-2012A-Q-046-01	09 ^h 59 ^m 38.44 ^s	02°33'13.9"	0.6603	2	X	
7	GS-2012A-Q-046-01	09 ^h 59 ^m 38.89 ^s	02°33'05.6"	0.7531	2	X	
8	GS-2012A-Q-046-01	09 ^h 59 ^m 43.03 ^s	02°32'00.1"	0.7259	2	X	✓
9	GS-2012A-Q-046-01	09 ^h 59 ^m 42.42 ^s	02°32'09.3"	0.7289	3	X	✓
10	GS-2012A-Q-046-01	09 ^h 59 ^m 42.27 ^s	02°31'34.6"	0.7265	2	X	✓
13	GS-2012A-Q-046-01	09 ^h 59 ^m 39.70 ^s	02°31'19.0"	0.7286	3	X	✓
14	GS-2012A-Q-046-01	09 ^h 59 ^m 42.19 ^s	02°32'36.8"	0.8893	3	X	
16	GS-2012A-Q-046-01	09 ^h 59 ^m 41.79 ^s	02°32'18.2"	0.5489	3	X	
17	GS-2012A-Q-046-01	09 ^h 59 ^m 40.25 ^s	02°31'10.9"	0.7332	3	X	✓
18	GS-2012A-Q-046-01	09 ^h 59 ^m 41.14 ^s	02°31'25.8"	0.7290	3	X	✓
19	GS-2012A-Q-046-01	09 ^h 59 ^m 42.36 ^s	02°30'45.3"	0.7270	3	X	✓
20	GS-2012A-Q-046-01	09 ^h 59 ^m 38.94 ^s	02°30'59.6"	0.7271	3	X	✓
21	GS-2012A-Q-046-01	09 ^h 59 ^m 39.66 ^s	02°30'52.1"	0.7186	3	X	✓
23	GS-2012A-Q-046-01	09 ^h 59 ^m 43.95 ^s	02°29'52.3"	0.7294	3	X	✓
25	GS-2012A-Q-046-01	09 ^h 59 ^m 40.35 ^s	02°30'19.2"	0.4748	2	X	
26	GS-2012A-Q-046-01	09 ^h 59 ^m 40.97 ^s	02°29'58.6"	0.7309	3	X	✓
29	GS-2012A-Q-046-01	09 ^h 59 ^m 40.95 ^s	02°29'16.9"	0.4053	3	X	
33	GS-2012A-Q-046-01	09 ^h 59 ^m 38.40 ^s	02°28'40.2"	0.7542	3	X	
35	GS-2012A-Q-046-01	09 ^h 59 ^m 40.88 ^s	02°28'46.8"	0.2494	3	X	
1	GS-2012A-Q-046-02	09 ^h 59 ^m 46.92 ^s	02°33'46.3"	0.6901	2	X	
5	GS-2012A-Q-046-02	09 ^h 59 ^m 43.78 ^s	02°31'54.5"	0.4687	3	X	
8	GS-2012A-Q-046-02	09 ^h 59 ^m 40.81 ^s	02°31'34.3"	0.7286	3	X	✓
11	GS-2012A-Q-046-02	09 ^h 59 ^m 39.41 ^s	02°33'00.1"	0.4703	3	X	
12	GS-2012A-Q-046-02	09 ^h 59 ^m 38.57 ^s	02°33'06.8"	0.7515	3	X	
15	GS-2012A-Q-046-02	09 ^h 59 ^m 39.41 ^s	02°32'20.4"	1.1040	3	X	
16	GS-2012A-Q-046-02	09 ^h 59 ^m 38.58 ^s	02°32'12.6"	0.4419	3	X	
19	GS-2012A-Q-046-02	09 ^h 59 ^m 40.65 ^s	02°31'15.9"	0.7295	3	X	✓
20	GS-2012A-Q-046-02	09 ^h 59 ^m 39.45 ^s	02°30'38.5"	0.7242	3	X	✓
23	GS-2012A-Q-046-02	09 ^h 59 ^m 42.80 ^s	02°30'08.8"	0.7248	3	X	✓
25	GS-2012A-Q-046-02	09 ^h 59 ^m 38.38 ^s	02°30'16.4"	0.7295	3	X	✓
26	GS-2012A-Q-046-02	09 ^h 59 ^m 40.52 ^s	02°30'02.4"	0.7308	3	X	✓
31	GS-2012A-Q-046-02	09 ^h 59 ^m 40.67 ^s	02°29'32.9"	0.9603	2	X	
33	GS-2012A-Q-046-02	09 ^h 59 ^m 39.64 ^s	02°28'37.8"	0.2489	3	X	
34	GS-2012A-Q-046-02	09 ^h 59 ^m 40.88 ^s	02°28'46.8"	0.2495	3	X	

Table B28. XMMXCSJ095940.7+023113.4: All columns are as explained in Table B23.

ID	Mask	RA(J2000)	Dec(J2000)	z	Quality	Identification	Member
2	GS-2010B-Q-046-03	11 ^h 24 ^m 00.44 ^s	05°27'13.8"	0.4726	3	X	
4	GS-2010B-Q-046-03	11 ^h 24 ^m 00.65 ^s	05°27'42.1"	0.3752	3	X	
5	GS-2010B-Q-046-03	11 ^h 24 ^m 00.16 ^s	05°27'43.0"	0.1554	3	X	
6	GS-2010B-Q-046-03	11 ^h 24 ^m 02.58 ^s	05°28'43.8"	0.3942	3	X	
11	GS-2010B-Q-046-03	11 ^h 23 ^m 58.50 ^s	05°28'10.8"	0.6544	3	X	
12	GS-2010B-Q-046-03	11 ^h 23 ^m 59.15 ^s	05°28'07.0"	0.5945	3	X	
13	GS-2010B-Q-046-03	11 ^h 23 ^m 57.11 ^s	05°28'34.9"	0.6514	3	X	✓
14	GS-2010B-Q-046-03	11 ^h 23 ^m 56.49 ^s	05°29'01.0"	0.6567	3	X	✓
15	GS-2010B-Q-046-03	11 ^h 23 ^m 59.97 ^s	05°29'13.0"	0.3750	3	X	
16	GS-2010B-Q-046-03	11 ^h 23 ^m 48.65 ^s	05°28'09.0"	0.5299	3	X	
17	GS-2010B-Q-046-03	11 ^h 23 ^m 51.43 ^s	05°28'49.7"	0.6569	3	X	✓
18	GS-2010B-Q-046-03	11 ^h 23 ^m 52.17 ^s	05°28'51.5"	0.6557	3	X	✓
19	GS-2010B-Q-046-03	11 ^h 23 ^m 50.28 ^s	05°29'13.9"	0.6557	3	X	✓
21	GS-2010B-Q-046-03	11 ^h 23 ^m 50.49 ^s	05°29'32.2"	0.6551	3	X	✓
25	GS-2010B-Q-046-03	11 ^h 23 ^m 53.46 ^s	05°29'04.3"	0.3747	3	X	
26	GS-2010B-Q-046-03	11 ^h 23 ^m 50.06 ^s	05°29'35.8"	0.6591	3	X	✓
27	GS-2010B-Q-046-03	11 ^h 23 ^m 43.65 ^s	05°26'58.6"	0.6552	3	X	✓
28	GS-2010B-Q-046-03	11 ^h 23 ^m 48.89 ^s	05°29'36.5"	0.6478	3	X	✓
30	GS-2010B-Q-046-03	11 ^h 23 ^m 46.52 ^s	05°29'52.2"	0.5826	3	X	
31	GS-2010B-Q-046-03	11 ^h 23 ^m 46.33 ^s	05°30'09.1"	0.6543	3	X	✓
32	GS-2010B-Q-046-03	11 ^h 23 ^m 47.45 ^s	05°29'57.6"	0.6389	3	X	
33	GS-2010B-Q-046-03	11 ^h 23 ^m 47.88 ^s	05°29'54.6"	0.6496	3	X	✓
2	GS2012AQ046-05	11 ^h 23 ^m 59.56 ^s	05°26'58.8"	0.4146	3	X	
7	GS2012AQ046-05	11 ^h 23 ^m 52.84 ^s	05°27'18.3"	0.6487	3	X	
14	GS2012AQ046-05	11 ^h 23 ^m 56.35 ^s	05°29'01.0"	0.2713	2	X	
15	GS2012AQ046-05	11 ^h 23 ^m 55.48 ^s	05°29'02.5"	0.6603	2	X	✓
16	GS2012AQ046-05	11 ^h 24 ^m 00.33 ^s	05°29'21.8"	0.6559	2	X	
19	GS2012AQ046-05	11 ^h 23 ^m 49.80 ^s	05°28'47.3"	0.6551	2	X	✓
20	GS2012AQ046-05	11 ^h 23 ^m 52.23 ^s	05°28'33.8"	0.2704	2	X	
23	GS2012AQ046-05	11 ^h 23 ^m 49.77 ^s	05°29'29.6"	0.6173	2	X	
26	GS2012AQ046-05	11 ^h 23 ^m 53.92 ^s	05°28'49.5"	0.6550	3	X	✓
32	GS2012AQ046-05	11 ^h 23 ^m 48.09 ^s	05°30'40.6"	0.2154	3	X	
3	GS2012AQ046-06	11 ^h 24 ^m 00.02 ^s	05°27'32.8"	0.4144	3	X	
6	GS2012AQ046-06	11 ^h 23 ^m 59.87 ^s	05°27'53.9"	0.4714	3	X	
12	GS2012AQ046-06	11 ^h 23 ^m 59.15 ^s	05°28'07.0"	0.5944	2	X	✓
13	GS2012AQ046-06	11 ^h 23 ^m 57.44 ^s	05°29'05.2"	0.6511	3	X	
14	GS2012AQ046-06	11 ^h 24 ^m 01.00 ^s	05°29'07.5"	0.3749	3	X	
15	GS2012AQ046-06	11 ^h 23 ^m 50.31 ^s	05°28'06.3"	0.6129	3	X	
17	GS2012AQ046-06	11 ^h 23 ^m 51.87 ^s	05°28'25.8"	0.5517	3	X	
18	GS2012AQ046-06	11 ^h 23 ^m 50.07 ^s	05°29'00.3"	0.6378	3	X	
19	GS2012AQ046-06	11 ^h 23 ^m 52.14 ^s	05°28'56.7"	0.6515	3	X	✓
20	GS2012AQ046-06	11 ^h 23 ^m 54.84 ^s	05°29'04.5"	0.6381	3	X	
23	GS2012AQ046-06	11 ^h 23 ^m 55.15 ^s	05°30'28.9"	0.3745	3	X	
27	GS2012AQ046-06	11 ^h 23 ^m 48.05 ^s	05°29'40.3"	0.8828	3	X	
28	GS2012AQ046-06	11 ^h 23 ^m 51.48 ^s	05°30'27.4"	0.4231	3	X	
30	GS2012AQ046-06	11 ^h 23 ^m 45.31 ^s	05°29'57.0"	0.5678	2	X	
32	GS2012AQ046-06	11 ^h 23 ^m 49.50 ^s	05°30'51.6"	0.6562	3	X	✓

Table B29. XMMXCSJ112349.4+052955.1: All columns are as explained in Table B23.

ID	Mask	RA(J2000)	Dec(J2000)	z	Quality	Identification	Member
3	GS-2012A-Q-046-07	11 ^h 35 ^m 58.38 ^s	-03°31'15.8"	1.0306	3	X	
5	GS-2012A-Q-046-07	11 ^h 35 ^m 59.26 ^s	-03°31'33.9"	0.8323	3	X	✓
6	GS-2012A-Q-046-07	11 ^h 35 ^m 59.51 ^s	-03°32'04.2"	0.8353	3	X	
8	GS-2012A-Q-046-07	11 ^h 36 ^m 01.95 ^s	-03°31'10.1"	0.8255	3	X	✓
9	GS-2012A-Q-046-07	11 ^h 36 ^m 02.76 ^s	-03°31'04.6"	0.8841	3	X	
11	GS-2012A-Q-046-07	11 ^h 36 ^m 01.15 ^s	-03°29'33.8"	0.8215	3	X	✓
12	GS-2012A-Q-046-07	11 ^h 36 ^m 04.68 ^s	-03°30'39.0"	0.8266	3	X	✓
13	GS-2012A-Q-046-07	11 ^h 36 ^m 04.36 ^s	-03°30'17.7"	0.8265	3	X	✓
14	GS-2012A-Q-046-07	11 ^h 36 ^m 03.15 ^s	-03°30'00.7"	0.8339	3	X	✓
15	GS-2012A-Q-046-07	11 ^h 36 ^m 04.33 ^s	-03°30'30.7"	0.8332	3	X	✓
16	GS-2012A-Q-046-07	11 ^h 36 ^m 06.69 ^s	-03°30'14.3"	0.7021	3	X	
17	GS-2012A-Q-046-07	11 ^h 36 ^m 04.13 ^s	-03°29'47.9"	0.8253	3	X	✓
18	GS-2012A-Q-046-07	11 ^h 36 ^m 03.74 ^s	-03°29'54.7"	0.8314	3	X	✓
20	GS-2012A-Q-046-07	11 ^h 36 ^m 00.34 ^s	-03°29'20.0"	0.8250	3	X	✓
21	GS-2012A-Q-046-07	11 ^h 36 ^m 01.38 ^s	-03°28'56.4"	0.9718	2	X	
22	GS-2012A-Q-046-07	11 ^h 36 ^m 01.43 ^s	-03°29'11.3"	0.8254	3	X	✓
23	GS-2012A-Q-046-07	11 ^h 36 ^m 10.03 ^s	-03°29'19.2"	0.6508	3	X	
24	GS-2012A-Q-046-07	11 ^h 36 ^m 09.58 ^s	-03°29'05.1"	0.6502	3	X	
25	GS-2012A-Q-046-07	11 ^h 36 ^m 05.87 ^s	-03°28'39.5"	0.8265	3	X	✓
26	GS-2012A-Q-046-07	11 ^h 36 ^m 04.83 ^s	-03°28'22.6"	0.8831	3	X	
28	GS-2012A-Q-046-07	11 ^h 36 ^m 03.95 ^s	-03°27'59.7"	0.8307	3	X	✓
34	GS-2012A-Q-046-07	11 ^h 36 ^m 02.55 ^s	-03°27'08.5"	0.6434	3	X	
36	GS-2012A-Q-046-07	11 ^h 36 ^m 04.01 ^s	-03°27'32.0"	0.8370	3	X	✓
9	GS-2012A-Q-046-08	11 ^h 36 ^m 04.48 ^s	-03°31'58.9"	0.5370	2	X	
11	GS-2012A-Q-046-08	11 ^h 35 ^m 58.58 ^s	-03°29'58.4"	0.2058	3	X	
12	GS-2012A-Q-046-08	11 ^h 36 ^m 00.27 ^s	-03°30'31.0"	0.7022	3	X	
13	GS-2012A-Q-046-08	11 ^h 36 ^m 03.65 ^s	-03°29'52.4"	0.8328	3	V	✓
15	GS-2012A-Q-046-08	11 ^h 36 ^m 02.47 ^s	-03°29'25.7"	0.6884	2	X	
16	GS-2012A-Q-046-08	11 ^h 36 ^m 05.41 ^s	-03°29'38.6"	0.8298	3	X	✓
17	GS-2012A-Q-046-08	11 ^h 36 ^m 04.64 ^s	-03°30'23.3"	0.8242	3	X	✓
18	GS-2012A-Q-046-08	11 ^h 36 ^m 06.05 ^s	-03°30'18.4"	0.8296	3	X	✓
19	GS-2012A-Q-046-08	11 ^h 36 ^m 02.55 ^s	-03°29'58.6"	0.8307	3	X	✓
20	GS-2012A-Q-046-08	11 ^h 36 ^m 02.67 ^s	-03°29'40.5"	0.8274	3	X	✓
22	GS-2012A-Q-046-08	11 ^h 36 ^m 03.71 ^s	-03°29'10.8"	0.4067	2	X	✓
24	GS-2012A-Q-046-08	11 ^h 36 ^m 04.25 ^s	-03°29'18.3"	0.8357	3	X	✓
30	GS-2012A-Q-046-08	11 ^h 36 ^m 04.70 ^s	-03°28'14.5"	0.1869	3	X	

Table B30. XMMXCSJ113602.9âũ32943.2: All columns are as explained in Table B23.

ID	Mask	RA(J2000)	Dec(J2000)	z	Quality	Identification	Member
4	GS-2012A-Q-046-10	13 ^h 42 ^m 58.07 ^s	-00°02′43.9″	0.8343	3	X	
5	GS-2012A-Q-046-10	13 ^h 42 ^m 59.51 ^s	00°00′08.0″	0.6925	3	X	✓
6	GS-2012A-Q-046-10	13 ^h 42 ^m 56.97 ^s	-00°00′47.4″	0.4383	3	X	
7	GS-2012A-Q-046-10	13 ^h 42 ^m 58.82 ^s	-00°00′53.6″	0.8342	3	X	
8	GS-2012A-Q-046-10	13 ^h 43 ^m 02.03 ^s	-00°01′17.4″	0.6829	3	X	✓
9	GS-2012A-Q-046-10	13 ^h 42 ^m 59.93 ^s	-00°01′20.0″	0.5510	3	X	
10	GS-2012A-Q-046-10	13 ^h 43 ^m 01.63 ^s	-00°01′41.7″	0.6833	3	X	✓
11	GS-2012A-Q-046-10	13 ^h 42 ^m 59.07 ^s	-00°01′45.5″	0.4123	3	X	
12	GS-2012A-Q-046-10	13 ^h 42 ^m 59.26 ^s	-00°01′33.3″	0.6865	3	X	✓
13	GS-2012A-Q-046-10	13 ^h 43 ^m 00.57 ^s	-00°01′23.8″	0.6962	3	X	✓
15	GS-2012A-Q-046-10	13 ^h 43 ^m 02.82 ^s	-00°00′28.3″	0.6956	3	X	✓
17	GS-2012A-Q-046-10	13 ^h 43 ^m 04.11 ^s	-00°01′50.1″	0.6896	3	X	✓
18	GS-2012A-Q-046-10	13 ^h 43 ^m 04.57 ^s	-00°00′56.4″	0.6912	3	X	✓
19	GS-2012A-Q-046-10	13 ^h 43 ^m 02.71 ^s	-00°01′13.1″	0.6913	3	X	✓
21	GS-2012A-Q-046-10	13 ^h 43 ^m 04.00 ^s	-00°00′55.2″	0.6849	3	X	✓
23	GS-2012A-Q-046-10	13 ^h 43 ^m 09.21 ^s	00°00′23.1″	0.6152	3	X	
24	GS-2012A-Q-046-10	13 ^h 43 ^m 06.79 ^s	00°00′09.5″	0.3847	2	X	
26	GS-2012A-Q-046-10	13 ^h 43 ^m 08.82 ^s	-00°00′04.8″	0.7017	2	X	
27	GS-2012A-Q-046-10	13 ^h 43 ^m 09.97 ^s	-00°01′11.0″	0.6906	3	X	✓
28	GS-2012A-Q-046-10	13 ^h 43 ^m 07.82 ^s	-00°00′51.4″	0.6911	3	X	✓
29	GS-2012A-Q-046-10	13 ^h 43 ^m 08.21 ^s	-00°00′30.5″	0.6958	3	X	✓
30	GS-2012A-Q-046-10	13 ^h 43 ^m 10.30 ^s	00°00′35.0″	0.6847	3	X	✓
31	GS-2012A-Q-046-10	13 ^h 43 ^m 09.80 ^s	00°00′25.8″	0.5491	3	X	
34	GS-2012A-Q-046-10	13 ^h 43 ^m 12.93 ^s	00°00′20.8″	0.2190	2	X	
35	GS-2012A-Q-046-10	13 ^h 43 ^m 13.05 ^s	-00°00′08.6″	0.6865	3	X	✓
36	GS-2012A-Q-046-10	13 ^h 43 ^m 13.85 ^s	-00°01′02.2″	0.7952	2	X	
3	GS-2012A-Q-046-11	13 ^h 42 ^m 54.94 ^s	-00°01′04.6″	0.8149	3	X	
8	GS-2012A-Q-046-11	13 ^h 43 ^m 02.43 ^s	-00°01′38.7″	0.6902	2	X	✓
10	GS-2012A-Q-046-11	13 ^h 43 ^m 00.20 ^s	-00°02′15.2″	0.6864	3	V	✓
11	GS-2012A-Q-046-11	13 ^h 43 ^m 00.10 ^s	-00°01′12.5″	0.6793	2	X	✓
13	GS-2012A-Q-046-11	13 ^h 42 ^m 59.42 ^s	-00°01′18.7″	0.6018	2	X	
14	GS-2012A-Q-046-11	13 ^h 43 ^m 02.31 ^s	-00°00′50.9″	0.6909	2	X	✓
15	GS-2012A-Q-046-11	13 ^h 43 ^m 03.97 ^s	-00°01′25.9″	0.6801	3	X	✓
16	GS-2012A-Q-046-11	13 ^h 43 ^m 05.18 ^s	-00°01′48.0″	0.5474	2	X	
18	GS-2012A-Q-046-11	13 ^h 43 ^m 04.65 ^s	-00°00′57.3″	0.6901	2	X	✓
19	GS-2012A-Q-046-11	13 ^h 43 ^m 04.77 ^s	-00°00′44.0″	0.6986	2	X	✓
21	GS-2012A-Q-046-11	13 ^h 43 ^m 07.84 ^s	00°00′19.6″	0.2707	2	X	
23	GS-2012A-Q-046-11	13 ^h 43 ^m 08.50 ^s	00°00′17.4″	0.7942	2	X	
30	GS-2012A-Q-046-11	13 ^h 43 ^m 12.41 ^s	00°01′23.7″	0.6895	2	X	✓
32	GS-2012A-Q-046-11	13 ^h 43 ^m 12.93 ^s	00°00′20.8″	0.8020	2	X	

Table B31. XMMXCSJ134305.1-000056.8: All columns are as explained in Table B23.

ID	Mask	RA(J2000)	Dec(J2000)	z	Quality	Identification	Member
1	Nastasi et al. (2014)	14 ^h 50 ^m 09.30 ^s	09°04′39.3″	0.6419	3		
2	Nastasi et al. (2014)	14 ^h 50 ^m 09.20 ^s	09°04′45.1″	0.6425	3		
3	Nastasi et al. (2014)	14 ^h 50 ^m 10.40 ^s	09°04′23.5″	0.6418	2		✓
4	Nastasi et al. (2014)	14 ^h 50 ^m 09.50 ^s	09°04′15.9″	0.6430	3		
5	Nastasi et al. (2014)	14 ^h 50 ^m 07.40 ^s	09°04′28.8″	0.6429	3		✓
6	Nastasi et al. (2014)	14 ^h 50 ^m 09.30 ^s	09°04′06.5″	0.6377	3		
7	Nastasi et al. (2014)	14 ^h 50 ^m 10.40 ^s	09°03′53.4″	0.6462	2		✓
8	Nastasi et al. (2014)	14 ^h 50 ^m 10.61 ^s	09°05′32.4″	0.6379	3		
9	Nastasi et al. (2014)	14 ^h 50 ^m 13.80 ^s	09°03′21.9″	0.6407	3		
10	Nastasi et al. (2014)	14 ^h 50 ^m 16.01 ^s	09°02′57.6″	0.6420	2		✓
11	Nastasi et al. (2014)	14 ^h 50 ^m 04.91 ^s	09°06′55.1″	0.6405	3		
3	GN-2012A-Q-070-05	14 ^h 50 ^m 12.84 ^s	09°02′45.1″	0.5093	3	X	
6	GN-2012A-Q-070-05	14 ^h 50 ^m 07.25 ^s	09°02′58.0″	0.5064	2	X	
9	GN-2012A-Q-070-05	14 ^h 50 ^m 10.22 ^s	09°02′50.9″	0.5889	3	X	
11	GN-2012A-Q-070-05	14 ^h 50 ^m 11.80 ^s	09°03′56.4″	0.6405	3	X	✓
12	GN-2012A-Q-070-05	14 ^h 50 ^m 09.37 ^s	09°04′06.5″	0.6367	2	X	✓
13	GN-2012A-Q-070-05	14 ^h 50 ^m 09.53 ^s	09°04′15.9″	0.6430	3	X	✓
14	GN-2012A-Q-070-05	14 ^h 50 ^m 09.97 ^s	09°04′36.0″	0.3242	3	X	
15	GN-2012A-Q-070-05	14 ^h 50 ^m 13.80 ^s	09°03′21.9″	0.6403	3	X	✓
16	GN-2012A-Q-070-05	14 ^h 50 ^m 09.86 ^s	09°04′27.2″	0.6412	2	X	✓
17	GN-2012A-Q-070-05	14 ^h 50 ^m 09.29 ^s	09°04′39.2″	0.6398	3	X	
22	GN-2012A-Q-070-05	14 ^h 50 ^m 11.94 ^s	09°05′40.3″	0.6455	3	X	✓
24	GN-2012A-Q-070-05	14 ^h 50 ^m 01.45 ^s	09°05′06.9″	0.6355	3	X	✓
27	GN-2012A-Q-070-05	14 ^h 50 ^m 02.90 ^s	09°05′45.5″	0.4828	3	X	
31	GN-2012A-Q-070-05	14 ^h 50 ^m 07.98 ^s	09°06′52.6″	0.3705	3	X	
1	GN-2012A-Q-070-06	14 ^h 50 ^m 09.49 ^s	09°01′54.0″	0.8757	2	X	
3	GN-2012A-Q-070-06	14 ^h 50 ^m 08.46 ^s	09°02′24.2″	0.2673	2	X	
4	GN-2012A-Q-070-06	14 ^h 50 ^m 09.14 ^s	09°02′21.3″	0.7059	2	X	
7	GN-2012A-Q-070-06	14 ^h 50 ^m 09.00 ^s	09°03′16.8″	0.6403	2	X	✓
10	GN-2012A-Q-070-06	14 ^h 50 ^m 09.73 ^s	09°04′11.7″	0.6372	3	X	✓
12	GN-2012A-Q-070-06	14 ^h 50 ^m 12.48 ^s	09°03′16.6″	0.5840	3	X	
15	GN-2012A-Q-070-06	14 ^h 50 ^m 09.12 ^s	09°04′25.8″	0.8099	3	X	
18	GN-2012A-Q-070-06	14 ^h 50 ^m 10.65 ^s	09°05′32.0″	0.6363	3	X	✓
21	GN-2012A-Q-070-06	14 ^h 50 ^m 14.62 ^s	09°05′46.7″	0.7252	3	X	
1	GN-2012A-Q-070-07	14 ^h 50 ^m 15.96 ^s	09°02′22.7″	0.5646	2	X	
6	GN-2012A-Q-070-07	14 ^h 50 ^m 07.24 ^s	09°02′45.5″	1.0768	3	X	
11	GN-2012A-Q-070-07	14 ^h 50 ^m 09.42 ^s	09°04′11.9″	0.6457	2	X	✓
12	GN-2012A-Q-070-07	14 ^h 50 ^m 13.56 ^s	09°03′51.6″	0.2948	3	X	
13	GN-2012A-Q-070-07	14 ^h 50 ^m 10.59 ^s	09°03′54.8″	0.2282	3	X	
14	GN-2012A-Q-070-07	14 ^h 50 ^m 08.87 ^s	09°04′18.6″	0.6444	3	X	✓
15	GN-2012A-Q-070-07	14 ^h 50 ^m 08.55 ^s	09°04′27.9″	0.7346	2	X	
16	GN-2012A-Q-070-07	14 ^h 50 ^m 09.51 ^s	09°03′59.3″	0.6413	2	X	✓
19	GN-2012A-Q-070-07	14 ^h 50 ^m 09.38 ^s	09°04′45.0″	0.6455	3	X	✓
22	GN-2012A-Q-070-07	14 ^h 50 ^m 01.03 ^s	09°04′50.5″	0.6417	3	X	✓
25	GN-2012A-Q-070-07	14 ^h 50 ^m 03.59 ^s	09°05′33.3″	0.6411	2	X	✓
26	GN-2012A-Q-070-07	14 ^h 50 ^m 03.83 ^s	09°06′15.5″	0.4833	3	X	
27	GN-2012A-Q-070-07	14 ^h 50 ^m 04.34 ^s	09°06′04.2″	0.6367	2	X	✓
32	GN-2012A-Q-070-07	14 ^h 50 ^m 07.98 ^s	09°06′52.6″	0.3702	3	X	

Table B32. XMMXCSJ145009.3+090428.8: All columns are as explained in Table B23.

ID	Mask	RA(J2000)	Dec(J2000)	z	Quality	Identification	Member
5	GS-2010B-Q-046-04	21 ^h 52 ^m 20.26 ^s	-27°28'46.6"	0.4662	2	X	
8	GS-2010B-Q-046-04	21 ^h 52 ^m 16.97 ^s	-27°28'39.8"	0.6330	3	X	
12	GS-2010B-Q-046-04	21 ^h 52 ^m 23.98 ^s	-27°30'29.9"	0.8217	3	X	✓
13	GS-2010B-Q-046-04	21 ^h 52 ^m 19.74 ^s	-27°30'32.1"	0.8262	2	X	✓
14	GS-2010B-Q-046-04	21 ^h 52 ^m 14.96 ^s	-27°30'00.0"	0.8293	3	X	✓
17	GS-2010B-Q-046-04	21 ^h 52 ^m 17.29 ^s	-27°29'22.2"	0.8297	2	X	✓
19	GS-2010B-Q-046-04	21 ^h 52 ^m 20.19 ^s	-27°29'52.9"	0.8281	2	X	✓
20	GS-2010B-Q-046-04	21 ^h 52 ^m 20.14 ^s	-27°30'22.7"	0.8203	2	X	✓
21	GS-2010B-Q-046-04	21 ^h 52 ^m 16.77 ^s	-27°29'44.6"	0.5923	3	X	
22	GS-2010B-Q-046-04	21 ^h 52 ^m 21.69 ^s	-27°30'05.5"	0.8308	2	X	✓
26	GS-2010B-Q-046-04	21 ^h 52 ^m 24.86 ^s	-27°30'59.8"	0.8076	3	X	
27	GS-2010B-Q-046-04	21 ^h 52 ^m 25.06 ^s	-27°31'42.7"	0.4450	3	X	
31	GS-2010B-Q-046-04	21 ^h 52 ^m 23.85 ^s	-27°31'20.3"	0.8287	2	X	✓
32	GS-2010B-Q-046-04	21 ^h 52 ^m 24.29 ^s	-27°32'05.7"	0.8240	3	X	
36	GS-2010B-Q-046-04	21 ^h 52 ^m 22.99 ^s	-27°32'50.7"	0.7358	3	X	
2	GS-2011B-Q-050-06	21 ^h 52 ^m 14.59 ^s	-27°28'22.5"	0.7984	2	X	
6	GS-2011B-Q-050-06	21 ^h 52 ^m 20.57 ^s	-27°29'08.9"	0.5914	3	X	
8	GS-2011B-Q-050-06	21 ^h 52 ^m 16.51 ^s	-27°28'45.2"	0.6038	3	X	
9	GS-2011B-Q-050-06	21 ^h 52 ^m 19.78 ^s	-27°28'45.5"	0.4569	3	X	
11	GS-2011B-Q-050-06	21 ^h 52 ^m 17.31 ^s	-27°29'43.8"	0.4667	2	X	
14	GS-2011B-Q-050-06	21 ^h 52 ^m 19.90 ^s	-27°29'23.0"	0.8057	2	X	
15	GS-2011B-Q-050-06	21 ^h 52 ^m 24.86 ^s	-27°30'54.4"	0.6334	3	X	
17	GS-2011B-Q-050-06	21 ^h 52 ^m 22.36 ^s	-27°29'59.0"	0.8292	3	X	✓
18	GS-2011B-Q-050-06	21 ^h 52 ^m 20.58 ^s	-27°30'26.0"	0.8264	3	X	✓
19	GS-2011B-Q-050-06	21 ^h 52 ^m 18.98 ^s	-27°30'50.1"	0.8271	2	X	✓
25	GS-2011B-Q-050-06	21 ^h 52 ^m 19.95 ^s	-27°31'28.2"	0.8251	3	X	✓
26	GS-2011B-Q-050-06	21 ^h 52 ^m 20.67 ^s	-27°30'18.8"	0.8240	3	X	✓
34	GS-2011B-Q-050-06	21 ^h 52 ^m 23.51 ^s	-27°32'34.8"	0.8111	2	X	
12	GS-2011B-Q-050-07	21 ^h 52 ^m 18.37 ^s	-27°30'18.4"	0.5314	3	X	
13	GS-2011B-Q-050-07	21 ^h 52 ^m 21.22 ^s	-27°30'21.3"	0.8305	3	X	✓
14	GS-2011B-Q-050-07	21 ^h 52 ^m 20.05 ^s	-27°30'34.2"	0.8313	3	X	✓
15	GS-2011B-Q-050-07	21 ^h 52 ^m 20.78 ^s	-27°29'43.1"	0.4419	3	X	
16	GS-2011B-Q-050-07	21 ^h 52 ^m 15.57 ^s	-27°29'12.9"	0.7362	3	X	
20	GS-2011B-Q-050-07	21 ^h 52 ^m 21.11 ^s	-27°30'37.5"	0.8383	3	X	
26	GS-2011B-Q-050-07	21 ^h 52 ^m 26.17 ^s	-27°31'26.5"	0.4950	2	X	

Table B33. XMMXCSJ215221.0ÅŞ273022.6: All columns are as explained in Table B23.

ID	Mask	RA(J2000)	Dec(J2000)	z	Quality	Identification	Member
1	GN-2012A-Q-070-10	23 ^h 02 ^m 39.79 ^s	08°42′48.1″	0.7148	3	X	✓
2	GN-2012A-Q-070-10	23 ^h 02 ^m 38.96 ^s	08°42′33.7″	0.7141	3	X	✓
4	GN-2012A-Q-070-10	23 ^h 02 ^m 39.70 ^s	08°42′25.3″	0.7169	3	X	✓
9	GN-2012A-Q-070-10	23 ^h 02 ^m 42.62 ^s	08°43′57.4″	0.7235	2	X	✓
11	GN-2012A-Q-070-10	23 ^h 02 ^m 43.85 ^s	08°43′55.2″	0.7291	3	X	✓
12	GN-2012A-Q-070-10	23 ^h 02 ^m 42.24 ^s	08°42′57.6″	0.7231	3	X	✓
14	GN-2012A-Q-070-10	23 ^h 02 ^m 43.02 ^s	08°42′48.4″	0.6239	3	X	
16	GN-2012A-Q-070-10	23 ^h 02 ^m 47.41 ^s	08°44′10.3″	0.7152	3	X	✓
17	GN-2012A-Q-070-10	23 ^h 02 ^m 48.36 ^s	08°43′54.2″	0.7192	3	X	✓
18	GN-2012A-Q-070-10	23 ^h 02 ^m 49.81 ^s	08°43′45.2″	0.7181	3	X	✓
19	GN-2012A-Q-070-10	23 ^h 02 ^m 47.90 ^s	08°43′23.0″	0.7107	3	X	✓
20	GN-2012A-Q-070-10	23 ^h 02 ^m 47.40 ^s	08°43′13.9″	0.8648	3	X	
22	GN-2012A-Q-070-10	23 ^h 02 ^m 51.32 ^s	08°45′14.6″	0.6157	3	X	
23	GN-2012A-Q-070-10	23 ^h 02 ^m 52.81 ^s	08°45′17.2″	0.4820	3	X	
25	GN-2012A-Q-070-10	23 ^h 02 ^m 53.25 ^s	08°44′37.2″	0.7244	3	X	✓
27	GN-2012A-Q-070-10	23 ^h 02 ^m 52.60 ^s	08°44′00.3″	0.7261	3	X	✓
28	GN-2012A-Q-070-10	23 ^h 02 ^m 51.71 ^s	08°43′52.4″	0.7104	3	X	✓
29	GN-2012A-Q-070-10	23 ^h 02 ^m 51.41 ^s	08°43′38.7″	0.7166	3	X	✓
31	GN-2012A-Q-070-10	23 ^h 02 ^m 54.65 ^s	08°46′40.9″	0.7212	3	X	✓
33	GN-2012A-Q-070-10	23 ^h 02 ^m 56.04 ^s	08°45′03.7″	0.4818	3	X	
34	GN-2012A-Q-070-10	23 ^h 02 ^m 55.68 ^s	08°44′52.0″	0.7171	2	X	✓
11	GN-2012A-Q-070-11	23 ^h 02 ^m 41.64 ^s	08°43′44.2″	0.7157	3	X	✓
13	GN-2012A-Q-070-11	23 ^h 02 ^m 47.90 ^s	08°44′45.5″	0.7377	3	X	
14	GN-2012A-Q-070-11	23 ^h 02 ^m 45.49 ^s	08°44′30.1″	0.7209	3	X	✓
18	GN-2012A-Q-070-11	23 ^h 02 ^m 45.16 ^s	08°43′12.6″	0.7113	3	X	✓
19	GN-2012A-Q-070-11	23 ^h 02 ^m 47.95 ^s	08°43′58.1″	0.7283	3	X	✓
20	GN-2012A-Q-070-11	23 ^h 02 ^m 46.70 ^s	08°44′00.6″	0.7253	3	X	✓
21	GN-2012A-Q-070-11	23 ^h 02 ^m 48.54 ^s	08°43′60.0″	0.7253	3	X	✓
32	GN-2012A-Q-070-11	23 ^h 02 ^m 55.72 ^s	08°45′01.7″	0.4828	3	X	
33	GN-2012A-Q-070-11	23 ^h 03 ^m 00.05 ^s	08°43′00.9″	0.8772	2	X	

Table B34. XMMXCSJ230247.7+084355.9: All columns are as explained in Table B23.

APPENDIX C: VELOCITY HISTOGRAMS

Velocity histograms of all the clusters in the sample to appear in the online version of the article.

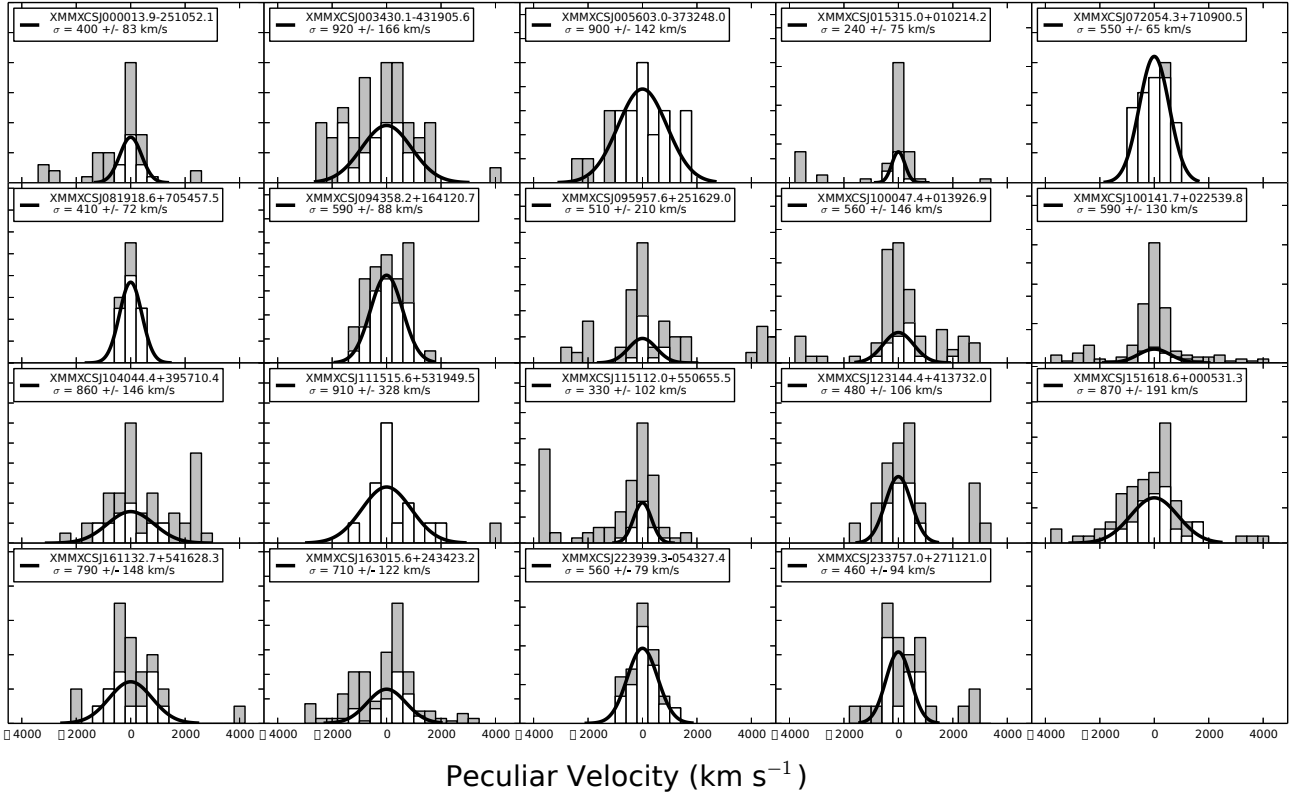


Figure C1. We depict a synthetic view of the tables found in Appendix B in the form of histograms for the low redshift sample. The solid grey blocks depict all the galaxies considered as possible members while the white blocks are the final chosen members. The solid black line shows the velocity dispersion calculated using the method described in the paper.

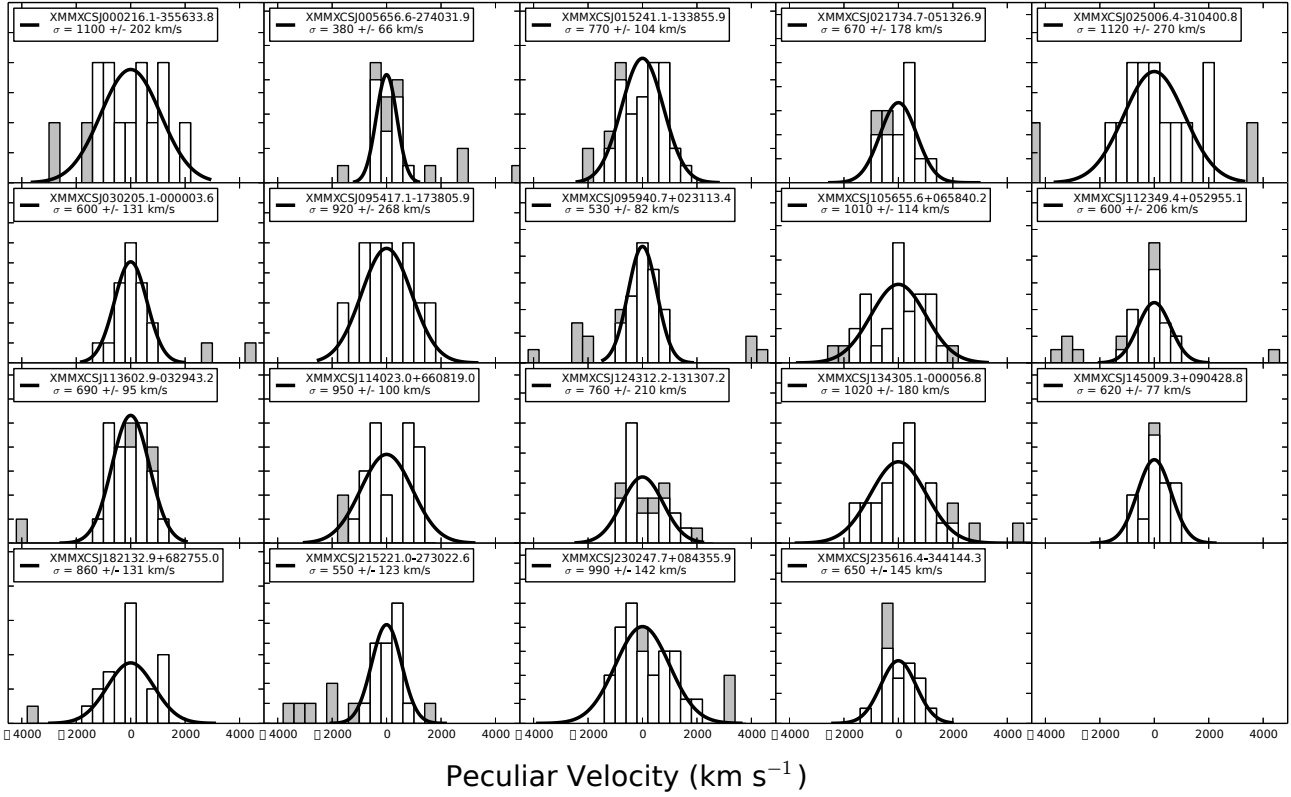


Figure C2. We depict a synthetic view of the tables found in Appendix B in the form of histograms for the high redshift sample. All blocks and lines are as in Figure C1.